



PONTIFICIA UNIVERSIDAD CATÓLICA DE CHILE
ESCUELA DE INGENIERÍA

OXYGEN MANAGEMENT DURING ALCOHOLIC FERMENTATION

MARÍA ISABEL MOENNE VARGAS

Thesis submitted to the Office of Research and Graduate Studies in
partial fulfillment of the requirements for the Degree of Doctor in
Engineering Sciences

Advisor:

EDUARDO AGOSIN T.

Santiago de Chile, December, 2013

© 2013, María Isabel Moenne Vargas



PONTIFICIA UNIVERSIDAD CATOLICA DE CHILE
ESCUELA DE INGENIERIA

OXYGEN MANAGEMENT DURING ALCOHOLIC FERMENTATION

MARIA ISABEL MOENNE VARGAS

Members of the Committee:

EDUARDO AGOSIN T.

EDMUNDO BORDEU

FELIPE LAURIE

RICARDO PEREZ-CORREA

JEAN-MARIE SABLAYROLLES

CRISTIAN VIAL

Thesis submitted to the Office of Research and Graduate Studies in partial fulfillment of the requirements for the Degree of Doctor in Engineering Sciences

Santiago de Chile, December, 2013

To my family, Juan Carlos, Silvia,
Cristóbal, René, Melita and Edith.

ACKNOWLEDGMENTS

First, I would like to thank my family for the unconditional love and support during all my life. I would also like to thank my advisor Eduardo Agosin for his patience and tutoring during my thesis, and to the professors, Ricardo, Felipe, Edmundo, Cristian and Jean-Marie, for their contribution to my thesis.

Big thanks María Carolina Zuñiga, Alexandra Lobos, Pauly Torres, Marianna Delgado, Marcelo Orellana, Martin Cárcamo, Carolina Pavez, Feña Silva, Carlos Galarce, Charlie Fontecilla, Benja Sánchez, Mane Valdebenito and all the staff of the biotechnology laboratory at Pontificia Universidad Católica de Chile for their friendship, time, patience, collaboration during the experiments and for all the good times that we spent together. Gracias por su apoyo, sus consejos, las tardes deportivas, las salidas en grupo, simplemente por estar cuando lo necesitaba y hacer de este recorrido un gran viaje.

Very big thanks to the staff of the INRA institute. Je tiens à remercier monsieur Jean-Marie SABLAYROLLES, directeur de l'UMR de Sciences pour l'oenologie de l'INRA de m'avoir reçue pour faire mon stage de recherche dans l'UMR. Je remercie spécialement à Jean-Roch MOURET et Vincent FARINES pour leur patience, leur aide et leur soutien au cours de mon stage et pour faciliter mon séjour en France, surtout après avoir renouvelé ma carte de séjour 3 fois! Je remercie également Christian PICOU pour son aide, sa patience de m'apprendre comment utiliser l'équipement de laboratoire et pour sa bonne humeur. Je tiens également à remercier Marc PEREZ pour l'aide apportée à traiter mes échantillons et pour me donner leurs deux CD de musique, Marc tu es un très bon musicien!!

Je remercie tout particulièrement Souhir MARSIT et Annalisa COI pour leur aide, leur soutien, votre amitié et pour tous les moments que on a partagé ensemble. Un grand

merci a Audrey SZARZYNSKI pour me accueillie quand je suis arrivé a la France, l'enseignement du français, sa amitié et ses conseils, vive la coloc!

Un autre grand merci à tous les personnes de l'INRA de Pech Rouge, plus particulièrement Magaly ANGENIEUX et Evelyne AGUERA, pour votre amitié et aidée dans les expérimentations. Ce un vrai plaisir de travailler avec vous!!!!

Finally, I would like to extend my gratitude to the National Fund for Scientific and Technological Development of Chile (FONDECYT) No. 1090520 for its economic support during the realization of this work and to the Chilean National Council of Scientific and Technological Research (CONICYT) for its doctoral fellowship.

LIST OF PUBLICATIONS

This thesis is based on the following publications.

Moenne, M.I., Saa, P.A., Laurie, V.F., Pérez-Correa, J.R., Agosin, E. 2013. Oxygen incorporation and dissolution during industrial-scale red wine fermentations. (*Accepted in Food and Bioprocess Technology; Manuscript number #FABT-D-13-01096R1*)

Saa, P.A., Moenne, M.I., Pérez-Correa, J.R., Agosin, E., 2012. Modeling oxygen dissolution and biological uptake during pulse oxygen additions in oenological fermentations. *Bioprocess and Biosystems Engineering* 35, 1167–1178.

Moenne, M.I., Mouret J-R, Sablayrolles J-M, Agosin E., Farines V., 2013. Control of Bubble-free Oxygenation with Silicone Tubing during Alcoholic Fermentation. *Process Biochemistry* 48, 1453-1461.

CONTENTS

	Pag.
ACKNOWLEDGMENTS.....	iii
LIST OF PUBLICATIONS	v
FIGURE INDEX.....	x
TABLE INDEX.....	xiv
ABBREVIATION INDEX	xv
ABSTRACT	xvi
RESUMEN.....	xix
1. BRIEF INTRODUCTION	1
1.1 Motivation.....	1
1.2 Objectives	1
1.3 Approach.....	2
1.3.1 Oxygen measurements at industrial scale	2
1.3.2 Studies at laboratory scale.....	3
2. GENERAL INTRODUCTION.....	5
2.1 Red wine making.....	5
2.2 Oxygen in wine making.....	7
2.3 Oxygen dissolution	9
2.3.1 Oxygenation by gas bubbles	10
2.3.2 Bubble-free oxygenation of media by membrane	14
2.3.3 Techniques for Oxygen Measurement	16
REFERENCES.....	18
3. OXYGEN INCORPORATION AND DISSOLUTION DURING INDUSTRIAL- SCALE RED WINE FERMENTATIONS.....	24
Abstract.....	24
3.1 Introduction.....	25

3.2	Materials and Methods.....	27
3.2.1	Wine fermentations	27
3.2.2	Oxygen incorporation due to different pump-over modes	28
3.2.3	Dissolved oxygen gradients inside large industrial wine tanks during open pump-overs.....	29
3.2.4	Oxygen dissolution and consumption kinetics during wine maceration and fermentation.....	31
3.2.5	Kinetics of oxygen consumption during pump-overs	32
3.2.6	Regression and statistics.....	32
3.3	Results and discussion	33
3.3.1	Oxygen incorporation by different pump-over modes.....	33
3.3.2	Dissolved oxygen gradients inside large industrial wine tanks during open pump-overs.....	36
3.3.3	Oxygen dissolution and consumption kinetics during wine maceration and fermentation.....	38
3.3.4	Kinetics of oxygen dissolution and consumption during alcoholic fermentations.....	41
3.4	Conclusion	44
	Acknowledgments	45
	References.....	46
4.	MODELLING OXYGEN DISSOLUTION AND BIOLOGICAL UPTAKE DURING PULSE OXYGEN ADDITIONS IN OENOLOGICAL FERMENTATIONS	50
	Abstract.....	50
	Abbreviations.....	51
	List of symbols.....	51
	Greek letters.....	52
4.1	Introduction.....	52
4.1.1	Model development.....	55
4.1.2	Oxygen mass balance	55
4.1.3	Oxygen solubility	56
4.2	Materials and methods	58
4.2.1	Yeast strain	58
4.2.2	Culture media and fermentation conditions	58

4.2.3 Analytical techniques	58
4.2.4 Oxygen additions.....	58
4.2.5 Dissolved oxygen	59
4.2.6 Oxygen solubility	59
4.2.7 k_{La} measurements in synthetic solution	60
4.2.8 Parameter fitting	60
4.2.9 Regression diagnostics	61
4.3 Results and discussion	62
4.3.1 Calibration of the oxygen solubility model.....	62
4.3.2 Oxygen uptake rate model calibration under perfect mixing conditions.....	64
4.3.3 Comparison of experimental results and model predictions	65
4.3.4 Oxygen uptake rate model calibration under non-agitated conditions.....	69
4.3.5 Influence of agitation conditions upon the oxygen uptake response time.....	69
4.3.6 Oxygen mass transfer under oenological conditions.....	71
4.3.7 Influence of the dissolved carbon dioxide upon the mass transfer coefficient	72
4.4 Conclusions.....	73
Acknowledgments	73
References.....	74

5. CONTROL OF BUBBLE-FREE OXYGENATION WITH SILICONE TUBING DURING ALCOHOLIC FERMENTATION.....	79
Abstract.....	79
5.1. Introduction.....	79
5.2. Materials and methods	82
5.2.1. Aeration system.....	82
5.2.2. Oxygen saturation concentration (C^*)	83
5.2.3. Volumetric transfer coefficient	83
5.2.4. Media composition	84
5.2.5. Viscosity and density	85
5.2.6. Fermentation.....	85
5.3. Results and discussion	86

5.3.1. Effect of physical parameters on the oxygen transfer rate	86
5.3.2. Model development.....	92
5.3.3. Model validation	97
5.4. Conclusions.....	98
Acknowledgments	99
Abbreviations.....	100
Symbols and abbreviations	100
References.....	101
6. Conclusions	105

FIGURE INDEX

Figure 2-1: Basic routes for the principal flavour groups during fermentation (Swiegers et al., 2005).....	9
Figure 2-2: Importance of define aroma and flavour specifications with the objective to attract the consumer to buy wines (Swiegers et al., 2005).....	9
Figure 2-3: Steps of oxygen transfer from a gas bubble to the individual cell (Nielsen et al., 2003).....	10
Figure 2-4: Simulation of a simultaneous measurement of OUR and $K_L \cdot a$ during fermentation, employing the dynamic method (Garcia-Ochoa et al., 2010).....	13
Figure 2-5: Schematic representation of mass transfer model for membrane oxygenation. The bulk oxygen concentrations are c_1 and c_2 (Schneider et al., 1995).....	15
Figure 3-1: Schematic experimental setups for studying oxygen incorporation and dissolution during pump-over operations in red wine industrial fermentations (p_{O_2} represent the points in which oxygen was measured). a Oxygen incorporation by different pump-over modes: closed, open and with Venturi; b Axial distribution of dissolved oxygen during open pump-overs at three heights in industrial wine tanks (40,000 L); c Oxygen dissolution and consumption kinetics during winemaking in 5,000-liter tanks (diagrams not to scale)	30
Figure 3-2: Boxplots of oxygen incorporation into industrial red wine fermentations by different types of pump-overs. a Closed pump-over; b Conventional open pump-over; c Open pump-over with Venturi. The abbreviations for grape varieties are: Cabernet Sauvignon (CAB), Carménère (CMR), Merlot (MER), Petit verdot (PVT), Cabernet franc (CAF), Carignan (CAR) and Alicante Henri Bouschet (AHB).....	35
Figure 3-3: Dissolved oxygen (DO) levels inside 40,000-liter industrial wine tanks during pump-overs in fermentations of Cabernet Sauvignon (<i>solid lines</i>) and Carménère musts (<i>dashed lines</i>). Panels a, b and c show DO at the top, middle and bottom of the tanks, respectively	38
Figure 3-4: Dissolved oxygen (DO) concentrations during maceration and fermentation of two Pinot noir. a Evolution of DO (<i>solid and dashed lines</i>) and the free SO_2 concentration (<i>filled squares</i>) during the maceration process; b Evolution of DO (<i>solid and dashed lines</i>) during alcoholic fermentation. The	

fermentation evolution is illustrated by the decrease of must's density (*filled circles*); c DO levels reached during open pump-overs in Pinot noir fermentations as a function of must densities 41

Figure 3-5: Oxygen dissolution and consumption kinetics during alcoholic fermentation. a A typical dissolution curve occurring during an open pump-over in a 5,000-liter wine tank during alcoholic fermentation (*black dots*). The arrow indicates the pump-over start and the onset of oxygen dissolution. The first part of the curve corresponds to the oxygen addition, in which the oxygen dissolution rate ($\Delta O_2/\Delta t$) can be estimated as the slope of the curve; while the second part describes the global oxygen consumption by the fermenting must which is modeled using Eq. (3); b Oxygen dissolution rate as a function of must's density in Pinot noir, Cabernet Sauvignon and Carménère wines. The thicker line represents a parabolic relation of the form between both variables ($R = 0.74$), while the thinner lines denote the 95% confidence interval of the trend of the fitted values (*black dots*); c Oxygen consumption constant for different fermentation stages: early fermentation (EF), tumultuous fermentation (TF) and stationary phase (SP)..... 44

Figure 4-1: A typical absorption-desorption cycle occurring during an oxygen impulse of 0.3 L/min under oenological fermentations, at 25°C. Biomass, ethanol and glucose concentrations were 4.0 g DW/L, 33.4 g/L and 70.5 g/L, respectively. The determination of the model parameters is carried out in two steps: first, the OUR model parameters and the oxygen stripping term ($k_{L,strip}$) are dynamically estimated from the desorption curve, using Eq.8; then, using these results –i.e., the experimental data of the absorption curve and Eq. 1 – the volumetric mass transfer coefficient for oxygen is calculated 61

Figure 4-2: Time-dependent normilized sensitivities of the OUR parameters model during the experiment. The *solid line* corresponds to the sensitivity of the parameter n , while the *dashed* and *dotted lines* represent the sensitivities of the $O_{2,crit}$ and $q_{O_2,max}$ parameters, respectively..... 65

Figure 4-3: Oxygen uptake rate model for different biomass concentrations during oenological fermentations at 25°C. The black squares and circles correspond to experimental measurements performed with biomass concentrations of 2.9 and 5.0 g DW/L, respectively. Solid lines represent model predictions. The fitted

parameters were $O_{2,crit}=0.3$ mg/L, $q_{O_2,max}=16.2$ mg O_2 /g DW·h and $n=1.5$ in the case of $X= 2.9$ g DW/L, while in the case of $X=5.0$ g DW/L the fitted parameters were $O_{2,crit}=0.3$ mg/L, $q_{O_2,max}=19.4$ mg O_2 /g DW·h and $n=2.3$ 67

Figure 4-4: Specific oxygen consumption kinetics by *Saccharomyces cerevisiae* and increase of the parameter n with the biomass concentration. a Behavior for different n values (*solid line* $n=1$, *dashed line* $n=2$ and *dotted line* $n=3$). b Fitting of n for different biomass concentrations (the higher the biomass concentration the larger the values of n). The *thicker line* represents a linear regression between both variables, while the *thinner lines* denote the 95% confidence interval of the trend of the fitted values (*black dots*) 67

Figure 4-5: Specific oxygen uptake rate optimization and biomass growth. a Evolution of the specific oxygen uptake rate with the biomass concentration. The *thicker line* represents a quadratic regression between both variables, while the *thinner lines* denote the 95% confidence interval of the trend of the fitted values (*black dots*). b Biomass concentration along the fermentation. *Black dots* represent biomass concentration measurements and the *solid line* represents the fermentation course 68

Figure 4-6: Comparison of different oxygen consumption dynamics for different hydrodynamic conditions. The biomass concentration in both cases was 4.0 g DW/L. For both experiments, the pH and temperature were maintained at 3.5 and 25°C, respectively. The *black circles* correspond to the oxygen uptake measurements at a stirring speed of 300 rpm, while the *black triangles* denote measurements without agitation. *Solid lines* represent model predictions. The fitted parameters were $O_{2,crit}=0.3$ mg/L, $q_{O_2,max}=19$ mg O_2 /g DW·h and $n=2.2$ in the case with agitation, while in the case without agitation the fitted parameter was $q_{O_2,max}/O_{2,s}=0.4$ L/g DW·h 70

Figure 4-7: Oxygen mass transfer under oenological conditions. a Correlation between the oxygen uptake rate and the estimated k_{La} . The *thicker line* represents a linear regression between both variables ($R=0.72$). b Comparison of different absorption curves in microbial culture (*black triangles*, $k_{La}=8.2$ 1/h) and in sterile medium (*black dots*, $k_{La}=16.6$ 1/h). *Solid lines* denote the model predictions. The biomass concentration was 2.9 g DW/L in the case of the medium with oxygen consuming yeast. The estimated oxygen solubilities were 34.2 mg/L in the sterile medium and 33.5 mg/L in the microbial culture 72

Figure 5-1: Schematic representation of the bubble-free oxygenation system	83
Figure 5-2: (A) Effect of the liquid flow rate on $K_L \cdot a$ at various temperatures: 20°C (x), 24°C (•), 28°C (). (B) Effect of the temperature on C^* with pure oxygen. (C) Effect of the liquid flow rate on the OTR_m at various temperatures: 20°C (x), 24°C (•), 28°C ().	88
Figure 5-3: Evolution of the OTR_m (histogram; □) and Reynolds number (line plot; •) with liquid flow rate for buffer solution at 20°C.	88
Figure 5-4: “Wilson plot” for oxygen adsorption and liquid flow inside the silicone tube, at three temperatures: 20°C (●), 24°C (*), 28°C (Δ).	90
Figure 5-5: Analysis of mass-transfer resistances (-) for oxygen absorption in liquid flowing inside the silicone tube at three temperatures: 20°C (●), 24°C (*), 28°C (Δ).	91
Figure 5-6: $K_L \cdot a$ (histogram; □), C^* (line plot; •) (A) and OTR_m (B) measured in model solution at 28°C and at a liquid flow rate of 337 mL/min. The concentration at saturation was measured using the same solutions.	92

TABLE INDEX

Table 3-1: Experimental data sets used in this work.....	27
Table 3-2: Oxygen incorporated in fermenting grape musts using different pump-over modes.	34
Table 4-1: Fitted parameters of the oxygen solubility model for temperatures ranging between 15 and 37°C.....	63
Table 4-2: Validation of the oxygen solubility model at 25°C.....	64
Table 4-3: Comparison of the different models	65
Table 5-1: Effect of gas flow rate, partial pressure of oxygen, and liquid flow rate on gas/liquid transfer. Experiments were carried out at 20°C with saline solution (containing 6 g/L of citric acid and 6 g/L of malic acid, adjusted to pH 3.3). the data reported are means with 95% confidence intervals.	87
Table 5-2: Effect of the medium composition on the $K_L \cdot a$ value. The data reported are means with 95% confidence intervals.	92
Table 5-3: Experimental conditions for the oxygen transfer experiments used to determine model coefficients	96
Table 5-4: Values of OTR_m obtained experimentally during Chardonnay fermentation at 28°C.....	98

ABBREVIATION INDEX

a	Interfacial Area per Unit Volume
C	Concentration of Dissolved Oxygen
C*	Oxygen Saturation Concentration
$\frac{dC}{dt}$	Oxygen Accumulation in the Liquid Phase
GC	Gas Chromatography
H	Henry's Constant
$K_L \cdot a$	Volumetric Transfer Coefficient
K_L	Global Transfer Coefficient
NOC	Non-respiratory Oxygen Consumption
OTR	Oxygen Transfer Rate
OTR_m	Maximum Oxygen Transfer Rate
OUR	Oxygen Uptake Rate
p_{O_2}	Oxygen Partial Pressure
$q_c(O_2)$	Specific Oxygen Uptake Rate
ROS	Reactive Oxygen Species
X	Biomass Concentration

PONTIFICIA UNIVERSIDAD CATÓLICA DE CHILE
ESCUELA DE INGENIERÍA

OXYGEN MANAGEMENT DURING ALCOHOLIC FERMENTATION

Thesis submitted to the Office of Research and Graduate Studies in partial fulfillment
of the requirements for the Degree of Doctor in Engineering Sciences by

MARÍA ISABEL MOENNE VARGAS

ABSTRACT

Oxygen additions are a common practice in winemaking, as oxygen has a positive effect in fermentative kinetics, biomass synthesis and improvement of color, structure and flavor in treated wines. However, most oxygen additions are carried out heuristically through pump-over operations solely on a *know-how* basis, which is difficult to manage in terms of the exact quantity of oxygen transferred to the fermenting must. It is important to estimate the amount of oxygen added because very slight additions are not effective and; excessive additions could lead to organoleptic defects, influencing the wine quality drastically. Therefore, oxygen management practices, including knowing the right amount of oxygen to add during winemaking (depending the desired results), the dynamics of oxygen transfer and consumption, and tools for regulating precisely the oxygen additions, are necessary for elaborating optimal quality wines.

The aim of the present study is cover these aspects, providing a better understanding of the oxygenation during alcoholic fermentation at industrial winemaking scale, *i.e.* how oxygen is distributed inside large tanks and how much oxygen is dissolved and biologically consumed. Such studies were performed firstly at industrial scale and, later, brought to the laboratory scale.

In these studies oxygen transfer was performed using two systems: direct oxygen bubbles sparging and through silicone membranes. The latter allows to transfer precise quantities of oxygen to the liquid phase and it could be used to study oxygen management and aroma compounds evolution during fermentation.

Industrial scale studies included the evaluation of different pump-overs modes: closed, open pump over and a pump-over with Venturi (that incorporates air to the circulating must). Results showed that closed pump-overs incorporated negligible amounts of oxygen, while pump-overs with a Venturi injector incorporated the highest dissolved oxygen, *i.e.* almost twice more oxygen than open pump-overs.

Oxygen distribution inside large tanks (40,000 L) was achieved by measuring with oxygen sensor probes at three different levels. Pump-overs resulted in a heterogeneous distribution of oxygen within the fermenting must, with almost 80% of the total oxygen added rapidly consumed at the top of the tank.

Oxygen consumption during industrial winemaking was followed in 5,000 L tanks, measuring on the middle of the tank. When analyzing oxygen dissolution during the maceration and fermentation stages, lower oxygen levels were encountered in the presence of high free SO₂ concentrations and reduced yeasts activity, respectively. Furthermore, the oxygen dissolution kinetics during fermentation was analyzed by estimating the oxygen dissolution rate and a global consumption constant for different fermentation stages. Results showed that the CO₂ has a negative impact on oxygen dissolution and, together with the elevated yeast biological uptake, are the main responsible for the low oxygen dissolution during the tumultuous fermentation. All-scale experiments were performed to better understand the industrial process and the oxygen dissolution.

A model of oxygen kinetics was developed and tested at laboratory scale, using a pore diffuser, under similar conditions of those encountered in oenological fermentations. Results indicated that the fermentation phase, liquid composition, mixing process and carbon dioxide concentration must be considered when performing oxygen addition during oenological fermentations. Nevertheless, oxygen added through the sparger system is difficult to control, making its implementation at industrial scale still complicated. For this reason, a bubble-free oxygenation system was developed and validated, which exhibited high reproducibility. The evaluation of various parameters on the maximum oxygen transfer rate (OTR_m) showed that, for fixed characteristics of the silicone tube and the partial pressure, dissolved CO₂ and

medium composition had negligible effects; and that the parameters with the biggest influence on the OTR_m were the liquid flow rate and the temperature. This information was used to build a mathematical model that allows to calculate the OTR in synthetic media and in real fermentation media. Furthermore, this bubble-free oxygenation system was used to manage precisely oxygen content (quantity and time of oxygen addition) during alcoholic fermentation, and to study the kinetics of relevant higher alcohols and esters produced during alcoholic fermentation by coupling the bubble-free oxygenation system to an on-line GC system (data not shown).

Altogether, the results of this study as well as the tools hereby developed will help developing better oxygen addition policies in wine fermentations on an industrial scale and this work makes a step toward innovative strategies for oxygen management during alcoholic fermentation through bubble-free oxygenation system.

Keywords: Alcoholic fermentation; Winemaking; Oxygen; *Saccharomyces cerevisiae*; Modeling; Bubbleless aeration; Pump-over.

Members of the Doctoral Thesis Committee:

Eduardo Agosin T.

Edmundo Bordeu

Felipe Laurie

Ricardo Perez-Correa

Jean-Marie Sablayrolles

Cristian Vial

Santiago, December, 2013

PONTIFICIA UNIVERSIDAD CATÓLICA DE CHILE
ESCUELA DE INGENIERÍA

MANEJO DEL OXÍGENO DURANTE FERMENTACIONES VÍNICAS

Tesis enviada a la Dirección de Investigación y Postgrado en cumplimiento parcial de los requisitos para el grado de Doctor en Ciencias de la Ingeniería.

MARÍA ISABEL MOENNE VARGAS

RESUMEN

Las adiciones de oxígeno son una práctica común durante el proceso de elaboración del vino, debido a que tienen un efecto positivo en la cinética de fermentación y la síntesis de biomasa, además de contribuir al color, estructura y aroma de los vinos tratados. A pesar de su importancia, la mayoría de las adiciones de oxígeno son realizadas de manera heurística, a través de remontajes basados sólo en el conocimiento de los enólogos, dificultándose así su manejo en términos de las cantidades exactas de oxígeno transferidas al mosto durante la fermentación. Por este motivo, es importante estimar la cantidad de oxígeno adicionado, ya que adiciones insuficientes de oxígeno no son efectivas, mientras que adiciones excesivas podrían generar defectos organolépticos, afectando drásticamente la calidad del vino final. Así, el manejo de la adición de oxígeno es crítica, tanto para determinar la cantidad adecuada de oxígeno a adicionar durante la elaboración del vino (dependiendo de los resultados deseados por el enólogo) o la dinámica de transferencia de oxígeno y su consumo, como para contar con herramientas que permitan regular precisamente las adiciones de oxígeno.

El propósito del presente estudio es cubrir estos aspectos, ampliando el conocimiento de la técnica de oxigenación durante la fermentación alcohólica a nivel industrial, es decir, como el oxígeno se distribuye dentro de los tanques y cuanto oxígeno se disuelve y consume biológicamente al interior de ellos. Estos estudios fueron

realizados primero a escala de industrial y luego llevados a escala de laboratorio (scale down).

La adición de oxígeno fue llevada a cabo mediante dos sistemas distintos: burbujeo directo de oxígeno y difusión de oxígeno a través de membranas de silicona. Estas últimas permiten transferir cantidades precisas de oxígeno a la fase líquida, por lo que dicho sistema se puede utilizar para estudiar políticas de adición de oxígeno y la evolución de compuestos aromáticos en fermentación.

A nivel industrial se contrastaron diferentes modos de operación de remontajes. Los resultados indican que los remontajes cerrados incorporan cantidades despreciables de oxígeno, mientras que los remontajes con venturi incorporan la mayor cantidad de oxígeno, aproximadamente 2 veces más que los remontajes abiertos con tina.

Al observar la distribución de oxígeno, en 3 puntos al interior de los tanques de fermentación (40,000L), se obtuvo una distribución heterogénea del oxígeno con relación a la altura del tanque; aproximadamente el 80% del total de oxígeno adicionado sólo alcanzó el nivel superior del tanque.

Para estudiar el consumo de oxígeno durante la elaboración industrial de vino, se emplearon tanques de 5,000L, llevándose a cabo las mediciones en, aproximadamente, el punto medio del tanque. Al analizar la disolución de oxígeno durante la maceración y fermentación, se encontraron bajos niveles de oxígeno en presencia de altas concentraciones de SO_2 libre y baja actividad de levaduras, respectivamente. Adicionalmente, se estudió la cinética de disolución de oxígeno durante fermentación, mediante la estimación de la tasa de disolución de oxígeno y la constante de consumo global de oxígeno para diferentes etapas de fermentación.

Los resultados sugieren que el CO_2 tiene un impacto negativo en la disolución de oxígeno y que, junto con el elevado consumo de oxígeno por parte de las levaduras, son los principales responsables de la baja disolución de oxígeno durante la fermentación tumultuosa.

Posteriormente, estudios de laboratorio permitieron desarrollar y probar un modelo cinético para el oxígeno, bajo condiciones similares a las de fermentaciones industriales y empleando un difusor. Los resultados indican que la fase de

fermentación, la composición del líquido, el mezclado y la concentración de CO₂ deben ser considerados cuando se realizan adiciones de oxígeno en fermentaciones enológicas. Sin embargo, se debe considerar que el oxígeno adicionado mediante burbujeo es difícil de controlar, haciendo compleja su implementación a nivel industrial. Por esta razón, un sistema de adición de oxígeno sin burbujas fue desarrollado y validado, sistema que mostró una alta reproducibilidad.

El estudio del sistema de adición de oxígeno por difusión, consideró la evaluación del efecto de diferentes parámetros sobre la máxima transferencia de oxígeno (OTR_m). Una vez fijadas las características del tubo de silicona y la presión parcial, empleadas para dicho estudio, los efectos del CO₂ disuelto y la composición del medio son despreciables; por consiguiente, los parámetros con la mayor influencia en la OTR_m son el caudal del líquido y la temperatura. Estos parámetros son los que se emplearon para construir un modelo matemático que permite calcular la OTR tanto en medio sintético como en medio real de fermentación. Además, el sistema de oxigenación sin burbujas puede ser utilizado para el manejo preciso del oxígeno (cantidad y tiempo de la adición de oxígeno) durante la fermentación alcohólica; o para estudiar la cinética de producción de aromas relevantes como alcoholes superiores y ésteres producidos durante fermentación, acoplado para esto el sistema de adición de oxígeno sin burbujas a un sistema GC en línea.

En conclusión, los resultados de este estudio, así como las herramientas desarrolladas ayudarán a desarrollar mejores políticas de adición de oxígeno a escala industrial y este trabajo constituye un paso hacia el uso de estrategias innovadoras para el manejo del oxígeno durante la fermentación alcohólica a través del uso de un sistema de oxigenación sin burbujas.

Palabras Claves: Fermentación alcohólica; Elaboración del vino; Oxígeno; *Saccharomyces cerevisiae*; Modelamiento; Aireación sin burbujas; Remontajes.

Miembros de la Comisión de Tesis Doctoral:

Eduardo Agosin T.

Edmundo Bordeu

Felipe Laurie

Ricardo Perez-Correa

Jean-Marie Sablayrolles

Cristian Vial

Santiago, Diciembre, 2013

1. BRIEF INTRODUCTION

1.1 Motivation

Chile is the fifth wine exporter worldwide (OIV, 2012). To maintain this position in a changing market, the wine industry requires to research continuously to improve the quality of wine, and thus increase our competitive advantage. In this context, oxygen is a relevant operational variable to tackle, because it is critical to fermentative kinetics and final color, structure and flavor of wines. To promote the beneficial effects of oxygen exposure during winemaking it is essential to understand the overall process of oxygen addition at industrial level and their effect in aroma compounds at laboratory scale. This knowledge will be important for winemaking industry, because nowadays the industrial process is mostly performed heuristically.

The present research work is a contribution to the study the addition of oxygen in fermentations, and the importance of taking into account the way oxygen is added to reach the desired oxygen level. Oxygen gradient inside a fermentation tank and the dissolution of oxygen during maceration and fermentation were also considered, with the objective to know the oxygen distribution patterns.

1.2 Objectives

The main objective of this thesis was to quantify the amount of oxygen added during winemaking through the traditional processes like pump-overs; how oxygen is distributed inside large tanks after its additions and how much oxygen is dissolved and biologically consumed. Based on that, studies of oxygen transfer were carrying out at laboratory scale (scale down). Scale down experiments were performed using a pore diffuser and a silicone membranes. The first allows to model oxygen transfer rate in similar conditions of those encountered in enological fermentations and the second allows to transfer precise quantities of oxygen to the liquid phase.

For this purpose, the specific objectives were the following:

At industrial scale:

- a.- Evaluation of oxygen addition with different pump-over modes (closed, open, and with Venturi injector).
- b.- Characterization of oxygen vertical distribution inside industrial tanks using open pump-overs.
- c.- Characterization of oxygen dissolution and consumption during red grape must maceration and fermentation stages in 5,000L open tanks.

At laboratory scale:

- d.- Development, calibration and validation of an oxygen kinetic model, under similar conditions of those encountered in oenological fermentations at an industrial scale.
- e.- Develop of a system for the estimation of oxygen solubility in defined medium and must.
- f.- Development and validation of a bubble-free oxygenation system at laboratory scale.

1.3 Approach

In this work, accurate measurement of oxygen was crucial. For this purpose, an optical oxygen sensor that does not consume oxygen was used (Dieval et al., 2010). This allowed to follow *in-line* and *on-line* the oxygen evolution using either a sensor dot glued inside a sight glass or dipping probes immersed inside tanks. The high versatility of this oxygen device to carry out these measurements in both industrial and laboratory scale, using the same equipment in all experiments.

1.3.1 Oxygen measurements at industrial scale

Oxygen addition with different pump-overs systems (open, closed and with venturi) was followed during the tumultuous and stationary fermentation stages. Seven different

wine varieties were studied: Cabernet Sauvignon, Carménère, Merlot, Petit verdot, Cabernet franc, Carignan and Alicante Henri Bouschet (Tintorera).

The concentration gradients of dissolved oxygen within industrial wine tanks during open pump-overs were measured at three different heights inside a 40,000-liter industrial tank, using fermenting Cabernet Sauvignon and Carménère.

Finally, oxygen dissolution and consumption kinetics of Pinot noir, Carménère and Cabernet Sauvignon enological fermentations were followed in closed and open pumping-over modes during carbonic maceration and fermentation stages. Dissolved oxygen concentration and temperature were determined inside the tanks at 1.3 m from the top (approx. the geometric center of the tank) during the whole fermentation.

All these results are presented in Chapter 3: “Oxygen incorporation and dissolution during industrial-scale red wine fermentations”.

1.3.2 Studies at laboratory scale

Research studies under tightly controlled conditions at laboratory scale were also performed to reproduce the industrial conditions of oxygen dissolution when an oxygen pulse is applied.

Culture conditions and oxygen additions encountered in industrial fermentations were simulated with a sparger system. Batch fermentations were carried out with synthetic medium MS300 to ensure reproducibility between experiments. The agitation effect on the oxygen consumption kinetics was studied and additionally, a model to measure the oxygen solubility was developed.

These results constitute the content of Chapter 4: “Modeling oxygen dissolution and biological uptake during pulse oxygen additions in oenological fermentations”.

Finally, we developed and validated a bubble-free oxygenation system to allow for fine-tuning of oxygen transfer rate to the liquid phase during alcoholic fermentation. This system allows air or oxygen addition through an external silicon contactor adapted from the system of Blateyron et al. (1998).

Six different variables were studied, *i.e.* the liquid flow rate inside the silicone tube, the temperature of the liquid, the presence of dissolved CO₂, the nature of the gas used for

oxygenation, the gas flow rate and the composition of the medium. Additionally, a model that predicts the oxygen transfer rate was developed.

The results of these studies are illustrated in Chapter 5: “Control of Bubble-free Oxygenation with Silicone Tubing during Alcoholic Fermentation”

2. GENERAL INTRODUCTION

2.1 Red wine making

Yeasts, particularly *Saccharomyces cerevisiae*, are the main microorganisms that carry out oenological fermentation. They have the ability to produce essentially ethanol, CO₂ and glycerol from sugars (*i.e.* glucose and fructose). Additionally, volatile metabolites like higher alcohols, esters, carbonyls and sulfur compounds are also produced during fermentation (Suomalainen and Lehtonen, 1978; Swiegers et al., 2005).

The process of red wine making considers the following steps (Ribéreau-Gayon et al., 2000):

- i) Destemming and crushing. These optional steps allow the separation of the berries from the stems and then break the berry skin to release the pulp and the juice. The resulting must (pulp, skin and seed) is transferred to a tank and it is sulfited. Generally, premium wine grapes are slightly crushed.
- ii) Maceration. Maceration is an optional step (mainly used in premium wines) and its purpose is to improve the extraction of pigments, phenolic compounds, aroma precursors, etc. in absence of ethanol. The maceration process can take several days depending on the extraction of desirable substances. There are two types of maceration: cool-temperature extraction (enhancing aromatic profile) and high-temperature extraction (enhancing phenolic extraction).
Pump-overs are performed during maceration, with the objective to improve the extraction of compounds from the pomace, homogenization and avoidance of the growth of aerobic microorganisms on the surface of pomace.

iii) Fermentation. The temperature of the tank is controlled between 25 and 30°C, temperature at which yeast cells convert the grape must sugars mainly into ethanol, CO₂ and glycerol. The bubbles of CO₂ produced during fermentation rise toward the surface of the tank, forming the cap of pomace. During fermentation the cap is regularly soaked with recirculating fermenting must to improve the extraction of its constituents, aerates the must, maintains the temperature and avoids spoilage of aerobic microorganism (Boulton et al., 1996).

Different processes can be used to oxygen additions: a) Pump-overs, with or without aeration: the fermenting must is pumped from the bottom of the tank and over onto the cap; b) Delestage or rack-and-return: in this case, the liquid (a third to a half of the tank) is drain to another tank and reintroduced by the top of the tank, allowing the immersion of the entire pomace and dissolving a higher quantity of oxygen; c) Direct sparging, by injection of oxygen or air: this technique could replace the traditional pump-overs; d) Cap immersion: hydraulic pistons control the immersion of the cap, enhancing the extraction and allowing oxygen addition.

iv) Malolactic fermentation. After fermentation, wine is separated from the pomace, and the malolactic bacteria, mainly heterofermentative *Oenococcus*, change the malic acid into lactic acid softening the wine and adding complexity (through diacetyl compound). Low temperatures and SO₂ inhibit these bacteria; hence, winemakers can arrest the onset of malolactic fermentation controlling these parameters.

v) Oak aging. At this optional stage the wine can be aged in different types of oak. French and American oak barrels are the most used. This operation allows the micro-oxygenation of the wine and gives wood character to wine, developing color, aroma and flavor.

vi) Clarification and stabilization. These steps eliminate particles in suspension that produce turbidity and prevent the formation of sediment in the bottle.

During red wine making, oxygen is incorporated by different techniques: pump-overs, sparging, rack-and-return, etc. Then, it is necessary to study the benefits of oxygen in winemaking to understand why this addition is carried out and why is so important to control it.

2.2 Oxygen in wine making

Wine fermentation is an anaerobic bioprocess. Under this condition, yeast cells are able to incorporate grape-derived sterols, promoting its initial growth and fermentative activity by substituting ergosterol in the cell membranes. However, if the absence of oxygen is maintained, the limitation of anaerobic growth factors and the rapid accumulation of phytosterols modify the physicochemical properties of the yeast cell membrane, limiting cell growth due to the difficulty to maintain membrane integrity and, therefore, yeast viability (Andreasen and Stier, 1954, 1953; Fornairon-Bonnefond et al., 2002; Salmon, 2006). Hence, at industrial level, the absence of oxygen can lead to stuck or sluggish fermentations, which are a major problem in the wine industry (Bardi et al., 1999; Salmon, 2006). Appropriate oxygen addition is therefore one of the keys to improve fermentation kinetics and biomass formation (Rosenfeld et al., 2003a). In fact, in anaerobic condition, yeast requires between 5 to 20 mg/L of oxygen to optimal growth and strong cell viability through fermentation (du Toit et al., 2006; Julien et al., 2000; Rosenfeld et al., 2003b; Sablayrolles and Barre, 1986). Particularly, the major effect of oxygen is achieved when the oxygen is added at the end of the yeast growth phase (Sablayrolles et al., 1996), where yeast cells have diluted their own reserves of sterols, the CO₂ production rate is the highest, and oxygen dissolution rate is at its minimum (Saa et al., 2013). Additionally, if oxygen incorporation is coupled with the addition of assimilable nitrogen, the risk of stuck fermentation significantly decreases (Blateyron and Sablayrolles, 2001; du Toit et al., 2006; Sablayrolles et al., 1996).

The effect of oxygen in sterol synthesis is due to the yeast have a high capacity to use oxygen as a substrate, but only 15 to 75% of oxygen is employed to sterol synthesis

after it is added (Rosenfeld et al., 2003a, 2002; Salmon et al., 1998). Thus, Rosenfeld et al. (2002) proposed that, if yeast is exposed to more oxygen than needed for sterol synthesis, the excess of oxygen will be consumed by **Non-respiratory Oxygen Consumption (NOC)** pathways. The issue of high oxygen dissolution is that the NOC pathways are associated with the production of **Reactive Oxygen Species (ROS)**, like H_2O_2 and O_2^- (Rosenfeld et al., 2002), leading to oxidative stress *i.e.* lipid peroxidation, oxidation of DNA and proteins.

During fermentation, yeast cells release volatile compounds from non-volatile precursors (varietal aromas) and synthesize volatile compounds, as well (fermentative aromas). These aromas influence the sensorial quality of wine, playing a key role for consumer choices. Accordingly, oxygen is not only related to sterol synthesis but, also it is beneficial to aroma diversity, astringency and color stability (Pérez-Magariño et al., 2007) (du Toit et al., 2006; Pérez-Magariño et al., 2007). A basic diagrammatic representation of the principal flavour pathways in *S. cerevisiae* is shown in Figure 2-1. Fariña et al. (2012) showed that the production of alcohols and isoacids (β -phenylethyl alcohol; 2-methyl 1-propanol; 2-methyl butanol; acetaldehyde; isovaleric and isobutanoic acids) decreased under low oxygen conditions (reductive medium); meanwhile, a high percentage of esters and fatty acids increased under the same condition (isobutyl acetate; isoamyl acetate; ethyl butanoate; ethyl hexanoate; ethyl decanoate and ethyl acetate). Other studies have also reported on the effect of oxygen in aroma compounds, showing that limited quantities of oxygen increase the higher alcohols concentration and alter the proportion of acetate to ethyl esters (Rojas et al., 2001; Saerens et al., 2010; Varela et al., 2012). Nevertheless, higher oxygen doses (*i.e.* 50mg/L) could be detrimental, resulting in color degradation, off-flavors production and wine oxidation (Adoua et al., 2010; Sablayrolles, 2009).

Considering that aroma compounds are the metabolic by-products that could be considered like quality indicators, the major advance for improving wine quality are focused in these compounds (Figure 2-2). Hence, the amount and time of oxygen addition during fermentation are essential to ensure an optimal wine quality, because of its influence on the metabolism of yeast and, consequently on aroma production.

2.3.1 Oxygenation by gas bubbles

This section, describes quantitatively how oxygen reach yeast cells from air bubbles. Oxygen can be added during fermentation either by: i) racking with aeration; ii) pumping over the must with a fritted stainless steel coupler or iii) pumping over the must after spraying into an *in-line* Venturi (Boulton et al., 1996).

During all of these processes, the oxygen from the air bubbles is transferred to the cell (Garcia-Ochoa et al., 2010; Nielsen et al., 2003), through the following steps (Figure 2-3):

1. Oxygen diffusion from the interior of the bubble to the gas-liquid interface.
2. Oxygen transport across the gas-liquid interface.
3. Oxygen diffusion through the region surrounding the gas bubble.
4. Oxygen transport across the bulk liquid.
5. Oxygen diffusion through the region adjacent to the cells.
6. Oxygen transport across the liquid-aggregate interface.
7. Oxygen diffusive transport.
8. Oxygen transport across the cell membrane.
9. Oxygen transport from the cell envelope to the site where the reactions are carrying out.

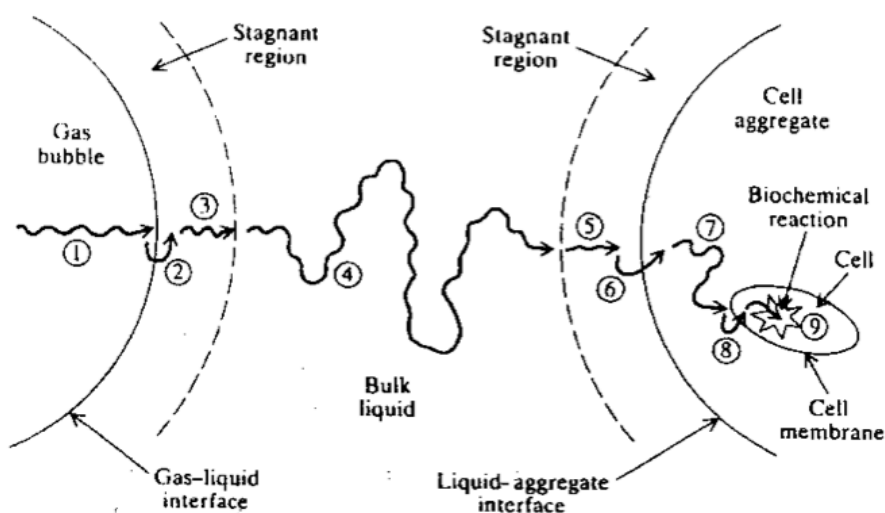


Figure 2-3: Steps of oxygen transfer from a gas bubble to the individual cell (Nielsen et al., 2003).

From all these steps, the major limitation to oxygen transfer is the liquid film adjacent to the gas bubble (Nielsen et al., 2003).

The efficiency of the oxygen transfer rate to the liquid phase depends on the volumetric transfer coefficient represented by $K_L \cdot a$, where “ K_L ” is the global transfer coefficient and “ a ” is the interfacial area per unit volume.

The gas–liquid mass transfer is generally modeled by the two-film theory introduced by Whitman (Lewis and Whitman, 1924; Whitman, 1923). This theory considers that the volumetric mass transfer rate of oxygen can be described as the product of $K_L \cdot a$, and a driving force in the liquid phase given by the difference between oxygen saturation concentration (C^*) and the actual concentration of dissolved oxygen (C):

$$\frac{dC}{dt} = K_L \cdot a \cdot (C^* - C) \quad (2.1)$$

Where $\frac{dC}{dt}$ is the oxygen accumulation in the liquid phase.

Under fermentation, yeast cells consume the oxygen that is incorporated during aeration. Therefore, it is necessary to add the oxygen uptake rate to Eq. 2.1. Additionally, the following assumptions are considered in the equations: the chemical oxygen consumption is negligible compared to biological consumption; the oxygen bubble distribution is homogeneous in the bioreactor; the oxygen dissolved is immediately consumed by yeast (Garcia-Ochoa et al., 2010); and the resistance of the liquid film surrounding the bubbles controls the oxygen transfer rate (Garcia-Ochoa and Gomez, 2009; Lewis and Whitman, 1924; Nielsen et al., 2003)).

The equation for the dissolved oxygen in the liquid phase can be worded as follows:

$$\frac{dC}{dt} = K_L \cdot a \cdot (C^* - C) - q_C(O_2) \cdot X \quad (2.2)$$

Where $q_C(O_2)$ is the specific **Oxygen Uptake Rate (OUR)**, X is the biomass concentration and $K_L \cdot a \cdot (C^* - C)$ is the **Oxygen Transfer Rate (OTR)**.

Moreover, using Henry’s law the oxygen concentration at saturation is given by:

$$C^* = \frac{p_{O_2}}{H} \quad (2.3)$$

Where p_{O_2} is the oxygen partial pressure in the gas phase and H is the Henry's constant. The $K_L \cdot a$ can be calculated using conventional kinetic saturation experiments. This method is adequate for non-biological oxygen consumption and it measures the rate of oxygen increase in the liquid medium. Basically, nitrogen or argon gas is added by bubbling until oxygen drops near 0 mg/L. Then pure oxygen or air is fed to the system, and the dynamic change in the concentration of dissolved oxygen is determined (Galaction et al., 2004; Garcia-Ochoa and Gomez, 2009; Özbek and Gayik, 2001; Van't Riet, 1979).

In the case of solutions with growing microorganisms, the dynamic method based on the technique described by Bandyopadhyay et al. (1967) is preferred. This method determines in the same experiment the $K_L \cdot a$ and OUR by first stopping the airflow for a certain time period, and then, turning it back on under the same operational conditions (Figure 2-4). Nevertheless, in the case of alcoholic fermentation, *i.e.* an anaerobic process, there are no reported techniques for the determination of $K_L \cdot a$ and OUR, without affecting the normal course of fermentation.

Different parameters can influence the OTR, for example when sparger systems are used, the OTR is affected by the pore size of the gas sparger, *i.e.* if the same gas flow rate is employed, a 100 μ m sparger gives bigger bubbles than a 40 μ m sparger, decreasing the oxygen transfer (Chiciuc et al., 2010; Kazakis et al., 2008). When the gas flow rate increases, more and smaller bubbles are generated. This increases the interfacial area and therefore the $K_L \cdot a$ value. The temperature has a positive effect on $K_L \cdot a$ parameter, because the K_L depends on the diffusion coefficient. Indeed, the viscosity of the liquid decreases when the temperature increases which leads to increases of diffusion coefficient (Devatine et al., 2007; Jamnongwong et al., 2010; Kazakis et al., 2008). However, the oxygen concentration at saturation decreases with temperature, so, only a small increase of oxygen transfer rate is achieved with temperature. Additionally, viscosity increases with increasing sugar concentration, which decreases the $K_L \cdot a$ value, it is expected that the oxygen transfer will be favored

at the end of fermentation, when ethanol is present (Chiciuc et al., 2010). During fermentation yeast cells saturate the liquid with CO_2 , and the presence of CO_2 in the medium desorbs and dilutes the oxygen, decreasing the OTR. In fact, when the concentration of CO_2 is 1.4 g/L and C^* is 41.1 mg/L (achieved with oxygen), the oxygen partial pressure in the leaving gas is divided by 4, showing the effect of the CO_2 input in the oxygen bubbles (Devatine et al., 2007).

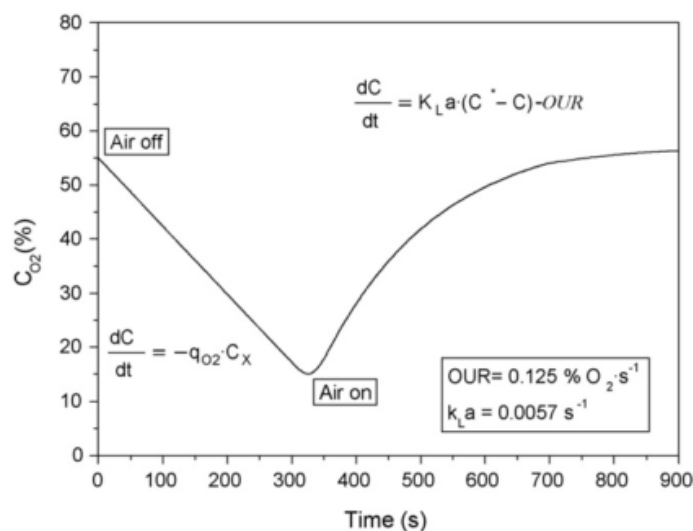


Figure 2-4: Simulation of a simultaneous measurement of OUR and $K_L \cdot a$ during fermentation, employing the dynamic method (Garcia-Ochoa et al., 2010).

On the other hand, the oxygen saturation concentration (C^*) depends on several factors, such as oxygen partial pressure in the gas phase (p_{O_2}), pH, media composition, and temperature (Chiciuc et al., 2010; du Toit, 2006; Singleton, 1987; van Stroe-Biezen et al., 1993). In this way, the oxygen concentration in wine saturated with air (at atmospheric pressure and room temperature) is approximately 8 mg/L or 6 mL/L (Singleton, 1987).

During red winemaking, the exposure to oxygen is a normal process, but how much oxygen dissolves into the liquid is variable, depending on the technological step (*i.e.* racking, pumping, etc). The traditional and currently widely employed way to add oxygen is through open pump-overs. In this technique, the fermenting must extracted from the racking valve of the tank is splashed over a vat connected to a pump that

drives the aerated juice to the top of the tank, adding about 2mg/L of oxygen (du Toit et al., 2006; Ribéreau-Gayon et al., 2000). Nevertheless, if no oxygen is desired a closed pump-over could be implemented. In closed pump-overs, the fermenting must is pumped out from the bottom of the tank and re-incorporated over the cap by means of flexible or fixed tubing (*i.e.* almost no air contact). Otherwise, oxygen additions can be achieved with an *in-line* Venturi valve that incorporate air to the circulating must. Other operations that add oxygen to wine are: transfer from tank to tank (up to 6mg/L); racking (3-5 mg/L); filtration (4-7 mg/L) and bottling (0.5-3 mg/L) (du Toit et al., 2006). An important fact to consider is pumps have no effect in the oxygen enrichment of the liquid medium. The average oxygen addition by these devices is from 0.1 to 0.2 mg/L, mainly at the beginning of the procedure (Castellari et al., 2004; Vidal et al., 2001).

Despite the significance of oxygen addition during fermentation, especially for the quality of final wine, there are only isolated reports about this topic (Bisson and Butzke, 2000; Bosso et al., 2009; Vidal and Aagaard, 2008). Also, the techniques to add oxygen during winemaking (*i.e.* sparging, pump-overs, racking) are not appropriate for ensuring a tight control the oxygen addition, due to the effect of medium composition (*i.e.* glucose, ethanol, fructose, CO₂, essentially) in the OTR during fermentation. Therefore, it would be interesting to carry out studies about other ways to add oxygen, for instance gas transfer using membranes.

2.3.2 Bubble-free oxygenation of media by membrane

Oxygenation by gas sparging is not precise enough. Moreover, oxygen could be lost due to the stripping effect of CO₂ and the addition is not constant because the liquid medium changes during fermentation (Grootjen et al., 1990; Rennie and Wilson, 1975). An alternative way to add a constant, precise and measurable quantity of oxygen during fermentation is the bubble-free oxygenation through membrane aeration with open-pore membranes or diffusion membranes (Blateyron et al., 1998; Côté, 1989; Grootjen et al., 1990; Haukeli and Lie, 1971; Rennie and Wilson, 1975). Another advantage of

the bubble-free system compared with the sparging systems is that the dissolved CO_2 does not affect the efficiency of the oxygen transfer rate (Devatine et al., 2007).

Gas permeable membranes can be used with circulating gas or liquid inside the tubing (Côté, 1989; Hirasu et al., 1991; Moulin et al., 1996; Robb, 1965). The more utilized membranes are the non-porous and microporous membranes; in the first case, the oxygen is dissolved into the membrane from the gas phase and, subsequently, the oxygen diffuses to the liquid medium (Mokrani, 2000; Moulin et al., 1996; Yasuda and Lamaze, 1972). An example of non-porous membrane is the silicone membrane, which has the advantage of working at a high gas pressure without bubbles formation (Ahmed and Semmens, 1992; Moulin et al., 1996). In the case of microporous membranes, the oxygen is transferred by diffusion through the membrane rather than dissolving into the membrane, because the gas and the liquid medium are in direct contact. To avoid bubbles formation, the gas should be operated at low pressures (Ahmed and Semmens, 1992; Schneider et al., 1995).

Gas transfer (air or oxygen) by membranes could be explained using a resistance model (Figure 2-5). Here, the overall resistance to mass-transfer is the result of three separate resistances in series: the gas film resistance, the membrane resistance and the liquid film resistance (Côté, 1989; Schneider et al., 1995).

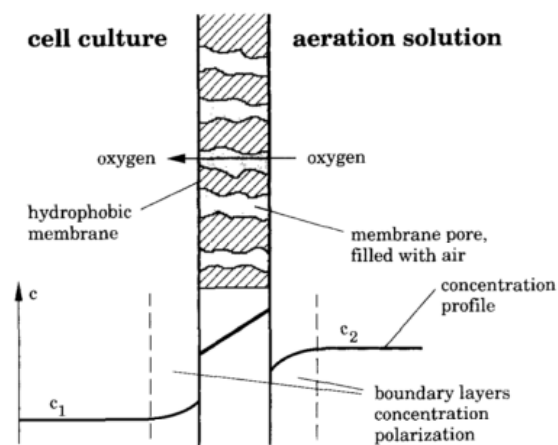


Figure 2-5: Schematic representation of mass transfer model for membrane oxygenation. The bulk oxygen concentrations are c_1 and c_2 (Schneider et al., 1995).

In the model, the gas film resistance can be considered negligible. Meanwhile, the membrane resistance depends on the permeability of oxygen and on the thickness of the membrane. So, very permeable and thicker membranes will have a membrane resistance smaller than the liquid film resistance. Scilicet, to reduce the mass transfer resistance it is necessary to reduce the liquid film resistance (Côté, 1989; Yang and Cussler, 1986).

The main parameters affecting the oxygen transfer through the membranes are: i) the oxygen concentration in the gas phase. If pure oxygen is employed, the driving force enhances the oxygen transfer rate; ii) the hydrodynamic conditions of the liquid phase. The resistance of liquid film is sensitive to the hydraulic conditions, decreasing when the Reynolds number increases and thus improving oxygen transfer; iii) the solubility of oxygen in the membrane. If the oxygen diffusion through the membrane is limited, the oxygen transfer will be also reduced due to the increase of membrane resistance; iv) the exchange area of the membrane. A large contact surface area, the transfer of oxygen is higher (Ahmed and Semmens, 1992; Côté, 1989; Hirasu et al., 1991; Schneider et al., 1995; Yasuda and Lamaze, 1972).

Notwithstanding, the significance of oxygen management during winemaking, by measuring the efficiency of oxygen transfer rate and the precise quantities of oxygen to transfer during all the alcoholic fermentation process have not been extensively studied.

2.3.3 Techniques for Oxygen Measurement

Most of the systems available to quantify dissolved oxygen are based on the Clark's electrode. These systems depend on the electrochemical-reduction of oxygen, and therefore have relatively long response times and consume oxygen while performing the measurement. For precise measurements, they require a setting in which the fluid flows through the sensor, thus complicating the measurement (Fernández-Sánchez et al., 2007; Nevares and del Alamo, 2008). Instead, recently developed optical sensors, based on luminescence, have been proposed as an alternative to solve these problems (Choi and Xiao, 1999; Fernández-Sánchez et al., 2007; Ogurtsov and Papkovsky,

2006). The measuring principle of these sensors is based on the fact that different concentrations of oxygen, reacting with an optical sensor, cause different degrees of luminescence decay when they are excited by a light (light emitting diode, laser, others) (Choi and Xiao, 1999; Nevares and del Alamo, 2008). Due to the advantages of the latter technique, this could be instrumental for following, and then, managing oxygen evolution during the winemaking process.

REFERENCES

- Adoua, R., Mietton-Peuchot, M., Milisic, V., 2010. Modelling of oxygen transfer in wines. *Chemical Engineering Science* 65, 5455–5463.
- Ahmed, T., Semmens, M.J., 1992. Use of sealed end hollow fibers for bubbleless membrane aeration: experimental studies. *Journal of Membrane Science* 69, 1–10.
- Andreasen, A., Stier, T., 1953. Anaerobic nutrition of *Saccharomyces cerevisiae* I. Ergosterol requirement for growth in a defined medium. *J. Cell. Comp. Physiol.* 41, 23–36.
- Andreasen, A., Stier, T., 1954. Anaerobic nutrition of *Saccharomyces cerevisiae* II. Unsaturated fatty acid requirement for growth in a defined medium. *J. Cell. Comp. Physiol.* 43, 271–281.
- Bandyopadhyay, B., Humphrey, A.E., Taguchi, H., 1967. Dynamic measurement of the volumetric oxygen transfer coefficient in fermentation systems. *Biotechnology and bioengineering* 9, 533–544.
- Bardi, L., Cocito, C., Marzona, M., 1999. *Saccharomyces cerevisiae* cell fatty acid composition and release during fermentation without aeration and in absence of exogenous lipids. *International journal of food microbiology* 47, 133–40.
- Bisson, L., Butzke, C., 2000. Diagnosis and Rectification of Stuck and Sluggish Fermentations. *Am. J. Enol. Vitic.*, 51, 168–177.
- Blateyron, L., Aguera, E., Dubois, C., Gerland, C., Sablayrolles, J.-M., 1998. Control of oxygen additions during alcoholic fermentations. *Vitic. Enol. Sci.* 53, 131–135.
- Blateyron, L., Sablayrolles, J.M., 2001. Stuck and slow fermentations in enology: statistical study of causes and effectiveness of combined additions of oxygen and diammonium phosphate. *Journal of bioscience and bioengineering*.
- Bosso, A., Guaita, M., Panero, L., Borsa, D., Follis, R., 2009. Influence of Two Winemaking Techniques on Polyphenolic Composition and Color of Wines. *Am. J. Enol. Vitic.* 60, 379–385.
- Boulton, R., Singleton, V., Bisson, L., Kunkee, R., 1996. Principles and practices of winemaking. Chapman and Hall.

- Castellari, M., Simonato, B., Tornielli, G.B., Spinelli, P., Ferrarini, R., 2004. Effects of different enological treatments on dissolved oxygen in wines. *Italian journal of food science* 16, 387–396.
- Chiciuc, I., Farines, V., Mietton-Peuchot, M., Devatine, A., 2010. Effect of Wine Properties and Operating Mode upon Mass Transfer in Micro-Oxygenation. *International Journal of Food Engineering* 6.
- Choi, M.M.F., Xiao, D., 1999. Linear calibration function of luminescence quenching-based optical sensor for trace oxygen analysis†. *The Analyst* 124, 695–698.
- Côté, P., 1989. Bubble-free aeration using membranes: Mass transfer analysis. *Journal of Membrane Science* 47, 91–106.
- Devatine, A., Chiciuc, I., Poupot, C., Mietton-Peuchot, M., 2007. Micro-oxygenation of wine in presence of dissolved carbon dioxide. *Chemical Engineering Science* 62, 4579–4588.
- Dieval, J.B., Aagaard, O., Vidal, S., 2010. Non-invasive measurements of total consumed oxygen in bottled wines, in: *Innovations in Grape and Wine Analyses*. Stuttgart.
- Du Toit, W.J., 2006. The effect of oxygen on the composition and microbiology of red wine. Stellenbosch University.
- Du Toit, W.J., Marais, J., Pretorius, I.S., du Toit, M., 2006. Oxygen in Must and Wine : A review. *S. Afr. enol. Vitic.* 27, 76–94.
- Fariña, L., Medina, K., Urruty, M., Boido, E., Dellacassa, E., Carrau, F., 2012. Redox effect on volatile compound formation in wine during fermentation by *Saccharomyces cerevisiae*. *Food chemistry* 134, 933–9.
- Fernández-Sánchez, J.F., Roth, T., Cannas, R., Nazeeruddin, M.K., Spichiger, S., Graetzel, M., Spichiger-Keller, U.E., 2007. Novel oxygen sensitive complexes for optical oxygen sensing. *Talanta* 71, 242–250.
- Fornairon-Bonnefond, C., Demaretz, V., Rosenfeld, E., Salmon, J.-M., 2002. Oxygen addition and sterol synthesis in *Saccharomyces cerevisiae* during enological fermentation. *Journal of bioscience and bioengineering* 93, 176–82.

- Galaction, a.-I., Cascaval, D., Oniscu, C., Turnea, M., 2004. Prediction of oxygen mass transfer coefficients in stirred bioreactors for bacteria, yeasts and fungus broths. *Biochemical Engineering Journal* 20, 85–94.
- Garcia-Ochoa, F., Gomez, E., 2009. Bioreactor scale-up and oxygen transfer rate in microbial processes: an overview. *Biotechnology advances* 27, 153–76.
- Garcia-Ochoa, F., Gomez, E., Santos, V.E., Merchuk, J.C., 2010. Oxygen uptake rate in microbial processes: An overview. *Biochemical Engineering Journal* 49, 289–307.
- Grootjen, D., van der Lans, R., Luyben, K., 1990. Controlled addition of small amounts of oxygen with membranes. *Biotechnology Techniques* 4, 149–154.
- Haukeli, A., Lie, S., 1971. Controlled Supply of Trace Amounts of Oxygen in Laboratory Scale Fermentations. *Biotechnology and bioengineering* XIII, 619–628.
- Hirasa, O., Ichijo, H., Yamauchi, A., 1991. Oxygen transfer from silicone hollow fiber membrane to water. *Journal of Fermentation and Bioengineering* 71, 206–207.
- Jamnongwong, M., Loubiere, K., Dietrich, N., Hébrard, G., 2010. Experimental study of oxygen diffusion coefficients in clean water containing salt, glucose or surfactant: Consequences on the liquid-side mass transfer coefficients. *Chemical Engineering Journal* 165, 758–768.
- Julien, A., Roustan, J., Dulau, L., Sablayrolles, J., 2000. Comparison of Nitrogen and Oxygen Demands of Enological Yeasts : Technological Consequences 51, 215–222.
- Kazakis, N. a., Mouza, a. a., Paras, S.V., 2008. Experimental study of bubble formation at metal porous spargers: Effect of liquid properties and sparger characteristics on the initial bubble size distribution. *Chemical Engineering Journal* 137, 265–281.
- Lewis, W.K., Whitman, W.G., 1924. Principles of gas absorption. *Industrial and Engineering Chemistry* 16, 1215–1220.
- Mokrani, T., 2000. Transport of gases across membranes. Cape peninsula university of technology.

- Moulin, P., Rouch, J.C., Serra, C., Clifton, M.J., Aptel, P., 1996. Mass transfer improvement by secondary flows: Dean vortices in coiled tubular membranes. *Journal of Membrane Science* 114, 235–244.
- Nevarés, I., del Alamo, M., 2008. Measurement of dissolved oxygen during red wines tank aging with chips and micro-oxygenation. *Analytica chimica acta* 621, 68–78.
- Nielsen, J., Villadsen, J., Lidén, G., 2003. *Bioreaction Engineering Principles*, Second ed. ed. Kluwer Academic/ Plenum Publishers, New York.
- Ogurtsov, V.I., Papkovsky, D.B., 2006. Application of frequency spectroscopy to fluorescence-based oxygen sensors. *Sensors and Actuators B: Chemical* 113, 608–616.
- OIV, 2012. Statistical report on world vitiviniculture.
- Özbek, B., Gayik, S., 2001. The studies on the oxygen mass transfer coefficient in a bioreactor. *Process Biochemistry* 36, 729–741.
- Pérez-Magariño, S., Sánchez-Iglesias, M., Ortega-Heras, M., González-Huerta, C., González-Sanjosé, M.L., 2007. Colour stabilization of red wines by microoxygenation treatment before malolactic fermentation. *Food Chemistry* 101, 881–893.
- Rennie, H., Wilson, R.J.H., 1975. A method for controlled oxygenation of worts. *J. Inst. Brew.* 81, 105–106.
- Ribéreau-Gayon, P., Dubourdieu, D., Doneche, B., Lonvaud, A., 2000. *Handbook of Enology Volume 1 The Microbiology of Wine and Vinifications* 2 nd Edition. John Wiley and Sons, Ltd.
- Robb, W.L., 1965. Thin silicone membranes-their permeation properties and some applications. *Annals of the New York Academy of Sciences* 1, 119–135.
- Rojas, V., Gil, J. V, Piñaga, F., Manzanares, P., 2001. Studies on acetate ester production by non-saccharomyces wine yeasts. *International journal of food microbiology* 70, 283–9.
- Rosenfeld, E., Beauvoit, B., Blondin, B., Salmon, J., 2003a. Oxygen Consumption by Anaerobic *Saccharomyces cerevisiae* under Enological Conditions: Effect on Fermentation Kinetics 69, 113–121.

- Rosenfeld, E., Beauvoit, B., Blondin, B., Salmon, J., Segalen, V., Ii, B., *Icrobiol, A.P.P.L.E.N.M.*, 2003b. Oxygen Consumption by Anaerobic *Saccharomyces cerevisiae* under Enological Conditions : Effect on Fermentation Kinetics 69, 113–121.
- Rosenfeld, E., Beauvoit, B., Rigoulet, M., Salmon, J.-M., 2002. Non-respiratory oxygen consumption pathways in anaerobically-grown *Saccharomyces cerevisiae*: evidence and partial characterization. *Yeast (Chichester, England)* 19, 1299–321.
- Saa, P.A., Perez-Correa, J.R., Celentano, D., Agosin, E., 2013. Impact of carbon dioxide injection on oxygen dissolution rate during oxygen additions in a bubble column. *Chemical Engineering Journal* 232, 157–166.
- Sablayrolles, J., Barre, P., 1986. Evaluation des besoins en oxygene de fermentations alcooliques en conditions oenologiques simulees. *Sci. Alim.* 6, 373–383.
- Sablayrolles, J.-M., Dubois, C., Manginot, C., Roustan, J.-L., Barre, P., 1996. Effectiveness of combined ammoniacal nitrogen and oxygen additions for completion of sluggish and stuck wine fermentations. *Journal of Fermentation and Bioengineering* 82, 377–381.
- Sablayrolles, J.M., 2009. Control of alcoholic fermentation in winemaking: Current situation and prospect. *Food Research International* 42, 418–424.
- Saerens, S.M.G., Delvaux, F.R., Verstrepen, K.J., Thevelein, J.M., 2010. Production and biological function of volatile esters in *Saccharomyces cerevisiae*. *Microbial Biotechnology* 3, 165–177.
- Salmon, J.-M., 2006. Interactions between yeast, oxygen and polyphenols during alcoholic fermentations: Practical implications. *LWT - Food Science and Technology* 39, 959–965.
- Salmon, J.M., Fornairon, C., Barre, P., 1998. Determination of Oxygen Utilization Pathways in an Industrial Strain of *Saccharomyces cerevisiae* during Enological Fermentation. *Journal of Fermentation and Bioengineering* 86, 154–163.
- Schneider, M., Reymond, F., Marison, I.W., von Stockar, U., 1995. Bubble-free oxygenation by means of hydrophobic porous membranes. *Enzyme and Microbial Technology* 17, 839–847.

- Singleton, V., 1987. Oxygen with Phenols and Related Reactions in Musts , Wines , and Model Systems : Observations and Practical Implications. *Am. J. Enol. Vitic.* 38, 69–77.
- Suomalainen, H., Lehtonen, M., 1978. The production of aroma compounds by yeast. *J. Inst. Brew.* 85, 149–156.
- Swiegers, J.H., Bartowsky, E.J., Henschke, P. a., Pretorius, I.S., 2005. Yeast and bacterial modulation of wine aroma and flavour. *Australian Journal of Grape and Wine Research* 11, 139–173.
- Van Stroe-Biezen, S. a. M., Janssen, a. P.M., Janssen, L.J.J., 1993. Solubility of oxygen in glucose solutions. *Analytica Chimica Acta* 280, 217–222.
- Van't Riet, K., 1979. Review of Measuring Methods and Results in Nonviscous Gas-Liquid Mass Transfer in Stirred Vessels. *Industrial & Engineering Chemistry Process Design and Development* 18, 357–364.
- Varela, C., Torrea, D., Schmidt, S., Ancin-Azpilicueta, C., Henschke, P., 2012. Effect of oxygen and lipid supplementation on the volatile composition of chemically defined medium and Chardonnay wine fermented with *Saccharomyces cerevisiae*. *Food chemistry* 135, 2863–71.
- Vidal, J.C., Dufourcq, T., Boulet, J.C., Moutounet, M., 2001. Les apports d'oxygène au cours des traitements des vins. Bilan des observations sur site, 1ère partie. *Revue Française d'Oenologie*.
- Vidal, S., Aagaard, O., 2008. Oxygen management during vinification and storage of Shiraz wine. *The Australian and New Zealand Wine Industry Journal* 23, 56–63.
- Whitman, W.G., 1923. A preliminary experimental confirmation of the two-film theory of gas absorption. *Chem. Met. Eng.* 29.
- Yang, M.-C., Cussler, E.L., 1986. Designing hollow-fiber contactors. *AIChE Journal* 32, 1910–1916.
- Yasuda, H., Lamaze, C.E., 1972. Transfer of gas to dissolved oxygen in water via porous and nonporous polymer membranes. *Journal of Applied Polymer Science* 16, 595–601.

3. OXYGEN INCORPORATION AND DISSOLUTION DURING INDUSTRIAL-SCALE RED WINE FERMENTATIONS

María Isabel Moenne, Pedro Saa, V. Felipe Laurie, Ricardo Pérez-Correa and Eduardo Agosin

Accepted in Food and Bioprocess Technology; Manuscript number #FABT-D-13-01096R1

Funding

This work was carried out with the support of FONDECYT Project N° 1090520 and FONDEF grant N° D11I1139. M. Isabel Moenne was supported by a doctoral fellowship from the Chilean National Council of Scientific and Technological Research (CONICYT).

Abstract

Oxygen management is critical to ensure the appropriate development of yeast and avoid its detrimental effects on sensory quality of wine. Oxygen additions during alcoholic fermentation are typically carried out through pump-over operations, which contributions have not been appropriately quantified. In this work, we designed a set of experiments with different pump-over modes (closed, open, and with Venturi) to evaluate oxygen dissolution and consumption during industrial scale fermentations. Closed pump-overs incorporate negligible oxygen amounts, while open pump-overs with Venturi incorporate the highest *i.e.* 3 mg/L (approximately twice more oxygen than the conventional open pump-overs). A highly heterogeneous vertical distribution of dissolved oxygen was also found, as approx. 80% of the total concentrated at the top of the tanks. When analyzing oxygen dissolution during the maceration, initial low oxygen levels were encountered in spite of the high free SO₂ concentrations (enzymatic inhibitor of oxidases). We speculate that the latter is due to the high initial CO₂ content, which prevents oxygen dissolution during the initial period. In the case of the fermentation stage, observed low oxygen concentrations are mainly due to elevated

yeasts activity. We also followed oxygen dissolution kinetics during fermentation by estimating the oxygen dissolution rate and a global consumption constant for different fermentation stages. Our results indicate the negative impact of CO₂ on oxygen dissolution and the elevated yeast biological activity of the tumultuous fermentation, as the main causes for the observed low dissolved oxygen levels. Overall, the present work will help improve the management of oxygen during fermentation and winemaking.

Key words: Oxygen; pump-over; wine fermentation; winemaking; *Saccharomyces cerevisiae*

3.1 Introduction

Discrete oxygen addition during alcoholic fermentation is a common practice in most wineries, as it promotes yeast biomass synthesis and contributes to a sound fermentation (Fornairon-Bonnefond et al., 2003; Rosenfeld et al., 2003). Several studies have shown that the risk of stuck and sluggish fermentations is reduced after oxygen additions of 10 to 20 mg/L (Rosenfeld et al., 2004; Sablayrolles & Barre, 1986), particularly when performed at the end of the yeast growth phase (Sablayrolles et al., 1996). Nevertheless, oxygen can also be detrimental when added in excess, enhancing wine oxidation, color degradation and the synthesis of off-flavors (Salmon, 2006). In spite of its importance, oxygen additions during wine fermentation are typically carried out heuristically through pump-over operations, which contribution to oxygen dissolution has not been appropriately characterized so far.

During red wine production, the fermenting must is pumped from the bottom of the tank and over onto the cap (*i.e.* pump-overs). The aims of pump-over operations are: the incorporation of oxygen into the must, favoring the extraction of color and flavor compounds from skin and seeds, avoid the spoilage of the must by keeping the cap in contact with the liquid, and remove metabolic heat formed during fermentation (Boulton et al., 1996).

Depending on the desired level of air exposure of the must, the pump-over operations are implemented either as closed, open or with an *in-line* Venturi. In closed pump-overs, the fermenting must is pumped out from the bottom of the tank and re-incorporated over the cap by means of flexible or fixed tubing (*i.e.* almost no air contact). In open pump-overs, the juice extracted from the racking valve of the tank is splashed over a vat (or a screened vat) connected to a pump that drives the aerated juice to the top of the tank. Finally, pump-overs with an *in-line* Venturi valve (*i.e.* a recently adopted technology) are also used for the incorporation of air into the circulating must. Surprisingly, there are only isolated reports on the amount of oxygen incorporated during these common winery operations (Bisson & Butzke, 2000; Bosso et al., 2009; Vidal & Aagaard, 2008), especially considering that the latter impacts the resulting wine quality, as it hinders oxygen addition management during the winemaking process.

The rate of dissolution within the liquid phase depends on its equilibrium concentration, which relates with the liquid temperature and composition, the amount of solids and the mixing provided by the bubbles of CO₂ produced by the yeast cells (Saa et al., 2012; Singleton, 1987). CO₂ has been shown to play opposite roles on the oxygen dissolution in wine fermentations. On one hand, it reduces the oxygen dissolution rate due to the dilution effect (Devatine et al., 2007; Saa et al., 2012, 2013), but on the other hand, CO₂ bubbling increases this rate due to enhanced mixing during the exponential growth phase (Garcia et al., 1994; Vlassides & Block, 2000). Overall, in small fermentation tanks CO₂ reduces the oxygen dissolution rate. Nevertheless, its impact at a larger scale remains to be assessed.

To date, several studies have characterized the oxygen concentration and distribution in pilot and industrial-scale winemaking during micro-oxygenation and aging (Adoua et al., 2010; Laurie et al., 2008; Nevares et al., 2008; Nevares et al., 2010); however, to the best of our knowledge, the fate of the oxygen added through pump-overs during wine fermentations in industrial tanks, has not been reported yet. Such studies should be essential to decide, on a quantitative basis, when and how much oxygen should be added.

In this work, the oxygen incorporation and dissolution during red wine fermentations were characterized at different positions within wine tanks, and after the use of different pump-overs modes. In addition, oxygen dissolution and consumption evolution during wine maceration and fermentation was evaluated.

3.2 Materials and Methods

3.2.1 Wine fermentations

Incorporation and dissolution of oxygen was measured during pump-overs accomplished in several red wine fermentations. For this study, data from 41 commercial red wine fermentations carried out during 2009, 2010 and 2013, was employed. The studied fermentations comprise 8 different wine varieties harvested in Chile: Cabernet Sauvignon, Carménère, Merlot, Petit verdot, Pinot noir, Cabernet franc, Carignan and Alicante Henri Bouschet (Table 3-1). The wine varieties tested in each experiment were selected depending on their availability at the different wineries.

Table 3-1: Experimental data sets used in this work

Experiment	Wine varieties ^a	Number of pump-overs
Oxygen incorporation by different pump-over modes: Closed, open and with Venturi	Cabernet Sauvignon (13), Carménère (7), Merlot (7), Petit verdot (2), Cabernet franc (2), Carignan (2), Alicante Henri Bouschet (2)	6 closed pump-overs, 10 open pump-overs and 19 with an <i>in-line</i> Venturi: 35 total
Dissolved oxygen gradients inside large industrial wine tanks during open pump-overs	Cabernet Sauvignon (1), Carménère (1)	32
Oxygen dissolution and consumption kinetics during wine maceration and fermentation	Pinot noir (2), Cabernet Sauvignon (1), Carménère (1)	76

3.2.2 Oxygen incorporation due to different pump-over modes

The amounts of oxygen incorporated by three types of pump-overs, either closed, open or with an *in-line* Venturi injector (Mazzei[®] Injector Company, LLC, Bakersfield, USA) (Fig. 3-1a), were determined *in-line* using optical mini planar oxygen sensors (PSt3, PreSens[®], Regensburg, Germany), glued to the inside of a sight glass fittings (stainless steel tubing with a glass section) with food-grade silicone. The oxygen level of the must could be followed from the outside by means of an oxoluminiscense-based dissolved oxygen meter 3 LCD-trace Fibox v7 (measuring span of 0-20 mg/L and 15 µg/L of O₂ detection limit) (PreSens[®], Regensburg, Germany). This optical sensor does not show the problems of the Clark's electrode, *e.g.* relatively long response times and oxygen consumption during the measurement (Fernández-Sánchez et al., 2007), and it is ideal for non-invasive measurements. Oxygen incorporation was calculated as the mean difference between the dissolved oxygen concentrations of the stream of must leaving and returning to the tank (measured after the point in which oxygen incorporation was achieved, *i.e.* vat or Venturi) in each trial. Oxygen concentration was recorded every 1 s at the two points as previously mentioned.

Depending on the pump-over mode, the glass fittings were coupled to one of racking valves of the tanks, the exit of the vat, the inlet and outlet of the Venturi and the exit of the impelling pump (Fig. 3-1a). This experimental set-up allowed assessing the contribution of each device (*i.e.* pump, vat, Venturi) to the total oxygen incorporation in the fermenting tanks.

The number of wines studied under each pump-over mode was as follows: 6 fermentations with closed pump-overs (during the early fermentation stages), 10 with open pump-overs and 19 with an *in-line* Venturi during the tumultuous and stationary fermentation stages. The varying number of trials in each case depended on the number of fermentation available at the wineries under each different mixing procedure. Seven different wine varieties were included in these experiments (Table 3-1). The type of pump employed was a positive displacement pump (Maxi80 Liverani[®], Lugo, Italy), with an average flow rate of 15 m³/h. Finally, the temperatures of the fermenting musts ranged between 17 and 27°C during the trials.

3.2.3 Dissolved oxygen gradients inside large industrial wine tanks during open pump-overs

The dissolved oxygen concentration within industrial wine tanks during open pump-overs was measured using PSt3 optical dipping probes (PreSens[®], Regensburg, Germany), at three different heights inside a 40,000-liter industrial tank. For this purpose, a 316 stainless steel tubing (2.5 cm diameter, 0.8 cm thick and 4.3 m long) with openings in the pipeline (7 cm width and 6 cm long) at three different heights (2.1, 3.2 and 4.3 meters from the top of the tank) was introduced into the center of the tank (Fig. 3-1b). The latter allowed to safely insert the optical oxygen and temperature probes (PT1000, PreSens[®], Regensburg, Germany) at a fix position within the tube, corresponding to the opening in the pipeline.

Cabernet Sauvignon and Carménère grapes were employed in this experiment (Table 3-1). Cabernet Sauvignon must (harvested with 26.3° Brix and initial must density of 1,110 g/L), inoculated with *Saccharomyces cerevisiae* yeast Zymaflore F15[®] (Laffort, Bordeaux, France), was first fermented; and later, the Carménère (harvested with 29° Brix and initial must density of 1,120 g/L), inoculated with *Saccharomyces cerevisiae* L2056[®] (Lalvin, Toulouse, France). Cabernet Sauvignon and Carménère musts were fermented at 22±1°C and 24±3°C, respectively. The type of yeast to utilize in each case was chosen by the winemakers based on technical considerations and their winemaking protocols.

During the Cabernet Sauvignon fermentation, a total of 18 pump-overs were performed during the 10 days of fermentation (the first 6 days corresponded to tumultuous fermentation); while for the Carménère, 14 pump-overs were conducted during the 6 days of fermentation (the first 4 days corresponded to tumultuous fermentation). Normally, two pump-overs per day were carried out for both fermentations. In both cases, the evolution of the fermentation was followed by the decrease of must density using appropriate hydrometers (Alla France[®], Chemillé, France). As a reference, fermentations were considered completed when the residual sugar content of the wine was lower than 2 g/L. The flow rate used during these experiences was approx. 15

m^3/h , as in the previous experiment, and the duration of pump-overs ranged between 20 and 30 min, according to the winemaking protocol of the winery.

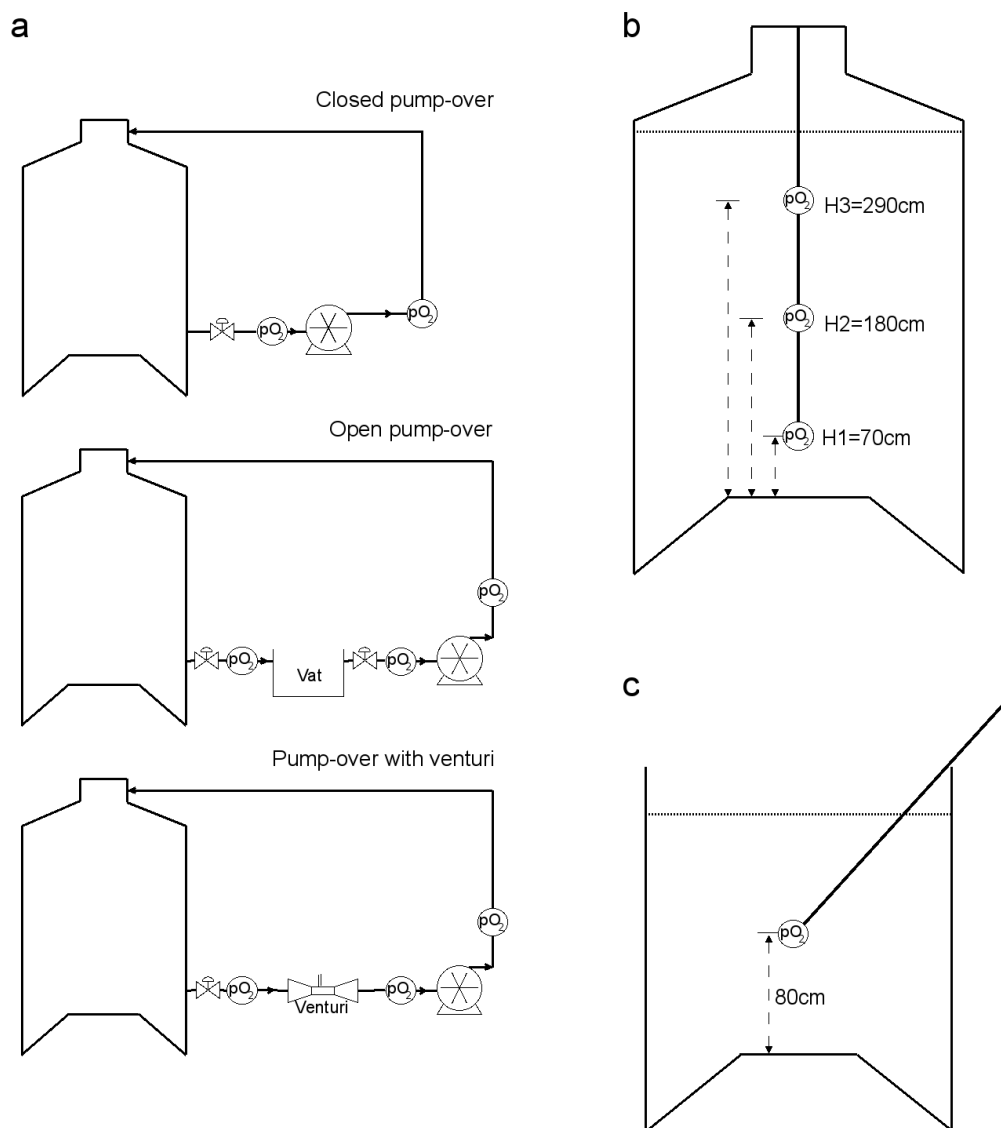


Figure 3-1: Schematic experimental setups for studying oxygen incorporation and dissolution during pump-over operations in red wine industrial fermentations (p_{O_2} represent the points in which oxygen was measured). **a** Oxygen incorporation by different pump-over modes: closed, open and with Venturi; **b** Axial distribution of dissolved oxygen during open pump-overs at three heights in industrial wine tanks (40,000 L); **c** Oxygen dissolution and consumption kinetics during winemaking in 5,000-liter tanks (diagrams not to scale)

3.2.4 Oxygen dissolution and consumption kinetics during wine maceration and fermentation

Oxygen dissolution and consumption kinetics of four red wine fermentations were followed in closed and open pump-over modes during pre-fermentative maceration and fermentation stages. The pre-fermentative maceration was performed by placing dry ice (solid CO₂) in the surface of the cap during the first days of the treatment, and adding 35 mg/L and 20 mg/L of SO₂ during the first and the second day of maceration, respectively. Again, fermentation evolution was periodically checked by the decrease of must density using appropriate hydrometers (Alla France[®], Chemillé, France) for all fermentations considered. The must density measurements were employed as an indicator of the fermentation evolution, which enabled the subsequent analysis of the dissolved oxygen content during different phases of wine fermentation.

Measurements were taken in two 5,000-liter open stainless steel tanks (Fig. 3-1c). First, the fermentation of two Pinot noir wines (harvested with 24.2° Brix and initial must density of 1,107 g/L) from Casablanca valley was followed; and later, one Carménère and one Cabernet Sauvignon from the same valley (harvested with 23.9° and 24.2° Brix and initial must densities of 1,104 g/L and 1,106 g/L, respectively) (Table 3-1). All these fermentations were carried out with native yeasts, *i.e.* without inoculation of commercial wine yeast strains. Pinot noir, Cabernet Sauvignon and Carménère musts were fermented at 22±2.6°C, 25±2.6°C and 25±1.4°C, respectively. SO₂ concentrations were also traced during the maceration and fermentation processes, employing the reference Ripper method (Buechsenstein & Ough, 1978).

Dissolved oxygen concentration was measured inside the tanks at 1.3 m from the top (approx. the geometric center of the tank), by placing a 316 stainless steel tubing (2.5 cm diameter and 0.8 cm thick) containing both the optical oxygen (PreSens[®], Regensburg, Germany) and temperature probes (PT1000, PreSens[®], Regensburg, Germany) as previously explained. A total of 18 pump-overs were performed for each Pinot noir (6 in maceration and 12 fermentation), while in the case of Cabernet Sauvignon and Carménère fermentations, 22 (6 in maceration and 16 fermentation) and 18 (4 in maceration and 14 fermentation) pump-overs were conducted, respectively

(usually 2 pump-overs per day during the fermentation). The flow rate employed during the pump-overs was approximately 5 m³/h and they lasted approximately 10 minutes, according to the winemaking protocol of the winery.

3.2.5 Kinetics of oxygen consumption during pump-overs

Oxygen consumption kinetics during industrial wine fermentations was described using the following mass balance equation (A Silva & Lambri, 2006),

$$\frac{dO_2}{dt} = -K_{\text{global}} \cdot O_2 \quad (1)$$

where K_{global} represents a kinetic constant which includes the biological, enzymatic and chemical consumption, and the physical desorption of CO₂. The latter expression can be analytically solved as follows:

$$O_2(t) = O_2(0) \cdot \exp(-K_{\text{global}} \cdot t) \quad (2)$$

where $O_2(0)$ represents the initial oxygen concentration.

3.2.6 Regression and statistics

Estimated consumption parameters were fitted by minimizing the sum of squared residual errors between predicted and experimental dissolved oxygen data, as indicated in Eq. (3)

$$\text{Min}_{K_{\text{global}}} \sum_{i=1}^N \left(O_2^{\text{model}} - O_2^{\text{meas}} \right)^2 \quad (3)$$

Where O_2^{model} represents predicted dissolved oxygen concentration, O_2^{meas} denotes the measured dissolved oxygen concentration, K_{global} is the consumption kinetic constant and N represents the number of measurements. We also developed an empirical correlation between the oxygen dissolution rate ($\Delta O_2/\Delta t$) and the must's density (ρ), in which case the estimated parameters were fitted using the same strategy (minimizing the sum of squared residual errors between the model and experimental data). In both cases, regressions were carried out using the non-linear optimization routine *fminsearch* of MATLAB[®]. To assess the confidence of the estimated parameters after

the regressions, the respective 95% confidence interval were calculated employing the MATLAB[®] functions *nlparci* and *nlpredci*. Finally, to compare the different treatments or group means, Student's *t*-test and one-way ANOVA analysis were employed (depending if two or more groups were compared), to determine whether the observed difference were statistically significant with 95% and 99% confidence levels. The MATLAB[®] Statistics Toolbox was used for these analyses.

3.3 Results and discussion

3.3.1 Oxygen incorporation by different pump-over modes

The amount of oxygen incorporated using the different pump-over modes (closed, open and with Venturi) was assessed by calculating the mean of the difference between the dissolved oxygen concentrations of the stream of must leaving and returning to the tank. According to the pump-over mode, different amounts of oxygen were incorporated into the fermenting must (Table 3-2). On average, closed, open and pump-overs with Venturi added 0.05 ± 0.02 , 1.4 ± 0.52 and 3.0 ± 1.3 mg/L of oxygen, respectively (mean plus one standard deviation). One-way ANOVA test at 99% confidence level yielded a *p*-value < 0.01 ($5.7 \cdot 10^{-6}$) which statistically support the observed difference upon the different modes of operation. Thus, closed pump-overs incorporate, in average, almost no oxygen, as would be expected due to the limited contact with air. In fact, this operation mode is mainly used for must circulation and homogenization purposes (Boulton et al., 1996). On the other hand, open pump-overs with Venturi were the most efficient configuration for oxygen addition, incorporating twice more oxygen than the traditional open one (*t*-test, *p*-value < 0.05).

Table 3-2: Oxygen incorporated in fermenting grape musts using different pump-over modes.

Pump-over mode	Min (mg/L)	Max (mg/L)	Average (mg/L)	Standard deviation (mg/L)	Coefficient of Variation (%)
Closed	0.02	0.11	0.05	$1.7 \cdot 10^{-2}$	38.4
Open	0.6	2.5	1.36	0.52	35.4
With Venturi	0.5	5.6	3.03	1.38	43
ANOVA	Sum of squares	Degrees of freedom	Mean square	<i>F</i>	<i>p</i> -value
Between groups	41.3	2	20.7	18.3	$5.7 \cdot 10^{-6}$
Within groups	35	31	1.13		
Total	76.3	33			

When it comes to comparing the oxygen incorporation during the fermentation of different red wine varieties (Fig. 3-2), no statistical differences were obtained at each operation mode (One-way ANOVA, p -value < 0.05). This trend is conserved among the grape varieties studied, suggesting that this tendency might be valid for most, if not all, red grape varieties. The latter is relevant, as it suggests that the pump-over mode must be chosen fundamentally on the oxygen dose to be added, independent of the grape variety to ferment.

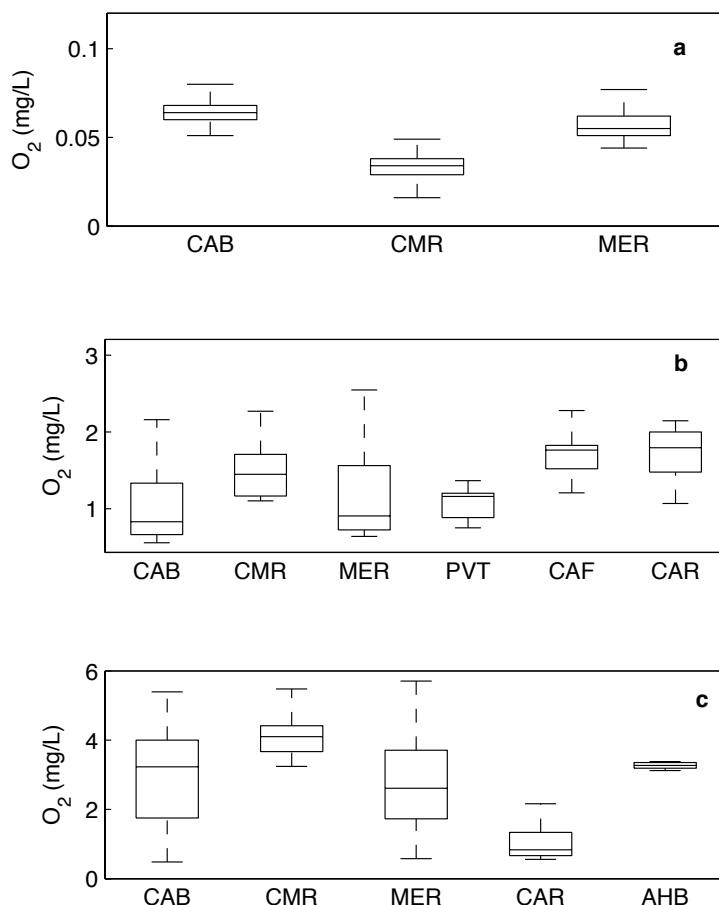


Figure 3-2: Boxplots of oxygen incorporation into industrial red wine fermentations by different types of pump-overs. **a** Closed pump-over; **b** Conventional open pump-over; **c** Open pump-over with Venturi. The abbreviations for grape varieties are: Cabernet Sauvignon (CAB), Carménère (CMR), Merlot (MER), Petit verdot (PVT), Cabernet franc (CAF), Carignan (CAR) and Alicante Henri Bouschet (AHB)

The partial contribution of each pump-over apparatus to the concentration of dissolved oxygen was as follows: in open pump-overs, the vat and the pump contribute similar amounts ($48.6 \pm 9.8\%$ for the vat, and $51.4\% \pm 29.5\%$ for the pump; equivalent to approximately 0.7 mg/L of dissolved oxygen each). For pump-overs with Venturi, the estimated contributions of the Venturi and the pump were $20.1 \pm 9.8\%$ and $79.9 \pm 14.9\%$ respectively, equivalent to 0.6 ± 0.4 and 2.5 ± 0.4 mg/L of dissolved oxygen. These findings seem contradictory at first sight, as we previously determined that closed pump-overs, incorporated almost no oxygen (approx. 0.05 mg/L). However, it has to be considered that the oxygen is dissolved in the liquid phase in two steps. First,

the inlet stream (oxygen-poor) comes in contact with the surrounding air, incorporating oxygen in form of bubbles. Then, the oxygen from the air bubbles is transferred through the gas–liquid interface into the liquid phase, where the oxygen dissolved. The rate upon which the oxygen gas is transferred to the liquid phase depends mainly on the hydrodynamic condition, among other factors (Gagnon et al., 1998). At this point, the pump plays a key role dissolving the air bubbles. When the liquid stream approaches the pump, the liquid turbulence is greatly enhanced, which improves the oxygen mass transfer by increasing the liquid velocity and the breakup of gas bubbles (Wang & Zhong, 1996a, 1996b). The latter can be used to explain the differences in the dissolved oxygen contributions of the vat, Venturi and pump in the different studied configurations. In conventional open pump-overs, the vat dissolves more oxygen than the Venturi, as the fermenting must is exposed to air for a longer period of time. On the other hand, the Venturi injector incorporates more oxygen than the vat, which explains the higher dissolved oxygen concentration of the leaving stream. Overall, the open pump-over with Venturi is more efficient at dissolving oxygen due to the combined effect of the Venturi injector and the pump.

Finally, another relevant factor during the operation of the different types of pump over was the variability in the amount of oxygen incorporated into the must. Indeed, it is not only important the average amount of oxygen added, but also its reproducibility in repeated trials. As shown in Table 3-2, oxygen additions with pump-overs are, in general, heterogeneous. The latter strengthens the importance of characterizing these modes of operation, to estimate, at least roughly, the amount of oxygen expected to be added in each operation.

3.3.2 Dissolved oxygen gradients inside large industrial wine tanks during open pump-overs

We found significant differences in the oxygen content of fermenting musts between the top and the bottom of 40,000-liter tanks following a pump-over (Fig. 3-3). Most of the oxygen added through pump-overs (approx. 80%) reaches only the upper portion of the must within the wine tank (2.9 m from the bottom of the tank). The other two points

(heights), measured at 0.7 and 1.8 m from the bottom of the tank, especially the lowest, received almost no oxygen during the course of the fermentation (< 1%). The latter can be explained by the form in which open-pump overs are performed (*i.e.* must exposed to air is added to the top) and the mixing regime present in wine fermentations. García et al. (1993) reported important gradients in pH, dry weight, sugars and ethanol concentrations, among others between different level of unagitated beer fermentations at pilot scale, inoculated at the top of the reactor. According to the authors, these results are due to the presence of poor mixing in the downwards direction, which is a direct result of the liquid recirculation patterns owed to the rise of CO₂ bubbles produced by the yeasts. Furthermore, it has been reported that during the high-CO₂ production stages (exponential growth phase), cell distribution is uniform in unagitated wine fermentors (Vlassides & Block, 2000), which discards any major influence of the yeast cells distribution in the observed dissolved oxygen distribution. Thus, the latter suggests that the mixing patterns resulting from the gaseous CO₂ bubbling are the main responsible of the observed dissolved oxygen distribution. This has been also observed in a recent work (P. A. Saa et al., 2013), where the CO₂ was shown to play a major role on the oxygen dissolution profile observed in an experimental bubble column, mimicking enological CO₂ generation.

Therefore, the efficiency of oxygen addition by pump-overs inside large wine tanks is limited. The presence of large oxygen gradients during pump-overs indicate that tank zones will be exposed longer to different dissolved oxygen concentrations. The latter could impact the fermentation evolution, as the yeast cells will be exposed to different amounts of oxygen during this process. Considering that wine yeasts require determined amounts of oxygen for successfully completing the fermentation (Sablayrolles & Barre, 1986), it is important to take into account this large heterogeneity in dissolved oxygen distribution when performing pump-overs at industrial scale.

Finally, there is a notorious difference in the dissolved oxygen concentrations reached in the top of the tank for the Cabernet Sauvignon and Carménère fermentations (Fig. 3-3a). For Cabernet Sauvignon, the highest dissolved oxygen concentration reached was

2.6 mg/L; while for Carménère, only 0.6 mg/L was achieved. The latter can result from the high dependency of this process on external features not fully controllable, such as operators, oxygen dissolution in the vat, time of exposure, among others. In fact, just in terms of oxygen incorporation, this operation possesses a variability of around 35% (Table 3-2) which, combined with external factors and the high working volumes, might be responsible for the large difference observed.

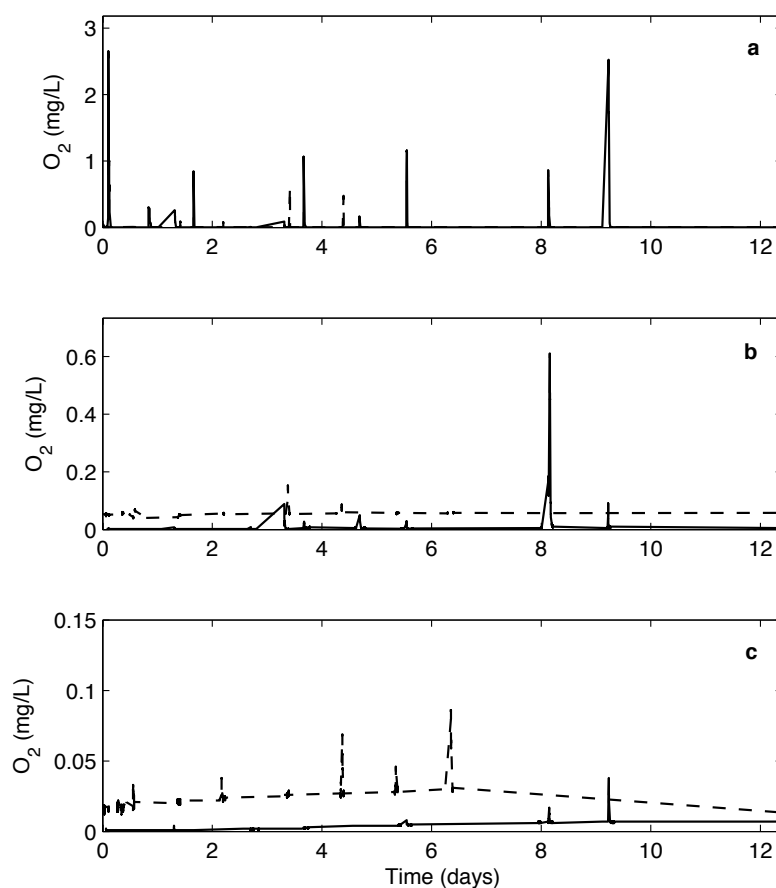


Figure 3-3: Dissolved oxygen (DO) levels inside 40,000-liter industrial wine tanks during pump-overs in fermentations of Cabernet Sauvignon (*solid lines*) and Carménère musts (*dashed lines*). Panels **a**, **b** and **c** show DO at the top, middle and bottom of the tanks, respectively

3.3.3 Oxygen dissolution and consumption kinetics during wine maceration and fermentation

The evolution of dissolved oxygen of grape musts from two commercial Pinot noir, a Cabernet Sauvignon and a Carménère was followed during the maceration and

fermentation processes. Figure 3-4 illustrates the dissolved oxygen evolution in Pinot noir musts.

Low oxygen dissolution was observed during the maceration process (Figures 3-4a). In musts, the main form of oxidation that takes place is enzymatic oxidation, which occurs at a much faster rate than chemical oxidation (Dubernet & Ribéreau-Gayon, 1973, 1974). This oxidation is conducted by polyphenol oxydases (PPO), using phenolic compounds (*e.g.* hydroxycinnamic acids, trans-caftaric and coumaric acid, among others) and oxygen as substrates (Macheix et al., 1991). Previously, it has been reported that SO₂ can inhibit PPO activity by 75% to 90% when 50 mg/L SO₂ are added to musts (Dubernet & Ribéreau-Gayon, 1974), which seems to disagree with the observed data (Fig. 3-4a). Indeed, lower oxygen levels were observed when SO₂ concentration were at its highest (beginning of the maceration). This contradictory result might be explained due to the “protective” effect of CO₂ against oxygen dissolution during the first days of the maceration. Devatine et al. (2011) have demonstrated that complete protection of wines and musts is obtained when CO₂ content is high. Moreover, the authors showed that micro-oxygenation is totally inefficient in the presence of initial high CO₂ concentrations, even if there is no production of CO₂. At this point, we speculate that because of the high additions of CO₂ during the first days of maceration, oxygen dissolution is very ineffective during this period (approx. until the second day, Fig. 3-4a). In fact, no oxygen dissolution is observed during the first two days of the maceration, despite the pump-overs carried out. Then, as the CO₂ escapes from the liquid to the gas phase due to the successive pump-overs and the SO₂ levels decrease, oxygen is able to dissolve in the must and to be consumed by enzymatic oxidation reactions. The latter is observed after the second day, in which oxygen dissolves into the must and is quickly consumed (Fig. 3-4a). Indeed, this hypothesis has to be properly validated and is by no means definitive, however it might explain the lower oxygen levels encountered at the beginning of the maceration. Finally, in terms of the dissolved oxygen evolution, overall heterogeneous levels were achieved during this stage in the different fermentations. Dissolved oxygen

concentrations obtained during pump-overs ranged between 0.2 and 3.6 mg/L, which reinforces the high variability of the open pump-over processes.

During the enological fermentation, the dissolved oxygen concentration was also very variable. Dissolved oxygen levels for Pinot noir ranged between 0.02 and 1.0 mg/L (Figures 3-4b), while for Cabernet Sauvignon and Carménère, oxygen values varied between 0.03 and 2.1 mg/L (data not shown). Nevertheless, it is noteworthy that for all four fermentations, higher dissolved oxygen concentrations were observed at the end of the fermentation, as indicated by the density plateau reached. This correlates well with the low yeasts activity, the major contributor of oxygen consumption during alcoholic fermentation (Salmon, 2006). Figures 3-4c show the dissolved oxygen levels reached in all the fermentations as a function of the must's density. Dissolved oxygen concentrations achieved are generally higher at the onset and at the offset of the alcoholic fermentation, *i.e.* when yeast concentration and activity are at their lowest, respectively. Therefore, must density might be regarded as a useful winemaking indicator of the capacity of the fermenting must to dissolve oxygen (see below).

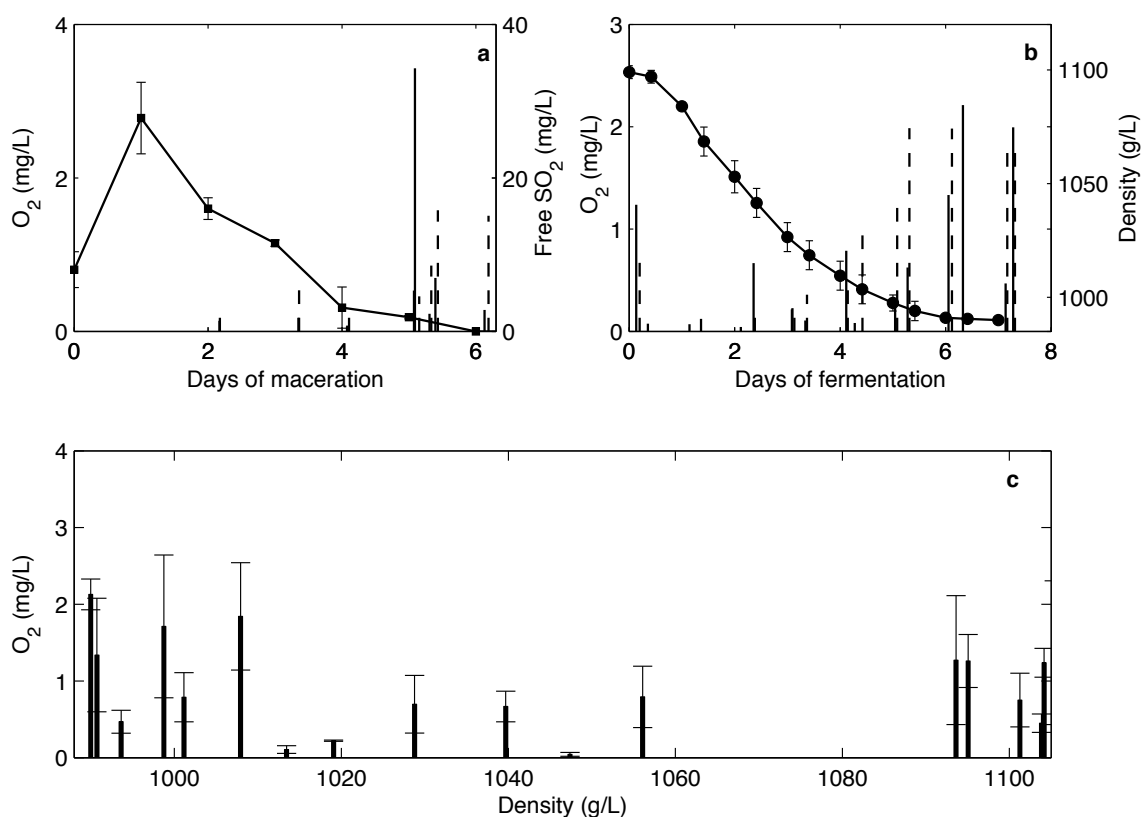


Figure 3-4: Dissolved oxygen (DO) concentrations during maceration and fermentation of two Pinot noir. **a** Evolution of DO (solid and dashed lines) and the free SO₂ concentration (filled squares) during the maceration process; **b** Evolution of DO (solid and dashed lines) during alcoholic fermentation. The fermentation evolution is illustrated by the decrease of must's density (filled circles); **c** DO levels reached during open pump-overs in Pinot noir fermentations as a function of must densities

3.3.4 Kinetics of oxygen dissolution and consumption during alcoholic fermentations

During the application of open pump-overs, the dissolved oxygen response followed the kinetics illustrated in Fig. 3-5a. Similar response curves were recently reported for unagitated alcoholic fermentations under enological conditions, on a laboratory scale (Saa et al., 2012). As shown in this figure, the first part of the response curve corresponds to the oxygen addition, in which the dissolved oxygen concentration increases as the pump-over advances. Then, when the pump-over is finished, the dissolved oxygen concentration decreases as the yeast cells consume the available oxygen. There are also other sinks for oxygen, such as chemical consumption and

physical desorption, which are, however, less important than the yeast activity during alcoholic fermentation (Aceituno et al., 2012; Saa et al., 2012; Salmon, 2006).

To better understand the dissolved oxygen dissolution and consumption kinetics, we examined both parts of the curve in detail for all the fermentations (Pinot noir, Cabernet Sauvignon and Carménère). Firstly, we computed the average oxygen dissolution rate ($\Delta O_2/\Delta t$) for all the pump-overs analyzed from the addition curve (Fig. 3-5a). This parameter was calculated by fitting a linear curve from the moment of the start of the oxygen addition until the end of the pump over (beginning of oxygen consumption). The slope of the fitted curve represents the oxygen dissolution rate and represents the average amount of oxygen that it is dissolved per unit of volume and time.

The main advantages of this parameter are that it does not solely rely on the particular oxygen concentration level determined at a particular point during the pump-overs (as shown before, pump-overs are quite variable in terms of oxygen incorporation), but it rather depends on the rate of change of the oxygen concentration; and secondly, it is very useful for managing oxygen doses as it indicates the amount of dissolved O_2 per unit of volume and time in a particular stage of the fermentation. A parabolic relationship between the must's density and the oxygen dissolution rate of the form $\Delta O_2/\Delta t = a \cdot \rho^2 + b \cdot \rho + c$ ($a = 7.76 \cdot 10^{-5} \pm 3.37 \cdot 10^{-5}$, $b = -1.65 \cdot 10^{-1} \pm 7.07 \cdot 10^{-2}$, $c = 8.75 \cdot 10 \pm 3.7 \cdot 10$, $R = 0.74$) was found (Figure 3-5b). At the fermentation's onset and offset (around 1100 and 990 g/L density, respectively), the oxygen dissolution rates are higher than during the tumultuous fermentation phase (between 1090 and 1020 g/L densities). The latter could be explained by the higher yeast activity and CO_2 production rates, typical of this phase (Casalta et al., 2010).

During tumultuous fermentation, yeast cells require oxygen to synthesize essential membrane components such as ergosterol, which allow them to thrive in the harsh conditions of alcoholic fermentations (Fornairon-Bonnefond et al., 2003; Fornairon-Bonnefond et al., 2002; Rosenfeld et al., 2002). This high demand can be illustrated by the higher consumption constants (K_{global}) fitted to the consumption curves during this

fermentation phase (Fig. 3-5c, TF). Nevertheless, this sole factor is not the only one responsible for the lower oxygen dissolution rate observed. The other key factor that impacts oxygen dissolution is the CO₂ production (Chiciuc et al., 2010; Devatine et al., 2011; Devatine et al., 2007; Devatine & Mietton-Peuchot, 2009; Saa et al., 2013). Saa et al. (2013) studied in a laboratory bubbling column the oxygen dissolution rate in water under CO₂ bubbling conditions similar to the ones encountered during the tumultuous phase of alcoholic fermentations. Under these conditions, the authors reported an average oxygen dissolution rate of approximately 0.3 mg O₂/(L·min), which is similar to the one estimated in this work under real conditions during the tumultuous phase – around 0.2 mg O₂/(L·min). The negative impact of the CO₂ production is related to its high concentration, and not to its specific production rate, *i.e.* stripping (Saa et al., 2012), as it favors the dilution of the dissolved oxygen added in the gas phase upon its transfer to the liquid phase (Devatine et al., 2011; Devatine & Mietton-Peuchot, 2009; Saa et al., 2013). As previously mentioned, CO₂ acts as a resistance to oxygen dissolution and not as a “physical sink” of consumption (Devatine et al., 2011). Combining the negative impact of CO₂ on the oxygen dissolution and the high biological uptake by the yeast cells during the exponential growth phase, one might be able to explain the significant contrast in the oxygen dissolution rates among the different fermentation phases.

Finally, the dissolved oxygen consumption during the different phases of the fermentation - early fermentation (EF), tumultuous fermentation (TF) and stationary phase (SP) - were also evaluated (Fig. 3-5c). Significant differences in the consumption constants for the different fermentation stages were determined (One-way ANOVA analysis; *p*-value < 0.01). On average, during the EF, TF and SP, the oxygen consumption constants were 0.17±0.08, 0.22±0.06 and 0.12±0.06 mg O₂/(L·min), respectively. These results agree with the evolution of the yeasts activity during the alcoholic fermentation. The differences between the EF and SP values could be explained by the free SO₂ remaining from the maceration process (Fig. 3-4a and 3-4c). These results suggest that the main source of oxygen consumption during alcoholic fermentation is the yeast metabolic activity.

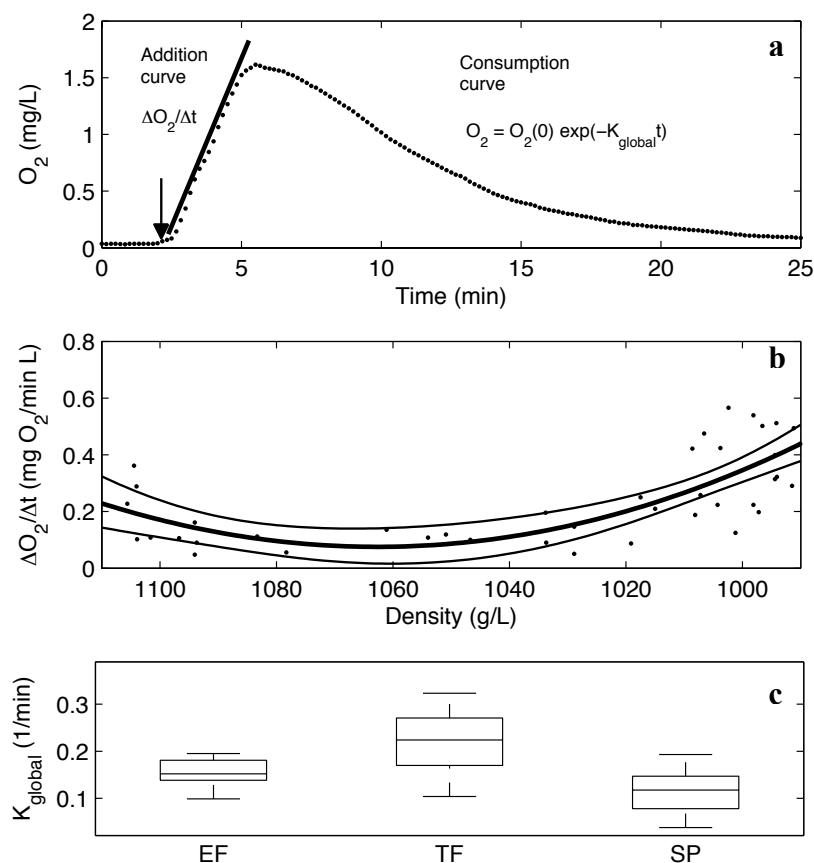


Figure 3-5: Oxygen dissolution and consumption kinetics during alcoholic fermentation. **a** A typical dissolution curve occurring during an open pump-over in a 5,000-liter wine tank during alcoholic fermentation (*black dots*). The arrow indicates the pump-over start and the onset of oxygen dissolution. The first part of the curve corresponds to the oxygen addition, in which the oxygen dissolution rate ($\Delta O_2 / \Delta t$) can be estimated as the slope of the curve; while the second part describes the global oxygen consumption by the fermenting must which is modeled using Eq. (3); **b** Oxygen dissolution rate as a function of must's density in Pinot noir, Cabernet Sauvignon and Carménère wines. The thicker line represents a parabolic relation of the form $\Delta O_2 / \Delta t = a \cdot \rho^2 + b \cdot \rho + c$ between both variables ($R = 0.74$), while the thinner lines denote the 95% confidence interval of the trend of the fitted values (*black dots*); **c** Oxygen consumption constant for different fermentation stages: early fermentation (EF), tumultuous fermentation (TF) and stationary phase (SP)

3.4 Conclusion

The present work comprises an integral study aiming to measure and better understand oxygen incorporation and dissolution through pump-overs during winemaking, at industrial scale. Regarding the operation mode of pump-overs, those with Venturi injectors incorporate approximately twice more oxygen than open pump-overs. Particular analysis of the contributions of the vat, the injector and the pump to the

oxygen dissolution during open pump-overs and with Venturi, suggests that the pump plays a key role in dissolving the oxygen incorporated by the former. Closed pump-overs, as expected, incorporated negligible amounts of oxygen, which make them ideal for homogenization purposes without oxygenating the must. In large wine tanks, a highly heterogeneous distribution of dissolved oxygen after pump-over was determined. We hypothesize that this results mainly from the yeast CO₂ bubbling during the fermentation, which generates poor mixing in the downwards direction, although this explanation should be validated under appropriate conditions. Finally, when analysing the course of oxygen dissolution and consumption, several findings stand out. During the maceration process, initial low levels of dissolved oxygen were found despite the presence of high concentrations of free SO₂, which is an effective oxidase inhibitor. We speculate that the latter is due to the high initial CO₂ content, which prevents oxygen dissolution during the initial period. Then, as the CO₂ escapes from the liquid and the SO₂ levels decrease, oxygen is able to dissolve in the must and to be consumed through enzymatic oxidation reactions. During the alcoholic fermentation, higher dissolved oxygen concentrations were observed at the end of the fermentation, which agrees well with the lower yeast activity in this stage. The kinetics of dissolved oxygen observed during this stage strongly suggests that both, the negative impact of CO₂ on the oxygen dissolution and the high biological uptake by the yeasts during the exponential growth phase, are the main variables responsible for the low dissolved oxygen levels achieved during the tumultuous fermentation phase. Overall, the present work will help improve the management of oxygen additions through pump-overs during winemaking at industrial scale.

Acknowledgments

We are grateful to Felipe Ibáñez from Viña Carmen, and to Rodrigo Soto and Sofía Araya from Viña Veramonte, who allowed us to carry out these studies in the cited wineries. We are particularly grateful to the reviewers for their thorough and constructive comments that contributed significantly to improve the final manuscript.

References

- Aceituno, F. F., Orellana, M., Torres, J., Mendoza, S., Slater, A. W., Melo, F., & Agosin, E. (2012). Oxygen response of the wine yeast *Saccharomyces cerevisiae* EC1118 grown under carbon-sufficient, nitrogen-limited enological conditions. *Applied and environmental microbiology*, *78*(23), 8340–52.
- Adoua, R., Mietton-Peuchot, M., & Milisic, V. (2010). Modelling of oxygen transfer in wines. *Chemical Engineering Science*, *65*(20), 5455–5463.
- Bisson, L., & Butzke, C. (2000). Diagnosis and Rectification of Stuck and Sluggish Fermentation. *American journal of enology and viticulture*, *51*(2), 168–177.
- Bosso, A., Guaita, M., Panero, L., Borsa, D., & Follis, R. (2009). Influence of Two Winemaking Techniques on Polyphenolic Composition and Color of Wines. *American journal of enology and viticulture*, *60*(3), 379–385.
- Boulton, R., Singleton, V., Bisson, L., & Kunkee, R. (1996). *Principles and Practices of Winemaking*. New York: Chapman Hall.
- Buechsenstein, J. W., & Ough, C. S. (1978). SO₂ determination by aeration-oxidation: a comparison with Ripper. *American journal of enology and viticulture*, *29*(3), 10–13.
- Casalta, E., Aguera, E., Picou, C., Rodriguez-Bencomo, J.-J., Salmon, J.-M., & Sablayrolles, J.-M. (2010). A comparison of laboratory and pilot-scale fermentations in winemaking conditions. *Applied microbiology and biotechnology*, *87*(5), 1665–1673.
- Chiciuc, I., Farines, V., Mietton-Peuchot, M., & Devatine, A. (2010). Effect of wine properties and operating mode upon mass transfer in micro-oxygenation. *International Journal of Food Engineering*, *6*(6).
- Danilewicz, J. C., Secombe, J. T., & Whelan, J. (2008). Mechanism of Interaction of Polyphenols, Oxygen, and Sulfur Dioxide in Model Wine and Wine. *American journal of enology and viticulture*, *59*(2), 128–136.
- Devatine, A., Chiciuc, I., & Mietton-Peuchot, M. (2011). The protective role of dissolved carbon dioxide against wine oxidation: a simple and rational approach. *Journal International des sciences de la vigne et du vin*, *45*(3), 189–197.

- Devatine, A., Chiciuc, I., Poupot, C., & Mietton-Peuchot, M. (2007). Micro-oxygenation of wine in presence of dissolved carbon dioxide. *Chemical Engineering Science*, *62*(17), 4579–4588.
- Devatine, Audrey, & Mietton-Peuchot, M. (2009). A mathematical approach for oxygenation using micro bubbles Application to the micro-oxygenation of wine. *Chemical Engineering Science*, *64*(9), 1909–1917.
- Fernández-Sánchez, J. F., Roth, T., Cannas, R., Nazeeruddin, M. K., Spichiger, S., Graetzel, M., & Spichiger-Keller, U. E. (2007). Novel oxygen sensitive complexes for optical oxygen sensing. *Talanta*, *71*(1), 242–250.
- Fornairon-Bonnefond, C., Aguera, E., Deytieux, C., Sablayrolles, J.-M., & Salmon, J.-M. (2003). Impact of oxygen addition during enological fermentation on sterol contents in yeast lees and their reactivity towards oxygen. *Journal of Bioscience and Bioengineering*, *95*(5), 496–503.
- Fornairon-Bonnefond, C., Demaretz, V., Rosenfeld, E., & Salmon, J. (2002). Oxygen addition and sterol synthesis in *Saccharomyces cerevisiae* during enological fermentation. *Journal of Bioscience and Bioengineering*, *93*(2), 176–182.
- Gagnon, H., Lounes, M., & Thibault, J. (1998). Power consumption and mass transfer in agitated gas-liquid columns: a Comparative study. *The Canadian Journal of Chemical Engineering*, *76*, 379–389.
- Garcia, A I, Pandiella, S. S., Garcia, L. A., & Diaz, M. (1994). Mechanism for mixing and homogenization in beer fermentation. *Bioprocess Engineering*, *10*(4), 179–184.
- Garcia, Ana I, Garcia, L. A., & Diaz, M. (1993). Mixing in unstirred batch fermenters. *Chemical Engineering Journal*, *51*(3), B57–B61.
- Laurie, V. F., Law, R., Joslin, W. S., & Waterhouse, A. L. (2008). In situ measurements of dissolved oxygen during low-level oxygenation in red wines. *American journal of enology and viticulture*, *59*(2), 215–219.
- Nevarés, I., Del Alamo, M., Cárcel, L. M., Crespo, R., Martín, C., & Gallego, L. (2008). Measure the Dissolved Oxygen Consumed by Red Wines in Aging Tanks. *Food and Bioprocess Technology*, *2*(3), 328–336.

- Nevarés, I., del Alamo, M., & González-Muñoz, C. (2010). Dissolved oxygen distribution during micro-oxygenation. Determination of representative measurement points in hydroalcoholic solution and wines. *Analytica chimica acta*, *660*, 232–239.
- Ribéreau-Gayon, P., Dubourdieu, D., Donèche, B., & Lonvaud, A. (2006). *Handbook of enology volume 2 The chemistry of wine stabilization and treatments* (2nd ed., pp. 341–344). Hoboken: Wiley.
- Rosenfeld, E., Beauvoit, B., Blondin, B., & Salmon, J. (2003). Oxygen Consumption by Anaerobic *Saccharomyces cerevisiae* under Enological Conditions: Effect on Fermentation Kinetics. *Applied and environmental microbiology*, *69*(1), 113–121.
- Rosenfeld, E., Beauvoit, B., Rigoulet, M., & Salmon, J.-M. (2002). Non-respiratory oxygen consumption pathways in anaerobically-grown *Saccharomyces cerevisiae*: evidence and partial characterization. *Yeast*, *19*(15), 1299–1321.
- Rosenfeld, E., Schaeffer, J., Beauvoit, B., & Salmon, J.-M. (2004). Isolation and properties of promitochondria from anaerobic stationary-phase yeast cells. *Antonie van Leeuwenhoek*, *85*, 9–21.
- Saa, P. A., Moenne, M. I., Pérez-Correa, J. R., & Agosin, E. (2012). Modeling oxygen dissolution and biological uptake during pulse oxygen additions in oenological fermentations. *Bioprocess and Biosystems Engineering*, *35*(7), 1167–1178.
- Saa, P. A., Pérez-Correa, J. R., Celentano, D., & Agosin, E. (2013). Impact of carbon dioxide injection on oxygen dissolution rate during oxygen additions in a bubble column. *Chemical Engineering Journal*, *232*, 157–166.
- Sablayrolles, J., & Barre, P. (1986). Evaluation des besoins en oxygène de fermentations alcooliques en conditions oenologiques simulées. *Sci. Alim.*, *6*, 373–383.
- Sablayrolles, J., Dubois, C., Manginot, C., Roustan, J.-L., & Barre, P. (1996). Effectiveness of combined ammoniacal nitrogen and oxygen additions for completion of sluggish and stuck wine fermentations. *Journal of Fermentation and Bioengineering*, *82*(4), 377–381.

- Salmon, J.-M. (2006). Interactions between yeast, oxygen and polyphenols during alcoholic fermentations: Practical implications. *LWT - Food Science and Technology*, 39(9), 959–965.
- Silva, A., & Lambri, M. (2006). Oxygen measures and consumption in must and wine. *Analytica Chimica Acta*, 563, 391–395.
- Singleton, V. L. (1987). Oxygen with phenols and related reactions in musts, wines and model systems: observations and practical implications. *American Journal of Enology and Viticulture*, 38(1), 69–77.
- Vidal, B. S., & Aagaard, O. (2008). Oxygen management during vinification and storage of Shiraz wine. *The Australian and New Zealand Wine Industry Journal*, 23, 56–63.
- Vlassides, S., & Block, D. (2000). Evaluation of cell concentration profiles and mixing in unagitated wine fermentors. *American journal of enology and viticulture*, 51(1), 73–80.
- Wang, S. J., & Zhong, J. J. (1996a). A novel centrifugal impeller bioreactor. II. Oxygen transfer and power consumption. *Biotechnology and bioengineering*, 51(5), 520–527.
- Wang, S. J., & Zhong, J. J. (1996b). A novel centrifugal impeller bioreactor. I. Fluid circulation, mixing, and liquid velocity profiles. *Biotechnology and bioengineering*, 51(5), 511–519.

4. MODELLING OXYGEN DISSOLUTION AND BIOLOGICAL UPTAKE DURING PULSE OXYGEN ADDITIONS IN OENOLOGICAL FERMENTATIONS

Pedro A. Saa, **M. Isabel Moenne**, J. Ricardo Pérez-Correa and Eduardo Agosin

Published in Bioprocess and Biosystems Engineering, February 2012, Vol. 35, No. 7, p. 1167-1178 (DOI 10.1007/s00449-012-0703-7)

Abstract

Discrete oxygen additions during oenological fermentations can have beneficial effects both on yeast performance and on the resulting wine quality. However, the amount and time of the additions must be carefully chosen to avoid detrimental effects. So far, most oxygen additions are carried out empirically, since the oxygen dynamics in the fermenting must are not completely understood. To efficiently manage oxygen dosage, we developed a mass balance model of the kinetics of oxygen dissolution and biological uptake during wine fermentation on a laboratory scale. Model calibration was carried out employing a novel dynamic desorption–absorption cycle based on two optical sensors able to generate enough experimental data for the precise determination of oxygen uptake and volumetric mass transfer coefficients. A useful system for estimating the oxygen solubility in defined medium and musts was also developed and incorporated into the mass balance model. Results indicated that several factors, such as the fermentation phase, wine composition, mixing and carbon dioxide concentration, must be considered when performing oxygen addition during oenological fermentations. The present model will help develop better oxygen addition policies in wine fermentations on an industrial scale.

Keywords: Oxygen uptake, Oxygen dissolution, Wine fermentation, *Saccharomyces cerevisiae*, Modeling

Abbreviations

AIC	Akaike's Information Criterion
gDW	Gram of dry weight
OTR	Oxygen transfer rate
OUR	Oxygen uptake rate
RSS	Sum of the squared residuals

List of symbols

C_j	Concentration of the j compound [g/L]
H_w	Henry's constant in pure water [atm L / mg O ₂]
H_{mix}	Henry's constant in a multicomponent solution [atm L / mg O ₂]
K_j	Sechenov's constant for the j compound [L/g]
k_{La}	Oxygen volumetric mass transfer coefficient [1/h]
$k_{La_{strip}}$	Oxygen volumetric mass transfer coefficient due to CO ₂ bubbles produced during the fermentation [1/h]
n	Oxygen uptake model affinity parameter [-]
O_2	Dissolved oxygen concentration [mg O ₂ / L]
O_2^*	Oxygen equilibrium concentration [mg O ₂ / L]
$O_{2,crit}$	Oxygen uptake model parameter under agitated condition [mg O ₂ / L]
$O_{2,s}$	Oxygen uptake model parameter under non-agitated condition [mg O ₂ / L]
p_{O_2}	Oxygen partial pressure [atm]
q_{O_2}	Specific uptake rate of oxygen [mg O ₂ / g DW·h]
$q_{O_2,max}$	Maximum specific uptake rate of oxygen (model parameter) [mg O ₂ / g DW·h]
$t_{95\%}$	Response time [min]
X	Biomass concentration [g DW / L]

Greek letters

β_j	Oxygen solubility model parameter for the j compound [1/K]
θ_i	Model parameter i

4.1 Introduction

Wine fermentation is an anaerobic bioprocess. However, discrete oxygen additions are common practice in most wineries because they favor fermentation kinetics and biomass formation [1], and are beneficial to aroma diversity and color stability [2, 3]. Yeast cells have an absolute requirement for oxygen for the synthesis of several intracellular components, particularly sterols and unsaturated fatty acids, which are essential for plasma membrane integrity [4]. Under anaerobiosis, yeasts are able to incorporate grape-derived sterols, which promote initial growth and fermentative activity by substituting ergosterol in the cell membranes. However, if oxygen deficiency is maintained, the rapid accumulation of these phytosterols modifies the physicochemical properties of the yeast cell membrane, leading to sluggish fermentations [3].

Growth of *Saccharomyces cerevisiae* during alcoholic fermentation requires oxygen concentrations of 5–7.5 mg O₂/L [5, 6]. Nevertheless, oxygen could also be detrimental when added at the wrong moment or in too high concentrations, resulting in wine oxidation, color degradation and off-flavors synthesis [7]. Therefore, the amount and opportunity of oxygenation must be carefully managed to avoid such undesirable effects.

At present, oxygen additions are performed mostly empirically, since the kinetics of oxygen dissolution and oxygen consumption in the fermenting must are still poorly studied. During oxygen additions, oxygen from the air bubbles is transferred through the gas–liquid interface followed by liquid phase diffusion/bulk transport to the cells. Although this is a multi-step serial transport, in a well-dispersed system, the major resistance to oxygen transfer is in the liquid film surrounding the gas bubble [8]. In the

case of oxygen, the gas–liquid mass transfer is commonly modeled by the two-film theory of Whitman [9]. According to this theory, the volumetric mass transfer rate of oxygen can be described as the product of a volumetric mass transfer coefficient, k_La , and a driving force, the difference between oxygen equilibrium concentration, O_2^* , and the actual concentration of dissolved oxygen. The oxygen equilibrium concentration depends on several factors, such as temperature, oxygen partial pressure in the gas phase, pH and composition of the fermenting must or wine [10]. For instance, at atmospheric pressure and room temperature, when using air, the oxygen saturation in wine is reached at 6 mg/L; if the saturation is carried out in the same conditions with pure oxygen, levels of 30 mg/L can be achieved [11]. To the best of our knowledge, and despite many isolated data, there is no systematic study to calculate oxygen solubility in fermenting musts and wine at different temperatures and compositions.

The oxygen transfer rate (OTR) to the liquid phase depends mainly on the k_La coefficient. This coefficient is affected by several factors, e.g., oxygen gas flow rate, temperature, rheological characteristics and composition of the medium and system's turbulence [12–15]. The last term accounts for the hydrodynamic condition of the culture and it is fundamental for determining the k_La value [16]. In the case of stirred bioreactors, this term is commonly associated with the energy input of the system, while in the case of bubble columns and airlift reactors it is mainly influenced by the bubbles produced by the gas injection [8].

Another factor that could influence the estimated k_La value is the biological oxygen uptake [17–19]. When absorption with chemical reaction occurs in a liquid, the concentration profiles are disturbed by the chemical reaction causing an increase in the gradient and, consequently, an enhancement of the mass transfer rate. The ratio of such a rate to the rate of absorption without chemical reaction is called the enhancement factor, E [18]. This factor is explained by several mechanisms, both physical and chemical, which are mainly influenced by the operation conditions and culture features [19]. Since oxygen absorption into a fermentation broth is similar to gas absorption accompanied by a chemical reaction, in that dissolved oxygen is consumed by microorganisms while it diffuses from the gas–liquid interface, the mass transfer rate is

expected to be enhanced, as compared with pure physical absorption [17]. The latter is normally observed in cultures with relatively high oxygen uptake rate (OUR) compared to the k_{La} coefficient. When the k_{La} coefficient is relatively high, no influence of the biological oxygen uptake can be detected, because the enhancement is relatively small [18].

To determine the k_{La} under abiotic conditions, the conventional dynamic method is commonly employed [20]. In the case of solutions with growing aerobic microorganisms, the dynamic method based on the technique described by Taguchi and Humphrey [21] is preferred. The latter determines simultaneously both, the k_{La} and the OUR, by first turning off momentarily the gas inlet and then turning it back on. Casas et al. [22] proposed a new approach for simultaneous calculation of the volumetric transfer rate and the oxygen consumption rate in pneumatically aerated bioreactors, without interrupting the gas inlet. Instead, a step change in composition of the aeration gas is imposed without altering its flow rate, and thus, without altering the microbial growth. However, in the case of anaerobic processes like wine fermentation, there are no reported methods for systematically determining the k_{La} and the OUR during fermentation, without affecting its normal course.

Once oxygen is dissolved in the liquid phase, it is immediately consumed by the microorganism [23]. The OUR depends on both the biomass concentration and the specific OUR, and therefore changes during the fermentation. In wine fermentation, maximum OUR values up to 18 mg O₂/L·h have been reported at the end of the growth phase, the optimal time for oxygen addition [24]. However, the oxygen consumption rate is commonly determined off-line, i.e., outside of the bioreactor, after culture sampling, which might not take into account the influence of several factors encountered under oenological conditions, e.g., limited mixing or high carbon dioxide concentrations. Moreover, considering the high carbon dioxide production rates observed during the exponential phase of fermentation—up to 1.2 g/L·h, [25, 26]—and the low amounts of oxygen added, it can be argued that significant amounts of the added oxygen are not being consumed by the yeast, but are lost due to CO₂ stripping.

Hence, oxygen losses by stripping must also be quantified in order to accurately estimate the biological consumption.

In this work, we developed a dynamic oxygen mass balance model to properly describe the kinetics of oxygen dissolution and consumption, during laboratory scale oenological fermentations. We evaluated the quality of the model by applying several regression diagnostics tests, *e.g.*, parameter sensitivity (how changes in parameter values affect response variables), parameter identifiability (detection of cross correlation between parameters) and parameter significance (determine parameter confidence intervals). These tests are crucial tools for model validation and optimization, as they allow us to identify the most significant correlations between parameters and to reduce model's uncertainty [27]. The current model includes the influence of agitation and medium composition on the oxygen mass transfer and on biological consumption, as well as the impact of CO₂ stripping on the oxygen dynamics.

4.1.1 Model development

The resulting dynamic, oxygen mass balance model describes the response of oxygen dissolution and consumption kinetics under oenological conditions when an oxygen pulse is applied. The main model assumptions are:

- . Liquid film resistance around bubbles controls the overall mass transfer rate [18].
- . Dissolved oxygen is immediately consumed by the yeast [23].
- . During the addition of oxygen, the bubbles are uniformly distributed in the bioreactor.
- . Chemical oxygen consumption is negligible compared to biological consumption.

4.1.2 Oxygen mass balance

The general mass balance for the dissolved oxygen in the liquid phase can be rearranged as:

$$\frac{dO_2}{dt} = k_L a \cdot (O_2^* - O_2) - q_{O_2} (O_2) \cdot X \quad (1)$$

where dO_2/dt is the oxygen accumulation specific rate in the liquid phase, $k_L a$ is the volumetric oxygen mass transfer coefficient, X is the total biomass measured, O_2^* is the oxygen equilibrium concentration and $q_{O_2}(O_2)$ is the specific oxygen uptake rate, which depends on the dissolved oxygen concentration. The latter can be described as the product of two terms, the maximum specific OUR, $q_{O_2,max}$ and a function of the dissolved oxygen, $f(O_2)$. The incorporation of this last term to Eq. 1 allowed describing heterogeneous mixing conditions in the bioreactor, which could account for the oxygen concentration gradients present in oenological fermentations. The choice of the $f(O_2)$ function for describing different hydrodynamic conditions was, therefore, based on its ability to reproduce empirical data. Under ideal mixing conditions, we found that $f(O_2)$ can be described by a sigmoid function, similar to the Hill equation [8].

$$f(O_2) = \frac{O_2^n}{O_{2,crit}^n + O_2^n} \quad (2)$$

where $O_{2,crit}$ and n are empirical model parameters. The former represents the dissolved oxygen level necessary to reach half of the consumption response, and the latter is an affinity parameter. Under non-agitated conditions, i.e., mechanical mixing was avoided, a different $f(O_2)$ function was chosen since the shape of the uptake kinetics changed. A linear, single parameter ($O_{2,s}$) function was sufficient to describe the observed oxygen consumption kinetics.

$$f(O_2) = \frac{O_2}{O_{2,s}} \quad (3)$$

4.1.3 Oxygen solubility

To estimate the oxygen solubility in terms of the fermenting medium composition, an empirical log additivity model was developed and calibrated with data taken from the literature [28–30]:

$$\log_{10} \left(\frac{H_{\text{mix}}}{H_w} \right) = \sum_j^m K_j(T) \cdot C_j \quad (4)$$

where H_{mix} and H_w denote the Henry's constants in the solution and in the pure water, respectively; C_j denotes the concentration of the compound j in the solution; and K_j is the Sechenov constant, which is slightly dependent on the temperature and is specific to the solute and the gas [31]. The compounds considered in this model are mainly sugars and alcohols. Rischbieter and Schumpe [28] have demonstrated that the Sechenov constant can be well represented by a linear function of the temperature. We found that a simple proportionality relation (Eq. 5) was sufficient to fit the experimental data to the proposed model.

$$K_j(T) = \beta_j T \quad (5)$$

Where β_j is a model parameter estimated from the experimental solubility data of solutions containing only the compound j for the specific gas and T is the temperature in Kelvin. The Henry's constant of oxygen in pure water can be calculated using the empirical equation proposed by Rettich [32],

$$\ln(H_w) = A + \frac{B}{T} + \frac{C}{T^2} \quad (6)$$

where A , B and C are model parameters calculated from the experimental data. Using Henry's law and Eqs. 4, 5 and 6, the dissolved oxygen concentration in equilibrium with the bulk gas phase is given by,

$$O_2^* = \frac{P_{O_2}}{H_{\text{mix}}} \quad (7)$$

where p_{O_2} is the oxygen partial pressure in the gas phase.

4.2 Materials and methods

4.2.1 Yeast strain

The commercial *S. cerevisiae* wine strain EC1118 Prise de Mousse (Lalvin, Zug, Switzerland) was used in these experiments. Yeasts were precultured in YPD medium at 28 °C in 125 mL Erlenmeyer flasks.

4.2.2 Culture media and fermentation conditions

Batch fermentations were carried out in a Bioflo IIc bioreactor (New Brunswick Scientific Co., Edison, N.J.) starting with 2.5 L of modified MS300 medium [33] containing (per liter): 120 g of glucose, 6 g of DL-malic acid, 6.32 g of citric acid monohydrate, 156 mg of $\text{CaCl}_2 \cdot 2\text{H}_2\text{O}$, 750 mg of KH_2PO_4 , 500 mg of K_2SO_4 , 250 mg of $\text{MgSO}_4 \cdot 7\text{H}_2\text{O}$, 200 mg of NaCl, 4 mg of $\text{MnSO}_4 \cdot \text{H}_2\text{O}$, 7.2 mg of $\text{ZnSO}_4 \cdot 7\text{H}_2\text{O}$, 1 mg of $\text{CuSO}_4 \cdot 5\text{H}_2\text{O}$, 1 mg of KI, 0.4 mg of $\text{CoCl}_2 \cdot 6\text{H}_2\text{O}$, 1 mg of H_3BO_3 , 1 mg of $\text{NaMoO}_4 \cdot 2\text{H}_2\text{O}$, 20 mg of myoinositol, 2 mg of nicotinic acid, 1.5 mg of calcium pantothenate, 0.25 mg of thiamine hydrochloride, 0.003 mg of biotin and 0.25 mg of pyridoxine hydrochloride. The ammoniacal nitrogen and amino acid concentration in the medium were the same used by Salmon and Barre [33], except that we did not use proline. The initial nitrogen concentration for batch fermentations was 300 mg/L. The inoculation was done to obtain 10⁶ cells/mL. The pH and temperature were maintained at 3.5 and 25 °C, respectively, while the stirring speed was set to 300 rpm throughout the cultivation.

4.2.3 Analytical techniques

Periodic samples were taken to analyze biomass (dry cell weight per liter) and the concentration of main metabolites, following the method described in Varela et al. [34].

4.2.4 Oxygen additions

During the fermentation course, addition of 0.3 L/min of pure oxygen (99.7% purity) was carried out during 1 min approximately, with and without agitation after the addition. To study the agitation effect on the oxygen consumption kinetics, oxygen

pulses without agitation were carried out during the exponential growth phase ($X > 2.5$ g DW/L). The additions were performed using a cylindrical pore diffuser with a pore mean diameter of ~ 20 μm at the bottom of the bioreactor. The oxygen pulse was stopped when dissolved oxygen reached 3–6 mg/L, levels that were reported to be beneficial for yeast performance [6].

4.2.5 Dissolved oxygen

The oxygen concentration was measured with a 3 LCD-trace Fibox v7 machine (PreSens[®], Regensburg, Germany) that included temperature compensation. This optical sensor does not have the problems of the Clark's electrode, e.g., relatively long response times and oxygen consumption during the measurement [35]. Moreover, most of these electrodes have a response time close to the characteristic time for the mass transfer process, and the measured concentrations are, therefore, influenced by the dynamics of the measurement device [8]. The oxygen kinetics were followed with two optical sensors PSt3 (PreSens[®], Regensburg, Germany) placed inside the reactor with ideal measurement ranges for dissolved oxygen between 0 and 45 mg/L: one measuring the dissolved oxygen within the liquid phase and the other the oxygen partial pressure inside the reactor headspace.

4.2.6 Oxygen solubility

Saturation experiments were performed with synthetic air (20% oxygen and 80% nitrogen from Indura, Santiago, Chile) and pure oxygen (99.7% purity also from Indura) using different test solutions in a 2.5-L agitated Bioflo IIc bioreactor and measured with the 3 LCD-trace Fibox v7 device. First, all dissolved gases were desorbed by nitrogen injection until oxygen concentrations lower than 40 $\mu\text{g/L}$ were reached. Then, pure oxygen or synthetic air was injected until the liquid phase reaches saturation with oxygen. Equilibrium concentration was recorded when dissolved oxygen concentration variations were less than $\pm 1\%$.

4.2.7 $k_L a$ measurements in synthetic solution

The estimation of the volumetric mass transfer coefficient in a model solution without biomass was performed using the conventional dynamic method described by Devatine et al. [20]. Measurements were carried out in a liquid medium that mimics the exponential growth phase (per liter): 80 g of glucose, 1.5 g of glycerol, 12.6 g of ethanol, 50 mg of nitrogen, 6.32 g of citric acid monohydrate, 6 g of DL-malic acid, 156 mg of $\text{CaCl}_2 \cdot 2\text{H}_2\text{O}$, 525 mg of KH_2PO_4 , 350 mg of K_2SO_4 , 160 mg of $\text{MgSO}_4 \cdot 7\text{H}_2\text{O}$, 140 mg of NaCl , 2.8 mg of $\text{MnSO}_4 \cdot \text{H}_2\text{O}$, 5 mg of $\text{ZnSO}_4 \cdot 7\text{H}_2\text{O}$, 0.7 mg of $\text{CuSO}_4 \cdot 5\text{H}_2\text{O}$, 0.7 mg of KI , 0.28 mg of $\text{CoCl}_2 \cdot 6\text{H}_2\text{O}$, 0.7 mg of H_3BO_3 and 0.7 mg of $\text{NaMoO}_4 \cdot 2\text{H}_2\text{O}$. The influence of dissolved carbon dioxide on the volumetric mass transfer coefficient was also assessed using this medium. Measurements were carried out in the synthetic medium without dissolved carbon dioxide and with carbon dioxide saturation concentrations of 1.2 g/L at 25 °C.

4.2.8 Parameter fitting

The most common and reproducible method for measuring the OUR is the standard dynamic method [23], which is only suitable for continuous aeration processes, but it is impracticable for wine fermentation. Instead, we propose a dynamic method for modeling the OUR and OTR during the addition of controlled oxygen pulses based on the absorption–desorption cycle shown in Fig. 4-1. First, the OUR model parameters ($q_{\text{O}_2, \text{max}}$, n and $\text{O}_{2, \text{crit}}$) and the oxygen stripping term ($k_L a_{\text{strip}}$) are dynamically estimated from the desorption curve until the dissolved oxygen concentration is $\sim 40 \mu\text{g/L}$. The oxygen mass balance during the desorption stage is given by,

$$\frac{d\text{O}_2}{dt} = -k_L a_{\text{strip}} \cdot \text{O}_2 - q_{\text{O}_2}(\text{O}_2) \cdot X \quad (8)$$

where $k_L a_{\text{strip}}$ corresponds to the volumetric oxygen mass transfer coefficient caused by the carbon dioxide bubbles naturally present during the fermentation. Then, the volumetric oxygen mass transfer coefficient ($k_L a$) is estimated from the absorption curve using the oxygen uptake model parameters previously fitted and the oxygen

solubility model, thus completing the cycle. In this case, Eq. 1 applies.

Model parameters were estimated in each stage by minimizing the sum of squared residual errors between predicted and experimental data,

$$\text{Min}_{\Theta} \sum_k^N (O_2^{\text{model}} - O_2^{\text{meas}})^2 \quad (9)$$

where Θ denotes the parameter space, O_2^{model} is the dissolved oxygen concentration predicted, O_2^{meas} is the dissolved oxygen concentration measured and N represents the number of measurements. This procedure was solved numerically using integration and non-linear optimization routines within MATLAB[®]. We found the local solver *fminsearch* to be effective for dynamic optimization of the oxygen mass balance model parameters and *nlinfit* for non-linear regression of the oxygen solubility model parameters. The function *ode113*, a variable order of Adams–Bashforth–Moulton solver, was employed for ODE integration.

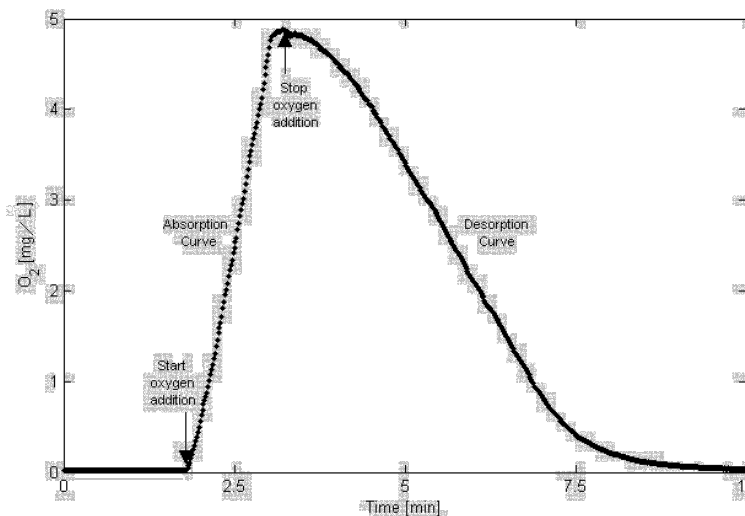


Figure 4-1: A typical absorption-desorption cycle occurring during an oxygen impulse of 0.3 L/min under oenological fermentations, at 25°C. Biomass, ethanol and glucose concentrations were 4.0 g DW/L, 33.4 g/L and 70.5 g/L, respectively. The determination of the model parameters is carried out in two steps: first, the OUR model parameters and the oxygen stripping term ($k_{L,a_{\text{strip}}}$) are dynamically estimated from the desorption curve, using Eq.8; then, using these results –i.e., the experimental data of the absorption curve and Eq. 1 – the volumetric mass transfer coefficient for oxygen is calculated

4.2.9 Regression diagnostics

The procedures required to test the quality of the parameter estimation consider the

calculation of the parameter sensitivity, parameter identifiability and parameter significance. These tests were performed as described by Sacher et al. [27], except that in the case of the 95% confidence interval calculation; the MATLAB® functions *nparci* and *nlpredci* were applied. The analysis of the results of the regression diagnostics allowed us to postulate models with different number of parameters. To compare goodness-of-fit of these models, Akaike's Information Criterion (AIC) was employed [36]. The AIC is calculated as [37]:

$$AIC = N \ln \left(\frac{RSS}{N} \right) + 2(p+1) + \frac{2(p+1)(p+2)}{(N-p-2)} \quad (10)$$

where RSS is the sum of the squared residuals and p is the number of parameters to fit. The model with the smallest AIC is the recommended choice [36].

4.3 Results and discussion

4.3.1 Calibration of the oxygen solubility model

The substances considered in the model were those with the higher concentrations during the fermentation course, i.e., ethanol, glucose and fructose. The influence of organic acids on oxygen solubility was neglected, because of their relatively low concentrations in wines [38]. Oxygen solubility data in pure water at different temperatures was obtained from the work of Wilhelm et al. [39], and then used to fit the parameters in Eq. 6. In the case of glucose and fructose, experimental results reported by Eya et al. [40] and Mishima et al. [41] were used, respectively. The situation is more complex in the case of oxygen solubility in hydroalcoholic solutions. Several authors [31, 42, 43] have shown that, at low ethanol concentrations, and depending upon the temperature, an increase or decrease of the oxygen solubility was observed [12]. For parameter calibration, we used the results obtained by Cargill [42] for hydroalcoholic solutions, where a decrease of oxygen solubility up to 0.15 ethanol mole fraction was reported. The fitted parameters are shown in Table 4-1 with their corresponding 95% confidence intervals.

Table 4-1: Fitted parameters of the oxygen solubility model for temperatures ranging between 15 and 37°C

Model	Parameter	Value
Henry's constant in pure water	A	-5.9 ± 1.2
$\ln(H_w) = A + \frac{B}{T} + \frac{C}{T^2}$	B	$3.0 \times 10^3 \pm 7.1 \times 10^2$
A [-], B [K], C [K ²]	C	$-6.9 \times 10^5 \pm 1.0 \times 10^5$
Sechenov constant	β_{glu}	$2.3 \times 10^{-6} \pm 1.7 \times 10^{-7}$
$K_j(T) = \beta_j T$	β_{fru}	$2.2 \times 10^{-6} \pm 1.5 \times 10^{-7}$
β_j [L / g·K]	β_{etOH}	$1.2 \times 10^{-6} \pm 8.2 \times 10^{-8}$

Model predictions agreed with validation experiments performed at 25 °C with a mean relative error of 2.1% (Table 4-2). Larger deviations in validation experiments are observed in saturation experiments performed with air, although the relative error is low (< 3%). This result can be explained because the model was calibrated using only solubility data with pure oxygen. Another possible source of error in the determination of oxygen solubility is that the oxygen partial pressure was not corrected by the water vapor pressure at 25°C, though its value is very low (~ 0.03 atm) under the conditions considered. We suspect that this term in our case can be neglected, since the experimental set-up for determining oxygen saturation concentration used a continuous flow of pure oxygen or synthetic air equilibrated at 1 atm. In fact, comparison with more complicated methods already published in the literature for measuring oxygen solubility in artificial media [44] show agreement with our solubility data. Finally, given that the experimental measurement error of the data used for parameter fitting and the precision of the validation experiments were around ± 1.5 and $\pm 1\%$, respectively, the proposed model showed satisfactory results which fell within the measurement's experimental error. These results also agreed with the results obtained using the solubility model proposed by Rasmussen and Rasmussen [44] for different artificial media.

Table 4-2: Validation of the oxygen solubility model at 25°C

Medium	O ₂ [*] with air in mg/L			O ₂ [*] with pure oxygen in mg/L		
	Exp.	Model	Rel. error (%)	Exp.	Model	Rel. error (%)
Distilled water	8.0	7.9	1.3	38.7	39.2	1.3
12% v/v ethanol	7.1	7.3	2.8	36.8	36.4	1.1
8% v/v ethanol, 55 g/L fructose, 25 g/L glucose	6.8	6.6	2.9	33.9	33.0	2.7
Fermentation medium ^a	7.0	6.8	2.9	34.8	34.2	1.7

^a Composition is the same used in k_{La} measurements in synthetic solution described in Materials and Methods

4.3.2 Oxygen uptake rate model calibration under perfect mixing conditions

To determine the optimal OUR model, we first performed calibrations considering the four model parameters for each pulse addition experiment. Parameter significance tests showed that during the stripping stage, $k_{La_{strip}}$ lacked statistical significance; hence, it could be discarded from the model. The latter was experimentally verified, by showing that almost no oxygen could be measured in the headspace after stopping oxygen addition (data not shown). Furthermore, oxygen balance showed that < 3.5% of the injected oxygen was lost by CO₂ stripping.

The model was then calibrated with three parameters: n , $q_{O_2;max}$ and $O_{2,crit}$. This reduced parameter model featured smaller confidence intervals and increased the significance of the parameter set; however, some identifiability problems were encountered, in particular, in the case of parameters $q_{O_2;max}$ and n . The estimated correlation coefficient, κ , for these parameters was 0.98 for the experimental time. On the other hand, the sensitivity analysis

showed that the $O_{2,crit}$ parameter presents a relatively low sensitivity (Fig. 4-2). In addition, fitted values ranged between 0.18 and 0.45 mg/L. Hence, to solve this lack of identifiability, $O_{2,crit}$ was arbitrarily set to 0.3 mg/L. Normally, one can fix those parameters whose values are given in the literature or can be obtained by independent experiments [45–48]; however, this was not our case, since there are no related data about this parameter. Nonetheless, the employed value agrees with the literature, since the saturation constant of oxygen for *S. cerevisiae*, K_o , is in the range of 1–10 μ M,

which corresponds approximately to oxygen concentrations of 0.03–0.33 mg/L at 25 °C and 1 atm of air [8].

The reduced parameter space improved the parameter significance and solved the lack of determinability. Model 3 showed the smallest AIC (Table 4-3), confirming that this was the best choice.

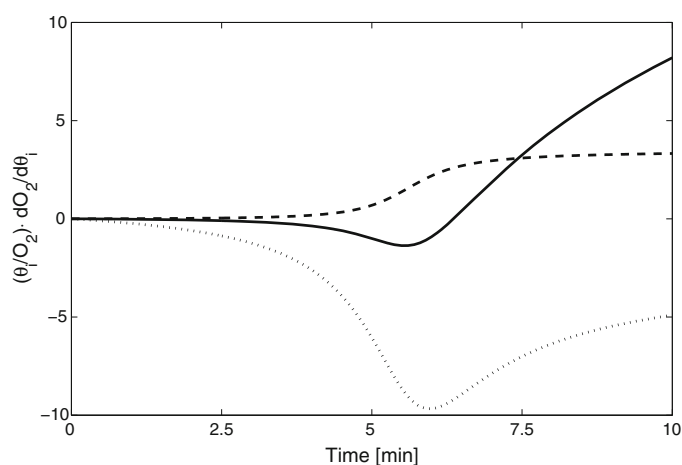


Figure 4-2: Time-dependent normalized sensitivities of the OUR parameters model during the experiment. The *solid line* corresponds to the sensitivity of the parameter n , while the *dashed* and *dotted lines* represent the sensitivities of the $O_{2,crit}$ and $q_{O_2,max}$ parameters, respectively

Table 4-3: Comparison of the different models

Model	Estimated parameters	Significant parameters	Correlated parameters	AIC
1	$k_L a_{strip}, n, q_{O_2,max}, O_{2,crit}$	$n, q_{O_2,max}, O_{2,crit}$	$k_L a_{strip}, q_{O_2,max}$	-828
2	$n, q_{O_2,max}, O_{2,crit}$	$n, q_{O_2,max}, O_{2,crit}$	$n, q_{O_2,max}$	-845
3	$n, q_{O_2,max}$	$n, q_{O_2,max}$	–	-867

4.3.3 Comparison of experimental results and model predictions

Oxygen consumption kinetics, as well as the two parameter OUR model fitting, are illustrated in Fig. 4-3. As previously mentioned, the decrease in the dissolved oxygen concentration corresponds to biological consumption of oxygen by the yeast. Oxygen consumption under anaerobic conditions is explained mainly by the oxygen utilization in sterols and unsaturated fatty acids pathways and other cellular processes that still are

not well characterized [49].

The proposed two parameter OUR model fits the data well, with mean relative differences with the experimental data of 2%. As expected, oxygen consumption rates strongly depend on the biomass concentration (Fig. 4-3). Under perfect mixing conditions, the first part of the oxygen consumption kinetics can be represented by a straight line, as in aerobic processes, at least until dissolved oxygen concentration reaches 0.6–0.8 mg/L ($\approx 2 \cdot O_{2,crit}$). When the dissolved oxygen falls below this critical level, the oxygen consumption rate decreased significantly, until a plateau was reached. This behavior is mainly described by the $f(O_2)$ function for low oxygen concentrations and agrees with Doran [50], who reports a critical level for dissolved oxygen concentration beyond which the specific oxygen consumption rate (q_{O_2}) by a microorganism reaches a maximum constant level $q_{O_2,max}$. Below this level, q_{O_2} is largely influenced by the dissolved oxygen concentration, falling in an oxygen-limiting region (Fig. 4-4a).

According to the proposed model, the specific OUR depends not only on $O_{2,crit}$ but also on n . When the value of n increases, the maximum specific OUR is reached faster in the oxygen-limiting region ($O_2 < 2O_{2,crit}$) (Fig. 4-4a). Considering that the higher the biomass concentration the larger the values of n (Fig. 4-4b), it appeared that the culture becomes more sensitive to low oxygen levels at higher biomass concentrations. The latter could also contribute to explain why oxygen additions performed at the end of the cell growth phase are key to completing the fermentation [24].

OUR depends on biomass content and the specific OUR. Model calibrations show that the specific OUR varies during the fermentation (Fig. 4-5). Maximum specific rates of 16.2–19.8 mg O_2 /g DW·h were observed during the exponential growth phase, i.e., for $X \approx 4.0$ g DW/L, while the oxygen consumption rate decreased at the end of the growth phase (11.8–14.4 mg O_2 /g DW·h). This trend is similar to the one observed for microorganisms growing in aerobic cultures; however, the computed values for *S. cerevisiae* wine strain are comparatively lower than those of similar aerobic microorganisms [23].

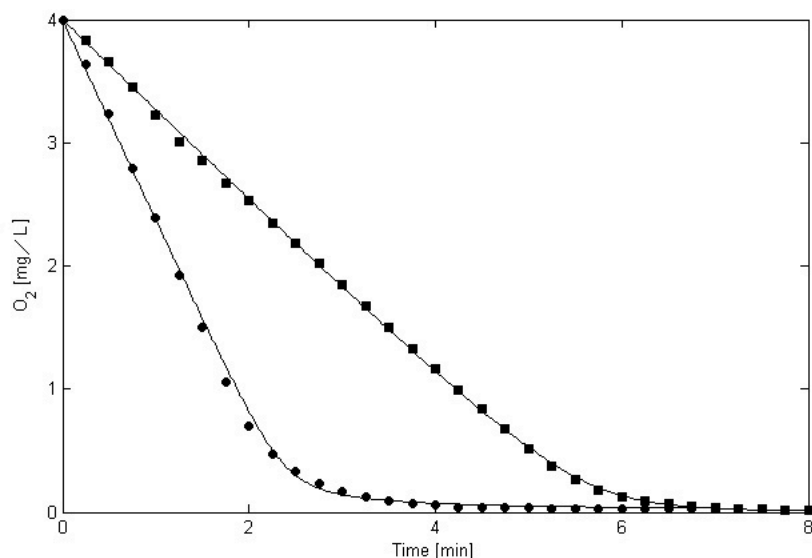


Figure 4-3: Oxygen uptake rate model for different biomass concentrations during oenological fermentations at 25°C. The black squares and circles correspond to experimental measurements performed with biomass concentrations of 2.9 and 5.0 g DW/L, respectively. Solid lines represent model predictions. The fitted parameters were $O_{2,crit}=0.3$ mg/L, $q_{O_2,max}=16.2$ mg O_2 /g DW·h and $n=1.5$ in the case of $X=2.9$ g DW/L, while in the case of $X=5.0$ g DW/L the fitted parameters were $O_{2,crit}=0.3$ mg/L, $q_{O_2,max}=19.4$ mg O_2 /g DW·h and $n=2.3$

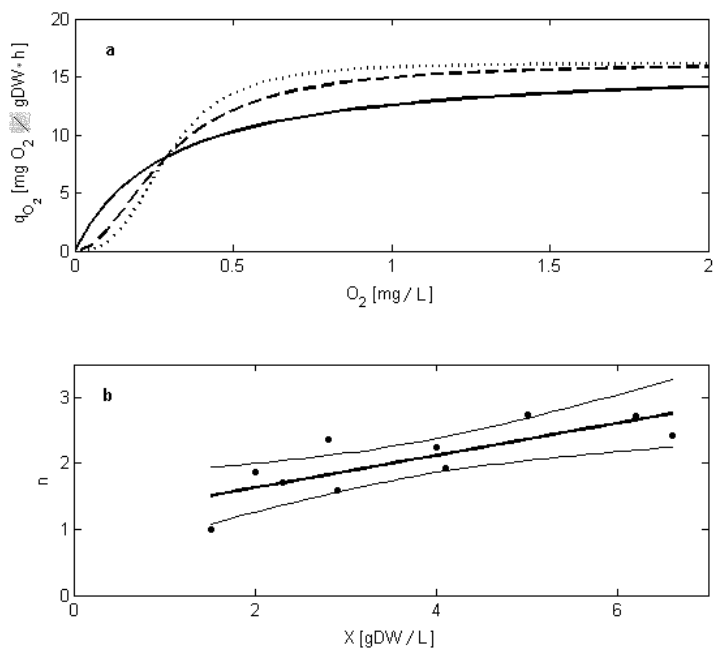


Figure 4-4: Specific oxygen consumption kinetics by *Saccharomyces cerevisiae* and increase of the parameter n with the biomass concentration. **a** Behavior for different n values (*solid line* $n=1$, *dashed line* $n=2$ and *dotted line* $n=3$). **b** Fitting of n for different biomass concentrations (the higher the biomass concentration the larger the values of n). The *thicker line* represents a linear regression between both variables, while the *thinner lines* denote the 95% confidence interval of the trend of the fitted values (*black dots*)

Maximum OUR values were reached at the end of the growth phase, as already reported by Sablayrolles [24]. However, OUR values estimated in the present research are considerably higher than the values reported in the literature. Maximum OUR values reached up to 108 mg O₂/L·h, which is approximately six times greater than the values reported in previous articles [6, 24]. This difference can be explained by the different methods employed for measuring the oxygen uptake. Previous works employed oxygen electrodes for measuring the oxygen uptake. These types of sensors require a continuous flow of oxygen through a prepared culture sample because they consume oxygen during the measurement. For this reason, they cannot be used to measure the consumption directly in the bioreactor. On the contrary, optical sensors such as those employed in this study allow measuring the dissolved oxygen concentration in situ under more realistic conditions and without interfering with the oxygen uptake because they do not consume oxygen.

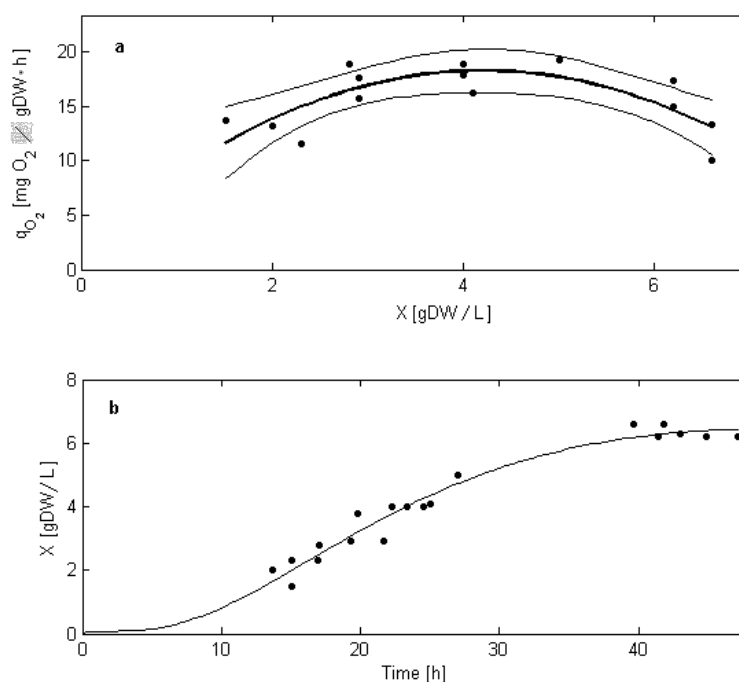


Figure 4-5: Specific oxygen uptake rate optimization and biomass growth. **a** Evolution of the specific oxygen uptake rate with the biomass concentration. The *thicker line* represents a quadratic regression between both variables, while the *thinner lines* denote the 95% confidence interval of the trend of the fitted values (*black dots*). **b** Biomass concentration along the fermentation. *Black dots* represent biomass concentration measurements and the *solid line* represents the fermentation course

4.3.4 Oxygen uptake rate model calibration under non-agitated conditions

In contrast with the model developed for agitated conditions, the model proposed for describing oxygen uptake kinetics under non-agitated conditions lacked structural identifiability, since the $q_{O_2, \max}$ and $O_{2,s}$ parameters are correlated ($\kappa = 1.0$). Considering that the $q_{O_2, \max}$ parameter changes continuously during the fermentation depending on the growth phase, and that we do not have reliable values for the $O_{2,s}$ parameter, we decided to estimate them together as one single key parameter, $q_{O_2, \max}/O_{2,s}$. As expected, this modification solved the model's identifiability problem.

4.3.5 Influence of agitation conditions upon the oxygen uptake response time

Figure 4-6 shows the different model fittings obtained with and without agitation for the same biomass concentration. Satisfactory fittings were obtained in the case of no agitation, confirming the suitability of the $f(O_2) = O_2/O_{2,s}$ function chosen. Mean relative differences with the experimental data were around 5%. As illustrated in Fig. 4-6, the oxygen response curve in non-agitated conditions is different from that in agitated conditions, both in shape and time of decay.

The influence of the mixing conditions on the oxygen uptake response time was assessed by comparing the response time for both kinetics [51]. The response time, $t_{95\%}$, is the time needed to reach the $\pm 5\%$ interval of its final value and to stay there. Using the respective expressions for the oxygen uptake under mixing and non-mixing cultivation, the response times in both conditions can be calculated as,

$$t_{95\%}^{\text{mixing}} = \frac{0.95 \cdot O_2(t=0)}{q_{O_2} \cdot X} \quad (11)$$

$$t_{95\%}^{\text{no mixing}} = \frac{\ln(20) \cdot O_{2,s}}{q_{O_2} \cdot X} \quad (12)$$

The estimated constants were statistically different—t test for unequal variances at 95% confidence level gave a p value of 6.4×10^{-3} —reaching 3.0 ± 0.8 and 7.9 ± 2.2 min for

the agitated and non-agitated conditions, respectively. Hence, the hydrodynamic condition significantly affects the response time of the oxygen uptake kinetics. When the culture is non-agitated, the response time increases by a factor of 1.5–2.6, confirming results reported in the literature of the importance of mixing during mass transfer in biological uptake processes [16]. Cascaval et al. [15] showed that a unique distribution of OTRs occurred within a stirred bioreactor, depending on the geometrical and operational characteristics of the vessel, medium composition and type and concentration of the microorganism, among other factors. In the case of *S. cerevisiae* broths, it was observed that the tendency of yeast cells to settle plays a key role in the OTRs distribution. This result can help to understand why the oxygen uptake response is different. Without agitation, yeast cells tend to accumulate at the bottom, slowing down the measured response at the location of the probe and changing the slope of the oxygen uptake curve.

Finally, oxygen partial pressure measurements at the reactor headspace found no significant differences in the oxygen lost by stripping between agitated and non-agitated cultures (mean relative difference < 1%).

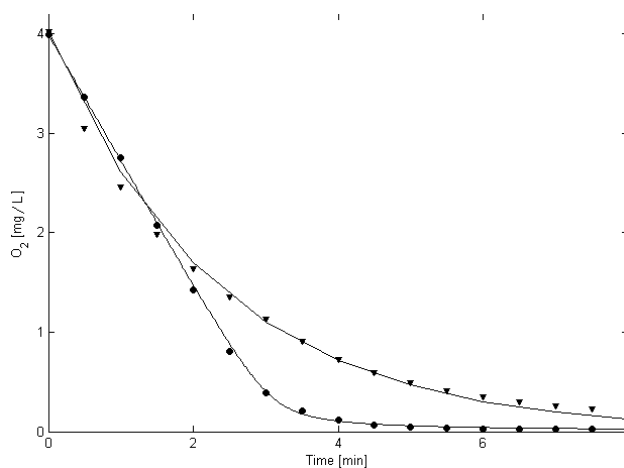


Figure 4-6: Comparison of different oxygen consumption dynamics for different hydrodynamic conditions. The biomass concentration in both cases was 4.0 g DW/L. For both experiments, the pH and temperature were maintained at 3.5 and 25°C, respectively. The *black circles* correspond to the oxygen uptake measurements at a stirring speed of 300 rpm, while the *black triangles* denote measurements without agitation. *Solid lines* represent model predictions. The fitted parameters were $O_{2,crit}=0.3$ mg/L, $q_{O_2,max}=19$ mg O₂/g DW·h and $n=2.2$ in the case with agitation, while in the case without agitation the fitted parameter was $q_{O_2,max}/O_{2,s}=0.4$ L/g DW·h

4.3.6 Oxygen mass transfer under oenological conditions

The developed models for oxygen solubility and OUR were employed to properly estimate the k_{La} coefficient during the absorption stage (Fig. 4-7a). The estimated k_{La} values increased from 5.14 to 13.43 1/h, when OUR increased from 20 to 108 mg O₂/L·h. Similar trends have been reported for aerobic cultures [52–55] also. Moreover, it was found that the k_{La} and the OUR can be linearly correlated. However, k_{La} values obtained when biomass was present are lower than the k_{La} estimated in a synthetic solution saturated with 1.2 g/L of CO₂ without biomass (16.7 ± 0.5 1/h). Thus, the oxygen transfer observed with biomass present is slower than without biomass (Fig. 4-7b). The latter could result from compositional changes of the culture, as well as from an increase in the broth's viscosity during the fermentation course. The increased medium viscosity increases the liquid film resistance to mass transport, negatively affecting the volumetric mass transfer coefficient [15, 23]. Hence, the positive effect of the OUR on the OTR is not large enough to compensate the increased mass transport resistance of the medium during the absorption of oxygen under oenological conditions.

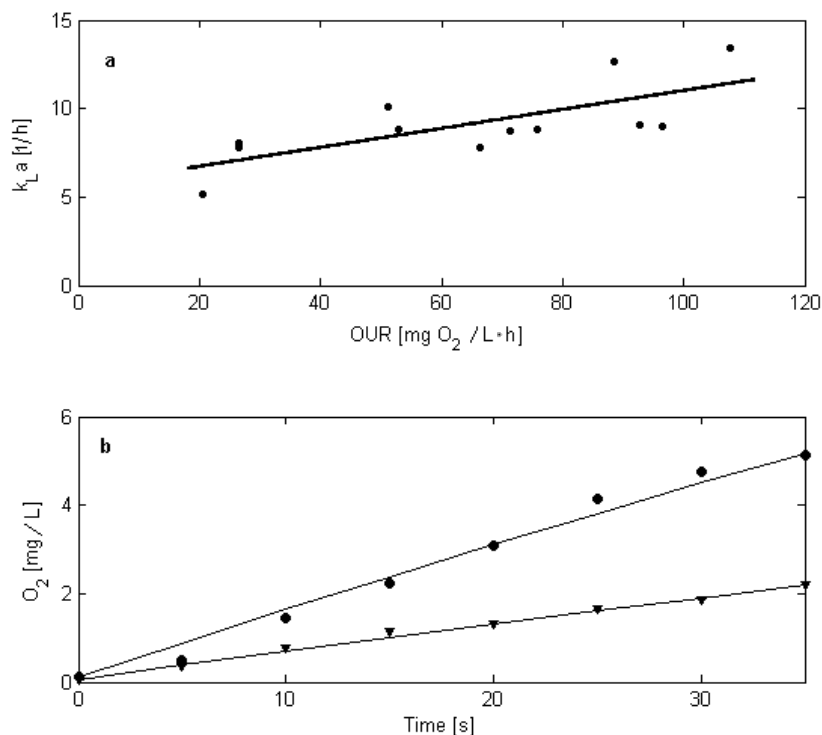


Figure 4-7: Oxygen mass transfer under oenological conditions. **a** Correlation between the oxygen uptake rate and the estimated k_{La} . The *thicker line* represents a linear regression between both variables ($R=0.72$). **b** Comparison of different absorption curves in microbial culture (*black triangles*, $k_{La}=8.2$ 1/h) and in sterile medium (*black dots*, $k_{La}=16.6$ 1/h). *Solid lines* denote the model predictions. The biomass concentration was 2.9 g DW/L in the case of the medium with oxygen consuming yeast. The estimated oxygen solubilities were 34.2 mg/L in the sterile medium and 33.5 mg/L in the microbial culture

4.3.7 Influence of the dissolved carbon dioxide upon the mass transfer coefficient

The dissolved carbon dioxide effect upon the estimated k_{La} in synthetic fermentation media was also assessed. Estimations of the k_{La} were carried using the conventional dynamic method [20]. The k_{La} value obtained in CO₂ free media was 47.2 ± 7.2 1/h, three times higher than the value obtained in the same solution saturated with 1.2 g/L carbon dioxide. Similar results were reported by Devatine et al. [20] for wines, thus confirming the negative influence of the carbon dioxide on the estimated k_{La} value in oenological fermentations.

4.4 Conclusions

The experimental methodology employed in this research allowed us to develop a model of the oxygen kinetics under similar conditions to those encountered in oenological fermentations on an industrial scale. The model accurately describes the oxygen kinetics observed during discrete oxygen additions under oenological conditions on a laboratory scale. We showed that the specific OUR of the *S. cerevisiae* wine strain strongly depends on the growth phase and that the oxygen mass transfer coefficient is modified by the biological uptake. Estimated k_La values increased from 5.14 to 13.43 1/h, when OUR increased from 20 to 108 mg O₂/L·h. However, our results suggest that the positive effect of the biological uptake on the oxygen mass transfer coefficient is not large enough to compensate the increased mass transport resistance of the medium due to compositional changes of the culture and the increased viscosity of the broth. The present model showed that agitation conditions have a significant effect on both the oxygen consumption response time and the shape of the response curve. Finally, experimental and model results confirmed the negative effect of high levels of carbon dioxide upon the mass transfer coefficient, although oxygen stripping due to CO₂ bubbles is negligible during uptake.

Acknowledgments

This work was carried out with the support from the National Fund for Scientific and Technological Development of Chile (FONDECYT) No. 1090520. M. Isabel Moenne is supported by a doctoral fellowship from the Chilean National Council of Scientific and Technological Research (CONICYT). We are particularly grateful to Claudio Gelmi for providing the sensitivity and determinability MATLAB[®] routines, to Claudia Sanchez (INDURA S.A., Santiago, Chile) for supplying the certified gases used for calibration of the Presens instrument and to the reviewers for their thorough and constructive comments that contributed significantly to improve the final manuscript.

References

1. Fornairon-Bonnefond C, Demaretz V, Rosenfeld E, Salmon J (2002) Oxygen addition and sterol synthesis in *Saccharomyces cerevisiae* during enological fermentation. *J Biosci Bioeng* 93: 176–182
2. Pérez-Magariño S, Sánchez-Iglesias M, Ortega-Heras M, González-Huerta C, González-Sanjosé M (2007) Colour stabilization of red wines by microoxygenation treatment before malolactic fermentation. *Food Chem* 101:881–893
3. Salmon J (2006) Interactions between yeast, oxygen and polyphenols during alcoholic fermentations: practical implications. *LWT Food Sci Technol* 39:959–965
4. Blayteron L, Sablayrolles J (2001) Stuck and slow fermentations in enology: statistical study of causes and effectiveness of combined additions of oxygen and diammonium phosphate. *J Biosci Bioeng* 91:184–189
5. Rosenfeld E, Schaeffer J, Beauvoit B, Salmon J (2004) Isolation and properties of promitochondria from anaerobic stationary- phase yeast cells. *Antonie Van Leeuwenhoek* 85:9–21
6. Sablayrolles J, Barre P (1986) Evaluation des besoins en oxygene de fermentations alcooliques en conditions oenologiques simulees. *Sci Alim* 6:373–383
7. Adoua R, Mietton-Peuchot M, Milisic V (2010) Modelling of oxygen transfer in wines. *Chem Eng Sci* 65:5455–5463
8. Villadsen J, Nielsen J, Lidén G (2011) *Bioreaction engineering principles*. Springer, New York
9. Whitman W (1923) A preliminary experimental confirmation of the two-film theory of gas absorption. *Chem Metal Eng* 29: 146–148
10. Singleton V (1987) Oxygen with phenols and related reactions in musts, wines and model systems: observations and practical implications. *Am J Enol Vitic* 38:69–77
11. Singleton V (2000) A survey of wine aging reactions, especially with oxygen. In: *Proceedings of the ASEV, 50th Anniversary Annual Meeting*, pp 323–336
12. Chiciuc I, Farines V, Mietton-Peuchot M, Devatine A (2010) Effect of wine properties and operating mode upon mass transfer in micro-oxygenation. *Int J Food Eng*. doi:10.2202/1556-3758. 1770

13. García-Ochoa F, Gómez E, Santos V (2000) Oxygen transfer and uptake rates during xanthan gum production. *Enzyme Microb Technol* 27:680–690
14. Jamnongwong M, Loubiere K, Dietrich N, Hébrard G (2010) Experimental study of oxygen diffusion coefficients in clean water containing salt, glucose or surfactant: consequences on the liquid-side mass transfer coefficients. *Chem Eng J* 165:758–768
15. Casçaval D, Galaction A, Turnea M (2011) Comparative analysis of oxygen transfer rate distribution in stirred bioreactor for simulated and real fermentation broths. *J Ind Microbiol Biotechnol* 38:1449–1466
16. Gagnon H, Lounes M, Thibault J (1998) Power consumption and mass transfer in agitated gas-liquid columns: a comparative study. *Can J Chem Eng* 76:379–389
17. Merchuk J (1977) Further considerations on the enhancement of oxygen transfer in fermentation broths. *Biotechnol Bioeng* 19:1885–1889
18. García-Ochoa F, Gómez E (2009) Bioreactor scale-up and oxygen transfer rate in microbial processes: an overview. *Biotechnol Adv* 27:153–176
19. Ruthiya K, Van der Schaaf J, Kuster B, Schouten J (2003) Mechanisms of physical and reaction enhancement of mass transfer in a gas inducing stirred slurry reactor. *Chem Eng J* 96:55–69
20. Devatine A, Chiciuc I, Poupot C, Mietton-Peuchot M (2007) Micro-oxygenation of wine in presence of dissolved carbon dioxide. *Chem Eng Sci* 62:4579–4588
21. Taguchi H, Humphrey A (1966) Dynamic measurement of the volumetric oxygen transfer coefficient in fermentation systems. *J Ferment Technol* 44:881–889
22. Casas J, Rodríguez E, Oller I, Ballesteros M, Sánchez J, Fernández J, Chisti Y (2006) Simultaneous determination of oxygen consumption rate and volumetric oxygen transfer coefficient in pneumatically agitated bioreactors. *Ind Eng Chem Res* 45:1167–1171
23. García-Ochoa F, Gómez E, Santos V, Merchuk J (2010) Oxygen uptake rate in microbial processes: an overview. *Biochem Eng J* 49:289–307
24. Sablayrolles J (1996) Effectiveness of combined ammoniacal nitrogen and oxygen additions for completion of sluggish and stuck wine fermentations. *J Ferment Bioeng* 82:377–381

25. Casalta E, Agüera E, Picou C, Rodríguez-Bencomo J, Salmon J, Sablayrolles J (2010) A comparison of laboratory and pilot-scale fermentations in winemaking conditions. *Appl Microb Biotechnol* 87:1665–1673
26. Morakul S, Mouret J, Nicolle P, Trelea I, Sablayrolles J, Athes V (2011) Modelling of the gas–liquid partitioning of aroma compounds during wine alcoholic fermentation and prediction of aroma losses. *Process Biochem* 46:1125–1131
27. Sacher J, Saa P, Cárcamo M, López J, Pérez-Correa R, Gelmi C (2011) Improved calibration of a solid substrate model. *Electron J Biotechnol*. doi:10.2225/vol14-issue5-fulltext-7
28. Rischbieter E, Schumpe A (1996) Gas solubilities in aqueous solutions of organic substances. *J Chem Eng Data* 41:809–812
29. Schumpe A, Quicker G, Deckwer W (1982) Gas solubilities in microbial culture media. *Adv Biochem Eng Biotechnol* 24:1–38
30. Gros J, Dussap C, Catté M (1999) Estimation of O₂ and CO₂ solubility in microbial culture media. *Biotechnol Prog* 15:923–927
31. Kutsche I, Gildehaus G, Schuller D, Schumpe A (1984) Aqueous alcohol solutions. *J Chem Eng Data* 29:286–287
32. Rettich T (2000) Solubility of gases in liquids. 22. High-precision determination of Henry's law constants of oxygen in liquid water from T = 274 K to T = 328 K. *J Chem Thermodyn* 32:1145–1156
33. Salmon J, Barre P (1998) Improvement of nitrogen assimilation and fermentation kinetics under enological conditions by derepression of alternative nitrogen-assimilatory pathways in an industrial *Saccharomyces cerevisiae* strain. *Appl Environ Microbiol* 64:3831–3837
34. Varela C, Pizarro F, Agosin E (2004) Biomass content governs fermentation rate in nitrogen-deficient wine musts. *Am Soc Microbiol* 70:3392–3400
35. Fernández-Sánchez J, Roth T, Cannas R, Nazeerudin Md, Spichiger S, Graetzel M, Spichiger-Keller U (2007) Novel oxygen sensitive complexes for optical oxygen sensing. *Talanta* 71:242–250
36. Bonate P (2011) Pharmacokinetic-pharmacodynamic modeling and simulation.

Springer US, Boston

37. Wang M, Tang S, Tan Z (2011) Modeling in vitro gas production kinetics: derivation of logistic–exponential (LE) equations and comparison of models. *Anim Feed Sci Technol* 165:137–150
38. Castiñeira A, Peña R, Herrero C, García-Martín S (2002) Analysis of organic acids in wine by capillary electrophoresis with direct UV detection. *J Food Compos Anal* 15:319–331
39. Wilhelm E, Battino R, Wilcock R (1977) Low-pressure solubility of gases in liquid water. *Chem Rev* 77:219–262
40. Eya H, Mishima K, Nagatani M, Iwai Y, Arai Y (1994) Measurement and correlation of solubilities of oxygen in aqueous solutions containing glucose, sucrose and maltose. *Fluid Phase Equilibria* 97:201–209
41. Mishima K, Matsuo N, Kawakami A, Komorita M, Nagatani M, Ouchi M (1996) Measurement and correlation of solubilities of oxygen in aqueous solutions containing galactose and fructose. *Fluid Phase Equilibria* 118:221–226
42. Cargill R (1993) The solubility of gases in water–alcohol mixtures. *Chem Soc Rev* 22:135–141
43. Lühring P, Schumpe A (1989) Gas solubilities (H₂, He, N₂, CO, O₂, Ar, CO₂) in organic liquids at 293.2 K. *J Chem Eng Data* 34:250–252
44. Rasmussen H, Rasmussen U (2003) Oxygen solubilities of media used in electrochemical respiration measurements. *Anal Biochem* 319:105–113
45. Degenring D, Froemel C, Dikta G, Takors R (2004) Sensitivity analysis for the reduction of complex metabolism models. *J Process Control* 14:729–745
46. Ingalls B, Sauro H (2003) Sensitivity analysis of stoichiometric networks: an extension of metabolic control analysis to non- steady state trajectories. *J Theor Biol* 222:23–36
47. Schwacke J, Voit E (2005) Computation and analysis of time- dependent sensitivities in generalized mass action systems. *J Theor Biol* 236:21–38
48. Zak D, Stelling J, Doyle F (2005) Sensitivity analysis of oscillatory (bio)chemical systems. *Comput Chem Eng* 29:663–673

49. Rosenfeld E, Beauvoit B, Rigoulet M, Salmon J (2002) Non-respiratory oxygen consumption pathways in anaerobically- grown *Saccharomyces cerevisiae*: evidence and partial characterization. *Yeast* 19:1299–1321
50. Doran P (1995) *Bioprocess engineering principles*. Academic Press, London
51. Stephanopoulos G (1984) *Chemical process control: an introduction to theory and practice*. Prentice-Hall, New Jersey
52. Vashitz O, Sheintuch M, Ulitzur S (1989) Mass transfer studies using cloned-luminous strain of *Xanthomonas campestris*. *Biotechnol Bioeng* 34:671–680
53. Çalik G, Vural H, Ozdamar T (1997) Bioprocess parameters and oxygen transfer effects in the growth of *Pseudomonas dacunhae* for L-alanine production. *Biotechnol Bioeng* 65:109–116
54. Çalik P, Yilgor P, Ayhan P, Demir A (2004) Oxygen transfer effects on recombinant benzaldehyde lyase production. *Chem Eng Sci* 59:5075–5083
55. Djelal H, Larher F, Martin G, Amrane A (2006) Effect of the dissolved oxygen on the bioproduction of glycerol and ethanol by *Hansenula anomala* growing under salt stress conditions. *J Biotechnol* 125:95–103

5. CONTROL OF BUBBLE-FREE OXYGENATION WITH SILICONE TUBING DURING ALCOHOLIC FERMENTATION

María Isabel Moenne, Jean-Roch Mouret, Jean-Marie Sablayrolles, Eduardo Agosin and Vincent Farines

Published in *Process Biochemistry*, July 2013, Vol. 48, p. 1453-1461

Abstract

The addition of oxygen is a common practice during winemaking to improve fermentation kinetics. However, an important limitation of standard oxygenation systems is that it is difficult to determine the exact quantity of oxygen transferred to wine or must. Tools enabling precise and reproducible oxygen addition would be useful. We developed and validated a bubble-free oxygenation system, at laboratory and pilot scale. In this system, oxygen is added by diffusion through a silicone membrane tube.

We evaluated the effects of various parameters on the maximum oxygen transfer rate (OTR_m). For fixed characteristics of the silicone tube and the partial pressure, the effects of dissolved CO₂ and medium composition were negligible; parameters with the biggest influence on the OTR_m were the liquid flow rate and the temperature.

These data were used to construct a mathematical model that calculates the OTR as a function of the operating parameters. This phenomenological model allows comprehensive description of physical parameters influencing the OTR_m. The model's predictions were very accurate both for the validation experiments in synthetic media and in real fermentation conditions. This work makes a step toward innovative strategies for oxygen management during alcoholic fermentation.

5.1. Introduction

In winemaking conditions, anaerobiosis limits cell growth because the lack of oxygen prevents fatty acid and sterol biosynthesis [1,2]. Very low lipid concentrations in musts

can lead to stuck or sluggish fermentations, which are a major problem in the wine industry [3–5]. Oxygen has a positive influence on the biosynthesis of fatty acids and sterols leading to a better cell viability and growth. Appropriate oxygen availability is therefore one of the keys to improve fermentation kinetics during alcoholic fermentation [1,5]. Indeed, addition of oxygen at the end of the yeast growth phase, coupled with the addition of assimilable nitrogen, greatly decreases the risk of stuck fermentation [6–8]. The amount of oxygen needed for the whole cycle of fermentation has been estimated to be in the range of 10–20 mg/L [9,10].

In wineries, oxygen can be added to fermenting must by various techniques, which differ in the amount of oxygen delivered: racking with aeration, pumping over the must with a fritted stainless steel coupler or pumping over the must after spraying into an open tub (for example, in-line venturi) [11]. However, it is not possible either to know or to control accurately the amounts of oxygen introduced into the medium by such practices. It is important to estimate the amount of oxygen added because very small additions are not effective and, at the other extreme, excessive additions may lead to organoleptic defects [6].

Direct sparging is a simple way to supply oxygen to the medium during fermentation. Micro-oxygenation techniques consist of generating micro-bubbles of air or pure gaseous oxygen (bubble diameter below 1.5 mm) inside the wine tank, using a porous gas diffuser. High oxygen transfer rates (OTR) can be obtained by oxygenation with spargers that have a large interfacial area (a) for bubbles [12]. The efficiency of the oxygen transfer from gas to liquid phase is given by the volumetric transfer coefficient ($K_L \cdot a$) where K_L is the global transfer coefficient and a is the interfacial area per unit volume. When using sparging systems, the $K_L \cdot a$ value is obviously affected by the size of the bubbles: the OTR increases as the size of the bubbles decreases. Bubble size is generally in the region of 4–6 mm with standard spargers (metal sparger, ring injector) or 0.1–1 mm with micro-spargers (e.g. those made of ceramic) [12,13]. However, the efficiency of the oxygen transfer also depends on the liquid phase composition. For example, the viscosity increases with increasing sugar concentration, which in turn leads to a significant decrease of the $K_L \cdot a$ value. Low ethanol concentrations in the

liquid phase (0.05% volume) strongly favor oxygen transfer [12]. Conversely, the presence of dissolved carbon dioxide in the fermenting must, which desorbs and dilutes the oxygen in the micro-bubbles, substantially decreases the efficiency of the transfer of oxygen to the liquid: the decrease is almost one order of magnitude when the carbon dioxide concentration changes from 0 to 1.4 g/L [14]. The composition of the medium (mainly glucose, fructose, ethanol and CO₂) evolves continuously during enological fermentation, and it is therefore not feasible to evaluate the efficiency of oxygen transfer throughout the fermentation process. Consequently, sparging techniques are not suitable for providing precisely controlled amounts of oxygen to the medium.

Bubble-free oxygenation of media by membrane aeration with open-pore membranes or diffusion membranes is an alternative approach to adding oxygen to the medium during fermentation [15–18]. Silicone membranes can be used because of their high permeability for oxygen, either with water or gas (air or oxygen) flowing inside the silicone tubing [19–21]. For microporous membranes, the medium is in direct contact with the gas in the micropores of the membrane. The characteristics of the gas–liquid interface in pores are dependent on pressure and hydrophobic forces. For nonporous membranes, oxygen diffuses first from the gas phase into the membrane and then into the liquid medium on the other side. Silicone membranes have the advantage of being nonporous and can be operated at high gas pressures without forming bubbles [22]. In such bubble-free oxygenation systems, the main factors affecting oxygen transfer are the oxygen concentration in the supply gas, the solubility of oxygen in the membrane and the exchange area of the membrane; the K_L value itself is influenced by the hydrodynamic conditions of the liquid phase [20,23,24].

The main drawback of the systems currently available for the addition of oxygen (i.e. pump-over or sparging) is the inaccuracy of determinations of the quantity of oxygen effectively transferred to the liquid phase. Indeed, except for the system designed by Blateyron et al. [15], it is not possible to measure the efficiency of the gas/liquid transfer precisely. We therefore tried to develop and validate a system for the transfer of precise quantities of oxygen to the liquid phase during alcoholic fermentations. We evaluated six different parameters that influence the OTR in our system: the liquid flow

rate inside the silicone tube, the temperature of the liquid, the presence of dissolved CO₂, the nature of the gas used for oxygenation, the gas flow rate and the composition of the medium. We also developed a model to predict the OTR from the operating parameters.

5.2. Materials and methods

5.2.1. Aeration system

The studies were carried out in a 10L reactor with temperature regulation. The reactor was filled with 9L of perfectly mixed solution. Air or oxygen was added through an external silicone tubing contactor (4.0 mm internal diameter and 4.5 mm external diameter) (Fig. 5-1) adapted from the system described by Blateyron et al. [15]. One meter of silicone tube develops an internal interfacial area (A) of $1.26 \times 10^{-2} \text{ m}^2$. During the aeration process, the liquid medium was pumped by a gear pump (Reglo-Z analog from Ismatec, Glattbrugg, Switzerland) and consequently circulated inside the silicone tube; pure oxygen (purity 99.7%) or air (20.95% oxygen) was continuously fed into the glass jar, to ensure a constant oxygen gradient around the silicone tube. All the peripheral connections were made with Norprene® tubing to avoid any air/oxygen transfer in these parts of the apparatus.

Dissolved oxygen concentrations were measured using an optical probe: a 3 LCD-trace Fibox v7 (PreSens®, Regensburg, Germany). The sensors employed were PSt3 spots (PreSens®, Regensburg, Germany). The measuring range of this sensor is between 0 and 20 mg/L for dissolved oxygen with a detection limit of 15 ppb. To determine the dissolved oxygen concentration in the loop of the aeration system (at the output of the tank and at the end of the silicone tube), two sight glasses with PSt3 spots glued inside were used (Fig. 5-1).

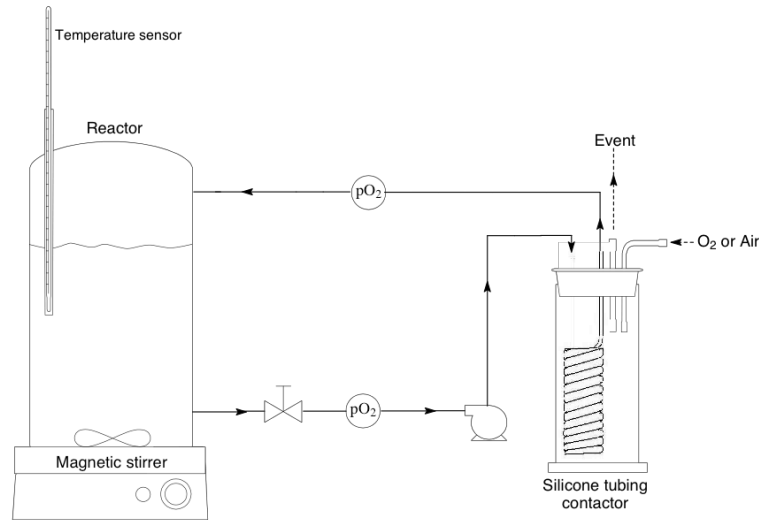


Figure 5-1: Schematic representation of the bubble-free oxygenation system

5.2.2. Oxygen saturation concentration (C^*)

The solubility of oxygen in a liquid phase is given by Henry's law:

$$C^* = \frac{p_{O_2}}{H} \quad (1)$$

where p_{O_2} is the partial pressure of oxygen in the gas phase in Pa; H is Henry's constant [$\text{Pa m}^3 / \text{kg}$] and C^* is the oxygen saturation concentration [kg/m^3].

H depends on the temperature and composition of the medium, such that for a given temperature, Henry's constants in water, must and wine are different [12,26]. The measured partial pressure is "converted" into the oxygen concentration in the liquid phase by the optical sensors using Henry's constant for water. Therefore, C^* was calculated using Eq. (1) and the model simulating oxygen solubility developed by Saa et al. [26] to take into account the effect of medium composition on the dissolved oxygen concentration in the liquid phase. The model's predictions of C^* agreed with validation experiments performed at 25°C with air and with pure oxygen and various synthetic media (from must to wine) with a mean relative error of 2.1%.

5.2.3. Volumetric transfer coefficient

For a given medium, the oxygenation capacity in a reactor is characterized by the overall volumetric transfer coefficient ($K_L \cdot a$). Conventional kinetic saturation

experiments can be used to determine $K_L \cdot a$. First, oxygen is desorbed from the liquid phase by argon sparging until the oxygen probe indicates an oxygen concentration lower than 200 $\mu\text{g/L}$. Then, the jar is continuously fed with air or pure oxygen at a controlled flow rate while the liquid solution is circulated in the loop at a constant flow rate.

Assuming a homogeneous concentration of oxygen in the reactor, the oxygen mass balance in the liquid phase is obtained from the following equation:

$$\frac{dC}{dt} = K_L \cdot a \cdot (C^* - C) \quad (2)$$

where dC/dt is the specific rate of oxygen accumulation in the liquid phase, C^* is the oxygen saturation concentration [mg/L], C is the oxygen concentration [mg/L] and $K_L \cdot a$ is the volumetric transfer coefficient [1/h].

Integrating Eq. (2) gives:

$$K_L \cdot a \cdot t = \ln \left(\frac{C^* - C_i}{C^* - C} \right) \quad (3)$$

where C_i is the initial dissolved oxygen concentration [mg/L] and C the oxygen concentration [mg/L] at the time t [h].

Hence, the value of $K_L \cdot a$ is obtained from the slope of Eq. (3). Finally, the OTR_m is defined by:

$$OTR_m = K_L \cdot a \cdot C^* \quad (4)$$

expressed in mg/L h.

5.2.4. Media composition

A buffer solution was prepared containing (per liter): 6 g of citric acid and 6 g of malic acid adjusted to pH 3.3 (with NaOH). For the model solution simulating a must, 180 g/L glucose was added. For the model solution simulating a wine, the buffer solution was supplemented with 10.8% (v/v) ethanol. For the model solutions simulating musts at different stages of fermentation, the buffer solution was supplemented with: (a) 140 g/L of glucose and 2.4% (v/v) of ethanol, or (b) 36 g/L of glucose and 8.6% (v/v) of ethanol. The resulting four media corresponded to 0, 22, 80, and 100% progression of the fermentation.

5.2.5. Viscosity and density

Dynamic viscosity μ of the various media (*cf* Section 2.4) was measured with a capillary viscometer (Viscometer AVS 470, SCHOTT-Instruments GmbH, Mainz, Germany) at 16, 20, 24 and 28°C. The density ρ of the same solutions at the same set of temperatures was measured with a densimeter (DMA 5000M, Anton Paar France S.A.S, Courtaboeuf, France).

5.2.6. Fermentation

5.2.6.1. Yeast strain

The commercial active dry wine yeast *Saccharomyces cerevisiae* UCD522 (MaurivinTM) was used. The tank was inoculated with 10g/hL of active dry yeast previously rehydrated for 20 min at 37°C.

5.2.6.2. Must, fermentation conditions and oxygen addition

A grape must of the Chardonnay variety from the South of France was used. This must was flash pasteurized and stored under sterile conditions. The concentration of sugar was 175 g/L and the assimilable nitrogen concentration was 143 mg/L. The must was supplemented with 40 g/hL of diammonium phosphate (DAP).

The fermentation was run in a stainless steel 10 L tank (the same reactor as for $K_L \cdot a$ measurements), containing 9 L of must. During the fermentation, the released CO₂ was automatically and accurately measured every 20 min with a gas mass flow meter to follow the rate of CO₂ production (dCO_2/dt) and to determine the progress of the fermentation. The initial pH was 3.3 and the temperature was maintained at 28°C.

Oxygen was added at various stages of fermentation using the external silicone tubing contactor described above.

5.3. Results and discussion

5.3.1. Effect of physical parameters on the oxygen transfer rate

Various experimental conditions were used to characterize the system for oxygen addition. For each parameter studied, its effects on the volumetric transfer coefficient ($K_L \cdot a$) and the OTR_m were determined and are reported. All these experiments involving model solutions, without yeast, were reproduced in triplicate for each operating condition.

5.3.1.1. Effect of gas parameters: flow rate, partial pressure of oxygen and dissolved CO_2

The length of the silicone tube was 3.1 m for an internal interfacial area of $3.9 \times 10^{-2} \text{ m}^2$ in all the experiments. The effect of gas flow rate was studied for saline solution containing only citric (6 g/L) and malic (6 g/L) acids, adjusted to pH 3.3. Four different gas flow rates were used: 0.25, 0.5, 1.0 and 2.0 L/min. Both pure oxygen and air were used to determine the effect of partial pressure on the OTR at two liquid flow rates: 167 and 337 mL/min (liquid velocity of 0.22 and 0.45 m/s, respectively).

Unsurprisingly, $K_L \cdot a$ was not influenced by the gas flow rate in the jar (Table 5-1). As a consequence, the variation of OTR_m with the flow rate was negligible (no more than 2% divergence from the average OTR_m).

The $K_L \cdot a$ value was independent of the oxygen partial pressure. However, the OTR_m was 79% lower with air than with pure oxygen. This can simply be attributed to the fact that the concentration at saturation is five times lower with air ($C^* = 9.03 \text{ mg/L}$ at 20°C) than with pure oxygen ($C^* = 43.1 \text{ mg/L}$ at 20°C), and is strictly correlated with the partial pressure of oxygen in the gas phase. Saturating the liquid phase with CO_2 before the oxygen absorption experiment had no effect on the $K_L \cdot a$, such that the OTR_m was unaffected (Table 5.1). Note that bubbleless aeration systems thus differ from sparging systems for which the presence of dissolved CO_2 strongly affects the efficiency of oxygen transfer [14].

Table 5-1: Effect of gas flow rate, partial pressure of oxygen, and liquid flow rate on gas/liquid transfer. Experiments were carried out at 20°C with saline solution (containing 6 g/L of citric acid and 6 g/L of malic acid, adjusted to pH 3.3). the data reported are means with 95% confidence intervals.

Parameter	Liquid flow rate (mL/min)	Nature of gas	Gas flow rate (L/min)	$K_L \cdot a$ (1/h)	OTR _m (mg/Lh)
Gas flow rate	337	O ₂	0.25	0.226 ± 0.007	9.74 ± 0.59
			0.5	0.238 ± 0.008	10.26 ± 0.37
			1.0	0.240 ± 0.008	10.34 ± 0.69
			2.0	0.238 ± 0.007	10.26 ± 0.62
Partial pressure and liquid flow rate	167	O ₂	0.5	0.173 ± 0.011	7.47 ± 0.47
	337			0.238 ± 0.008	10.26 ± 0.37
	167	Air	0.5	^a 0.232 ± 0.014	10.00 ± 0.60
	337			0.174 ± 0.020	1.57 ± 0.18
	167			0.237 ± 0.006	2.14 ± 0.05
	337				

^a Buffer solution was saturated with CO₂ (1480–1515 mg of CO₂/L) before the experiment.

5.3.1.2. Effect of the liquid flow rate and temperature

The effect of the liquid flow rate was studied using the buffered saline solution and six different liquid flow rates from 75 to 667 mL/min. Each flow rate was tested at three temperatures: 20, 24 and 28°C. The length of the tube was 3.1 m and pure oxygen was fed continuously into the jar at 0.5 L/min.

$K_L \cdot a$ increased with the liquid flow rate in a non-linear manner (Fig. 5-2A). The relationship between $K_L \cdot a$ and the liquid flow rate can be divided in two parts: Firstly, $K_L \cdot a$ increased rapidly with the liquid flow rate up to a rate of 330 mL/min. For example, at 28°C, the OTR_m was 59.5% higher for a liquid flow rate of 167 than for 75 mL/min.

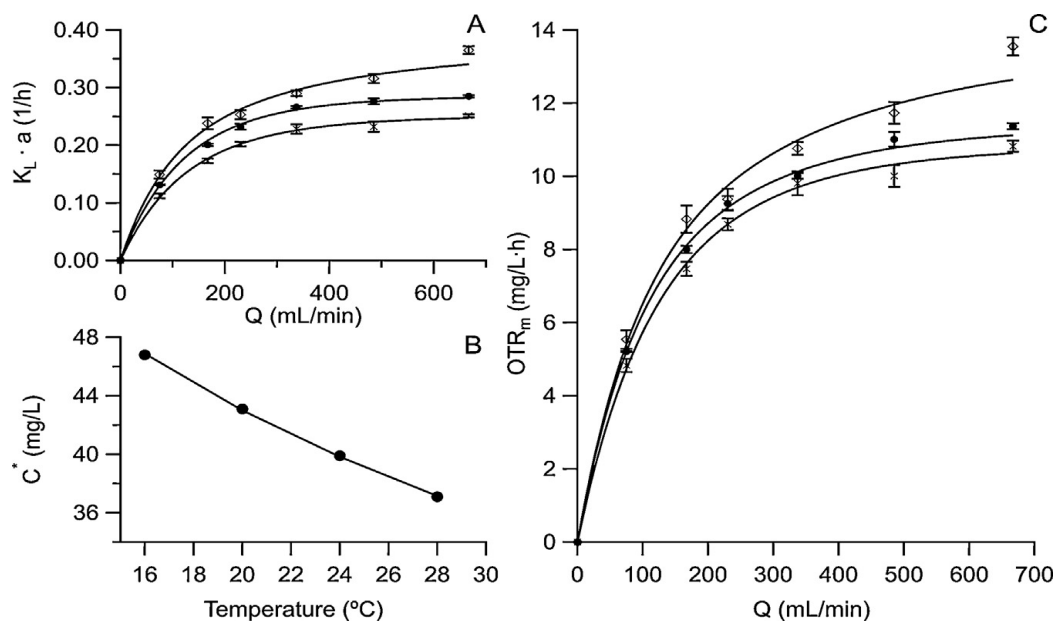


Figure 5-2: (A) Effect of the liquid flow rate on $K_L \cdot a$ at various temperatures: 20°C (x), 24°C (•), 28°C (◊). (B) Effect of the temperature on C^* with pure oxygen. (C) Effect of the liquid flow rate on the OTR_m at various temperatures: 20°C (x), 24°C (•), 28°C (◊).

Between 75 and 330 mL/min, the system was in laminar flow with Reynolds number between 396 and 1785 (Fig. 5-3). Therefore, the increase of $K_L \cdot a$ as a function of the liquid flow rate can be explained by a decrease of the resistance of the liquid film inside the silicone tube.

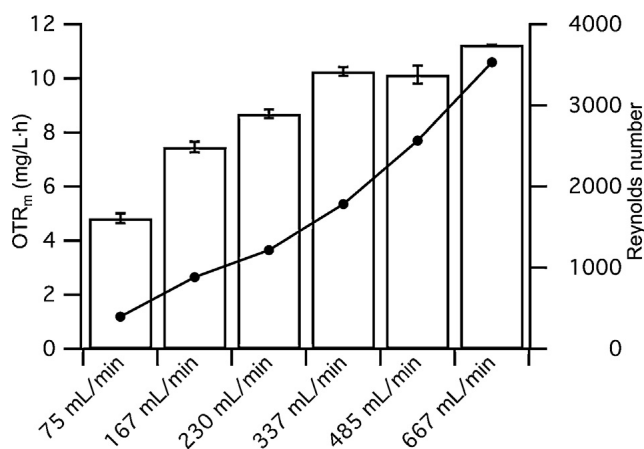


Figure 5-3: Evolution of the OTR_m (histogram; □) and Reynolds number (line plot; •) with liquid flow rate for buffer solution at 20°C.

Secondly, at liquid flow rates higher than 330mL/min, the hydrodynamic conditions were different, such that the liquid flow was no longer laminar. At the maximum liquid flow rate, the Reynolds number was close to 3530. In this range of liquid flow rates, $K_L \cdot a$ and OTR_m increased only slowly with increasing flow. For example, doubling in the liquid flow rate resulted in only a 12% increase of the OTR_m at 20 and 24°C (Fig. 5-3). However, at 28°C, the OTR_m increased by 26% when the liquid flow rate was increased from 330 to 660 mL/min. Beyond a threshold value of the liquid flow rate (≈ 330 mL/min), the stability of the value of $K_L \cdot a$ can be explained by the resistance of the silicone tube.

For oxygen to be transported from the outside of the silicone tubing to the targeted bulk liquid (inside the tubing), it must diffuse through the membrane wall of the tubing and through the liquid boundary layer. The overall resistance to mass-transfer ($1/K_L$) is therefore the result of three separate resistances in series: (1) the gas film resistance ($1/k_G$); (2) the membrane resistance ($1/k_M$); and (3) the liquid-film resistance ($1/k_L$). The gas film resistance can be considered to be negligible. The major determinant is the liquid-film resistance [20,27], which depends on the concentration boundary-layer thickness (δ) and the diffusivity (D) of oxygen in the liquid medium [28]:

$$k_L = \frac{D}{\delta} \quad (5)$$

Thus, a larger diffusivity or a thinner boundary layer will increase both the liquid-side mass-transfer coefficient and the overall rate of oxygen transfer. A minimum boundary layer thickness will maximize OTR, and this can be modulated by controlling the liquid velocity inside the tube. So, as for the gas flow rate in sparging aeration systems, the liquid flow rate appears to be the most appropriate lever for controlling the OTR in bubbleless aeration systems.

To determine the transfer coefficient of the silicone membrane, k_M , under these experimental conditions, $1/K_L$ was plotted against $1/v_L$ as a “Wilson plot” (Fig. 5-4). The gas-phase resistance in our system was negligible, i.e. $((1/K_G \cdot H) \approx 0$, such that the intercept in the “Wilson plot” (where $1/Q_L = 0$, implying $Q_L \rightarrow \infty$ and $1/k_L \approx 0$) corresponded to the resistance of the membrane of the silicone tube, $1/k_M$. A least

square regression analysis of the data gave values of $1/k_M = 4.67 \times 10^4$, 4.71×10^4 and 4.44×10^4 s/m at 20, 24 and 28°C, respectively. From these results, an average value for $k_M (= 2.17 \times 10^{-5}$ m/s) can be calculated. The analysis of individual mass-transfer resistances for oxygen absorption in buffer (three temperatures combined) is given in Fig. 5-5. It was evident from this figure that the liquid mass-transfer resistance decreased as the liquid flow increases, as a consequence of the decrease of the boundary layer thickness. Under the flow conditions used, the membrane resistance constituted from 32% at the lowest flow rate (75 mL/min i.e. $v=0.1$ m/s) to 91% at the highest flow rate (670 mL/min i.e. $v = 0.9$ m/s) of the total mass-transfer resistance. At the maximum flow rate, the total mass-transfer resistance was almost entirely due to material resistance alone.

The solubility of oxygen decreased as the temperature increased (Fig. 5-2B). However, the $K_L \cdot a$ value increased with increasing temperature (Fig. 5-2A). Nevertheless, although the OTR_m was higher at 28 than 20°C, the percentage difference depended on the flow rate: 20% at the maximum flow rate and 13% at the lowest flow rate.

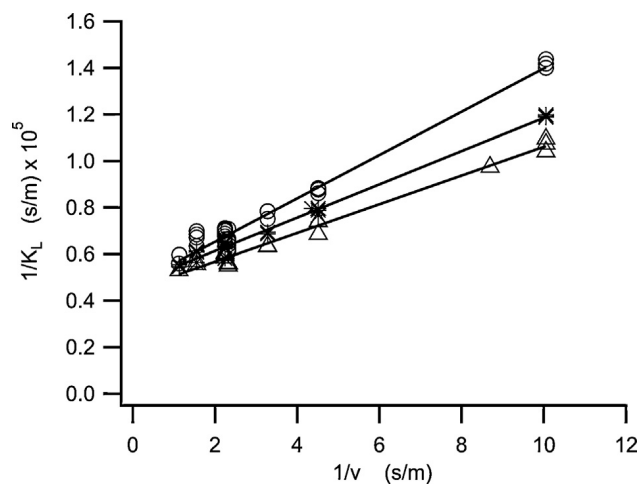


Figure 5-4: “Wilson plot” for oxygen adsorption and liquid flow inside the silicone tube, at three temperatures: 20°C (●), 24°C (*), 28°C (Δ).

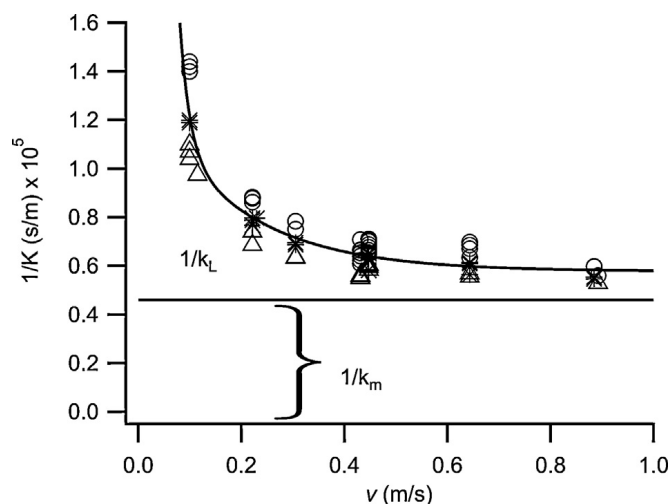


Figure 5-5: Analysis of mass-transfer resistances (-) for oxygen absorption in liquid flowing inside the silicone tube at three temperatures: 20°C (●), 24°C (*), 28°C (Δ).

5.3.1.3. Effect of the medium composition (acid salts, sugar, ethanol)

The solubility of oxygen depends on the composition of the liquid, and was calculated using the model described by Saa et al. [26]. The matrix composition (sugar and ethanol concentrations in particular) can also affect the OTR_m . $K_L \cdot a$ values were measured in model solutions corresponding to 0, 22, 80, and 100% progression of the fermentation. The $K_L \cdot a$ was studied in these model solutions at 28°C and with a liquid flow rate of 337 mL/min; the length of the tube was 3.1 m and oxygen was fed into the jar continuously at 0.5 L/min.

The salt (malic and citric acids) concentrations did not affect the value of $K_L \cdot a$; the values were similar for water and buffer solution (Table 5-2).

The C^* increased with the progress of fermentation (Fig. 5-6A). The solubility of oxygen was lower in musts with high sugar concentration than in the buffer solution, whereas the presence of ethanol increased the solubility of oxygen. Consequently, C^* increased by 25% between the start and the end of the fermentation process.

On the contrary, $K_L \cdot a$ decreased slightly during the fermentation (Table 5-2 and Fig. 5-6A). Consequently, the OTR_m remained almost constant (Fig. 5-6B).

Table 5-2: Effect of the medium composition on the $K_L \cdot a$ value. The data reported are means with 95% confidence intervals.

	$K_L \cdot a$ (1/h)
MilliQ water pH 3.3	0.27 ± 0.007
Buffer solution	0.28 ± 0.011
Model solution (% of fermentation progress)	
0	0.29 ± 0.020
22	0.31 ± 0.025
80	0.27 ± 0.014
100	0.28 ± 0.008

The model solutions simulating musts at 0, 22, 80 and 100% of fermentation progress respectively contain (i) 180, 140, 36, 0 g/L of glucose and (ii) 0.0, 2.4, 8.6 and 10.8% (v/v) of ethanol.

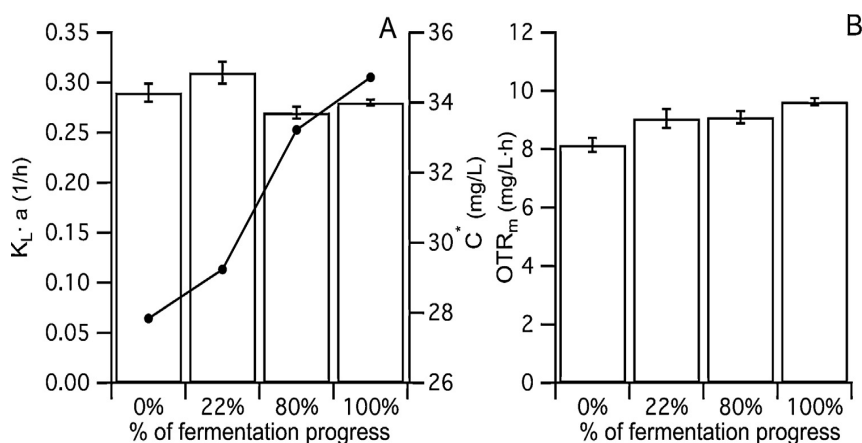


Figure 5-6: $K_L \cdot a$ (histogram; \square), C^* (line plot; \bullet) (A) and OTR_m (B) measured in model solution at 28°C and at a liquid flow rate of 337 mL/min. The concentration at saturation was measured using the same solutions.

5.3.2. Model development

We tried to develop a model to calculate the OTR for all values of fermentation progress, liquid flow rate, temperature of the medium, length of circular silicone tube and partial pressure of oxygen in the gas. We established that the OTR_m was mostly influenced by the liquid flow rate, up to a rate of 330 mL/min (see Fig. 5-2). Exceeding this value, the transfer was limited by the resistance of the material. The second parameter to be taken into account was the temperature: the OTR_m increased with temperature. The composition of the medium had only a negligible effect on the

OTR_m : at a fixed liquid flow rate and temperature, the OTR was almost unchanged as fermentation progressed (Fig. 5-6B).

Equation (6) gives the definition of the OTR:

$$OTR = K_L \cdot a \cdot (C^* - C) \quad (6)$$

To model the OTR, the three following constituents of Eq. (6) have to be determined:

(i) the interfacial area per unit volume a , (ii) the driving force of the transfer ($C^* - C$), and (iii) the overall liquid mass-transfer coefficient K_L .

5.3.2.1. Interfacial area per unit volume

The interfacial area A corresponds to the inner surface of the silicone tube. Indeed, the interfacial area per unit volume, for a given system, is a constant that depends on the physical characteristics of the silicone tube (diameter, d_{in} and length, L) and the volume of solution to be oxygenated (V):

$$a = \frac{\pi \cdot d_{in} \cdot L}{V} \quad (7)$$

5.3.2.2. Driving force

To calculate the driving force ($C^* - C$), C^* can be calculated by applying the oxygen solubility model developed by Saa et al. [26]. The calculation of the value of C^* allows the effect of the partial pressure of oxygen on the OTR to be taken into account.

For the value of C , two possibilities have to be considered. In the case of oxygen addition during fermentation, the consumption rate is usually higher than the transfer rate: no accumulation of oxygen in the fermentor is detected and thus $C = 0$. Consequently, the OTR corresponds to OTR_m as given in Eq. (4). In other cases, for example absorption experiments using solutions without yeast, oxygen accumulates such that $C \neq 0$. It is therefore necessary to estimate the quantities of dissolved oxygen at the exit of the circular silicone tube, C_{out} . This can be done by considering a space differential mass balance in the silicone tube contactor for steady-state conditions with a dissolved oxygen concentration on entry C_{in} :

$$dF = K_L \cdot dA \cdot (C^* - C) = Q_L \cdot dC \quad (8)$$

Also:

$$\frac{dC}{(C^* - C)} = \frac{K_L}{Q_L} \cdot dA \quad (9)$$

$$\int_{C_{in}}^{C_{out}} \frac{dC}{(C^* - C)} = \frac{K_L}{Q_L} \cdot \int_0^A dA \quad (10)$$

$$\left[\ln(C^* - C) \right]_{C_{in}}^{C_{out}} = -\frac{K_L}{Q_L} \cdot A \quad (11)$$

$$\frac{C^* - C_{out}}{C^* - C_{in}} = e^{-\frac{K_L}{Q_L} \cdot a} \quad (12)$$

$$C^* - C_{out} = (C^* - C_{in}) \cdot e^{-\frac{K_L}{Q_L} \cdot a} \quad (13)$$

The oxygen concentration at exit of the circular tube is thus:

$$C_{out} = C^* - (C^* - C_{in}) \cdot e^{-\frac{K_L}{Q_L} \cdot a} \quad (14)$$

From the value of C_{out} , it is possible to calculate the concentration of dissolved oxygen C in the fermentor, on the basis of the volume of solution to be aerated.

5.3.2.3. Overall liquid mass-transfer coefficient

A predictive model of OTR should allow access to K_L values in all aeration conditions (liquid flow rate, temperature, partial pressure of oxygen etc.). K_L can be determined using an adimensional numbers (Sherwood and Reynolds) approach. According to this approach, no differentiation needs to be made between k_L and k_M , even though we have already determined k_M to provide a better understanding of phenomena involved in mass transfer limitation.

Taking the overall liquid mass-transfer coefficient K_L into account instead of the liquid phase mass-transfer coefficient k_L , the modified Sherwood number for liquid flow inside the tube was obtained as follows, calculated from the measured values of $K_L \cdot a$ in absorption experiments:

$$Sh = \frac{K_L \cdot d_{out}}{D} \quad (16)$$

where D is the oxygen diffusivity in the liquid medium. This diffusion coefficient can be determined by using the Wilke and Chang equation [29]. This equation is commonly used to calculate diffusion coefficients of a solute B in water W , D_{BW} (m^2/s), and is:

$$D_{BW} = 7.4 \cdot 10^{-12} \cdot \frac{(\Phi \cdot M_w)^{0.5} \cdot T}{\mu_w \cdot V_B^{0.6}} \quad (17)$$

where Φ is the association factor which is equal to 2.6 for water [29], M_w is the molar mass of water (g/mol), T is the temperature (K), μ_w is the viscosity of water (cP) and V_B is the molar volume of solute B at its normal boiling temperature (cm^3/mol).

The Reynolds number for the liquid flow inside the tube was calculated using the expression:

$$Re = \frac{V_L \cdot d_m \cdot \rho}{\mu} \quad (18)$$

where ρ and μ are respectively the density (kg/m^3) and the dynamic viscosity ($Pa \cdot s$) of the liquid and V_L is the liquid velocity (m/s) inside the silicone tube.

To incorporate the effect of temperature, the changes of ρ and μ with the temperature were measured for the buffer solution, leading to the two following equations:

$$\rho = -0.25 \cdot T + 1009.22 \text{ with } R^2 = 0.9953 \quad (19)$$

$$\mu = -2.41 \cdot 10^{-5} \cdot T + 1.53 \cdot 10^{-3} \text{ with } R^2 = 0.9979 \quad (20)$$

where T is the temperature expressed in degrees Celsius. More than 120 tests (i.e. 40 experiments each done in triplicate) of oxygen absorption with buffer solution in various conditions (Table 5-3) were used to identify the model coefficients. The liquid-side K_L values including the material resistance (i.e. $k_L + k_M$) expressed in terms of the modified Sherwood numbers were plotted against the liquid flow rates in terms of the Reynolds numbers on a log–log scale. A least-squares regression of the data gave the following correlation:

$$Sh = 1.32 \cdot Re^{0.44} \quad (21)$$

The exponent of the Reynolds number was coherent with published values, most of which were between 0.3 for laminar flow and 0.8 for turbulent flow in a circular tube or a flat channel [30].

From Eqs. (16) and (21), K_L can be calculated as:

$$K_L = \frac{1.04 \cdot \text{Re}^{0.44} \cdot D}{d_{\text{out}}} \quad (22)$$

Table 5-3: Experimental conditions for the oxygen transfer experiments used to determine model coefficients

Parameter	Range
Gas flow rate	0.25–2 L/min
Liquid flow rate	75–670 mL/min
Temperature	20–28 °C
Length of silicone tube	0.4–3.1 m
Partial pressure of O ₂	20.95% (air) and 100% (pure oxygen)

5.3.2.4. Oxygen transfer rate

The OTR in mg/L h can be predicted with the following global expression:

$$OTR = \frac{1.04 \cdot [(v_L \cdot d_{in} \cdot (-0.25 \cdot T + 1009.22)) / (-2.41 \times 10^{-5} \cdot T + 1.53 \times 10^{-3})]^{0.44} \cdot D \cdot \frac{\pi \cdot d_{in} \cdot L}{V} \cdot (C^* - C) \cdot 3600}{d_{out}} \quad (23)$$

In this study, the effect of the Schmidt number, Sc , on the mass-transfer coefficient was not evaluated. The relevance of the Schmidt number to our model is limited because the model developed is self-sufficient. However, a 1/3 power dependence, as widely accepted in the literature, is plausible in the mass-transfer correlation [31].

The mean relative error between values predicted by the model and the values measured was calculated as follows:

$$E = \frac{1}{n} \sum_{j=1}^n \left| \frac{OTR_{\text{measured}} - OTR_{\text{predicted}}}{OTR_{\text{measured}}} \right| \cdot 100 \quad (24)$$

where n is the number of $K_L \cdot a$ measurements used for the construction of the model.

Applied to the 120 experiments in buffer solution and used to determine the model coefficients, the model allowed satisfactory prediction of OTR_m values with mean relative error of 4.9%.

5.3.3. Model validation

5.3.3.1. Model validation in synthetic media

Twenty-seven oxygen transfer experiments were done in various conditions to validate the model established in buffer solution. These experiments involved varying the following factors: (i) medium composition: model solutions simulating must (180g/L of sugar), wine (10.8% (v/v) of ethanol) and intermediate model solutions simulating musts at different stages of fermentation; (ii) liquid flow rate: 100–650 mL/min; (iii) temperature: 18–28°C; (iv) partial pressure of oxygen: 20.95% (air) and 100% (pure oxygen); and (v) length of silicone tube: 0.4 or 3.1 m.

The model provided good predictions of the OTR_m values determined experimentally with a mean relative error (*cf* Eq. (24)) of 4.6% for the validation experiments as a whole. This was a very satisfactory performance, because this mean relative error was close to that obtained for the determination of the coefficients of the model (4.9%).

Notably, the model predicted OTR_m with an error lower than 1% for two experiments conducted at a temperature of 18°C, thus outside of the range of temperatures used for the construction of the model (Table 5-3).

5.3.3.2. Model validation in real fermentation conditions

Oxygen was added using the external silicone tubing contactor (3.1 m) described above at various times during chardonnay fermentation ($V = 9$ L) at 28°C. For each oxygen addition, the liquid flow rate Q_L was set to 337 ml/min. In preliminary experiments, we verified that oxygen did not accumulate inside the reactor (*i.e.* $C=0$).

The OTR_m was calculated during fermentation using the following equation:

$$OTR_m = \frac{(C_{out} - C) \cdot Q_L}{V} \quad (25)$$

where C_{out} is the dissolved oxygen concentration at the exit of the tubing contactor.

The measured OTR_m values remained generally constant throughout fermentation (Table 5-4). The mean OTR_m measured was 9.74 ± 0.19 mg/L h. With these operating parameters (temperature, liquid flow rate, length of the silicon tube), the OTR_m calculated using the model Eq. (23) was 9.83 mg/L h. The mean relative error between

the values predicted by the model and the values measured was thus 0.4%, which is very satisfactory and demonstrates the accuracy of the model.

This result is particularly promising, because, by contrast, with sparging systems, the $K_L \cdot a$ value decreases with the presence of CO_2 in the liquid phase, decreasing the efficiency of the OTR_m due to the incorporation of gaseous CO_2 into the bubbles of O_2 [14]. Moreover, the gas–liquid mass transfer in sparging systems is also influenced by the liquid composition (mainly the sugar and ethanol contents) [12]. With our bubbleless system, the OTR_m remained relatively constant during fermentation, confirming that the effects of CO_2 and medium composition were negligible when the O_2 was added by diffusion through this system.

This result means that the main parameters determining the OTR_m are the liquid flow rate and the temperature (when the characteristics of the silicone tube and the partial pressure of O_2 are fixed). Therefore, we can use the model (Eq. (23)) to calculate the OTR_m precisely, for all must compositions and at all stages of fermentation.

Table 5-4: Values of OTR_m obtained experimentally during Chardonnay fermentation at 28°C.

Fermentation progress (%)	OTR_m (mg/Lh)
20	9.84 ± 0.15
40	9.84 ± 0.35
70	9.90 ± 0.25
80	9.28 ± 0.12
100	9.85 ± 0.10

5.4. Conclusions

We describe an innovative technique for controlling the amount of oxygen transferred during alcoholic fermentation under enological conditions at pilot scale. The bubble-free oxygenation system developed allows precise addition of oxygen by diffusion across a silicone tubing membrane with a perfectly controlled OTR. The OTR can be easily modulated, in particular by controlling the liquid velocity inside the silicone tube. Tested in real fermentation conditions, the OTR_m associated with this bubbleless aeration system was constant during the fermentation process, and was independent of

the dissolved CO₂ concentration in the liquid. Furthermore, we developed a model for the calculation of the OTR from the values of the liquid flow rate and temperature of the liquid phase, the characteristics of the silicone tube, and the oxygen partial pressure. The experimental and calculated OTR_m values agreed well, with a mean relative error of 4.6% for the validation experiments in synthetic media and 0.4% for the validation experiment in real fermentation conditions.

This work contributes to our understanding of oxygen assimilation in enological conditions, and this is important because controlling oxygen input into wine fermentations would be extremely beneficial. We will use this bubble-free oxygenation system to assess consequences of precise oxygen management (quantity and time of oxygen addition) on yeast metabolism during alcoholic fermentation.

In addition, new options for management of fermentation become possible if both “one-off” and continuous, tightly controlled additions of oxygen are feasible. The consequences of such addition strategies will be evaluated for both the bioconversion of sugar into ethanol and the production of fermentative aromas. Aroma production will be studied by coupling the bubble-free oxygenation system to an online GC system, such that the production kinetics of relevant higher alcohols and esters produced during the alcoholic fermentation of wine can be monitored accurately [32].

Acknowledgments

We thank Christian Picou for his help in designing the aeration pilot. We also thank Cristian Trelea for his help with modeling.

M. Isabel Moenne is supported by a doctoral fellowship from the Chilean National Council of Scientific and Technological Research (CONICYT). Part of this work was carried out with the support from the National Fund for Scientific and Technological Development of Chile (FONDECYT) No. 1090520.

Abbreviations

OTR	Oxygen transfer rate (mg/L h)
OTR _m	Maximum oxygen transfer rate (mg/L h)
Re	Reynolds number
Sh	Sherwood number

Symbols and abbreviations

δ	concentration boundary layer thickness (m)
ε	porosity of the silicone tube wall
ρ	density of the liquid (kg/m ³)
μ	dynamic viscosity of the liquid (Pa·s)
a	interfacial area per unit volume (m ² /m ³) ²
A	interfacial area (m ²)
C	instantaneous dissolved oxygen concentration in the fermentor (mg/L)
C^*	dissolved oxygen saturation concentration (mg/L)
C_{in}	dissolved oxygen concentration at the entry of the tubing contactor (mol/m ³)
C_{out}	dissolved oxygen concentration at the exit of the tubing contactor (mol/m ³)
C_i	initial dissolved oxygen concentration (mol/m ³)
dC/dt	specific rate of oxygen accumulation in the liquid phase (mg/L h)
d_{in}	internal diameter of the silicone tube (m)
d_{out}	outer diameter of the silicone tube (m)
D	diffusivity coefficient (m ² /s) = 2.5×10^{-9} m ² /s for oxygen in water
D_{BW}	diffusion coefficient of a solute B in water (m ² /s)
E	mean relative error
H	Henry's constant (atm L/mg)
k_G	transfer coefficient of the gas phase (m/s)
k_L	liquid phase mass-transfer coefficient (m/s)

K_L	overall liquid mass-transfer coefficient (m/s)
k_M	transfer coefficient of the silicone membrane (m/s)
L	length of silicone tube (m)
M_W	molar mass of water (g/mol)
n	number of experiments
p_{O_2}	oxygen partial pressure (Pa)
Q_L	volumetric flow-rate of the liquid (m^3/s)
T	temperature ($^{\circ}C$)
t	time (s)
V	volume of solution to be aerated (m^3)
V_B	molar volume of solute B at its normal boiling temperature (cm^3/mol)
v_L	liquid velocity (m/s)

References

- [1] Andreasen AA, Stier TJB. Anaerobic nutrition of *Saccharomyces cerevisiae*. I. Ergosterol requirement for growth in a defined medium. J Cell Compar Physiol 1953;41:23–36.
- [2] Fornairon-Bonnefond C, Demaretz V, Rosenfeld E, Salmon JM. Oxygen addition and sterol synthesis in *Saccharomyces cerevisiae* during enological fermentation. J Biosci Bioeng 2002;93:176–82.
- [3] Bardi L, Cocito C, Marzona M. *Saccharomyces cerevisiae* cell fatty acid composition and release during fermentation without aeration and in absence of exogenous lipids. Int J Food Microbiol 1999; 47:133–40.
- [4] Andreasen AA, Stier TJB. Anaerobic nutrition of *Saccharomyces cerevisiae*. II. Unsaturated fatty acid requirement for growth in a defined medium. J Cell Compar Physiol 1954; 43:271–81.
- [5] Rosenfeld E, Beauvoit B, Blondin B, Salmon JM. Oxygen consumption by anaerobic *Saccharomyces cerevisiae* under enological conditions: effect on fermentation kinetics. Appl Environ Microb 2003; 69:113–21.

- [6] DuToit WJ, Marais J, Pretorius IS, duToit M. Oxygen in must and wine: a review. *S Afr J Enol Vitic* 2006; 27:76–94.
- [7] Sablayrolles JM, Dubois C, Manginot C, Roustan JL, Barre P. Effectiveness of combined ammoniacal nitrogen and oxygen additions for completion of sluggish and stuck wine fermentations. *J Ferment Bioeng* 1996; 82:377–81.
- [8] Blateyron L, Sablayrolles JM. Stuck and slow fermentations in enology: statistical study of causes and effectiveness of combined additions of oxygen and diammonium phosphate. *J Biosci Bioeng* 2001; 91:184–9.
- [9] Sablayrolles JM, Barre P. Evaluation of oxygen requirement of alcoholic fermentations in simulated enological conditions. *Sci Alim* 1986; 6:373–83.
- [10] Julien A, Roustan JL, Dulau L, Sablayrolles JM. Comparison of nitrogen and oxygen demands of enological yeasts: technological consequences. *Am J Enol Vitic* 2000; 51:215–22.
- [11] Boulton R, Singleton VL, Bisson LF, Kunkee RE. Principles and practices of winemaking. New York: Chapman & Hall; 1996.
- [12] Chiciuc I, Farines V, Mietton-Peuchot M, Devatine A. Effect of wine properties and operating mode upon mass transfer in micro-oxygenation. *Int J Food Eng* 2010;6:6.
- [13] Kazakis NA, Mouza AA, Paras SV. Experimental study of bubble formation at metal porous spargers: effect of liquid properties and sparger characteristics on the initial bubble size distribution. *Chem Eng J* 2008; 137:265–81.
- [14] Devatine A, Chiciuc I, Poupot C, Mietton-Peuchot M. Micro-oxygenation of wine in presence of dissolved carbon dioxide. *Chem Eng Sci* 2007; 62:4579–88.
- [15] Blateyron L, Aguera E, Dubois C, Gerland C, Sablayrolles JM. Control of oxygen additions during alcoholic fermentations. *Vitic Enol Sci* 1998; 53:131–5.
- [16] Grootjen DRJ, Van der lans RGJM, Luyben KCAM. Controlled addition of small amounts of oxygen with membranes. *Biotechnol Tech* 1990; 4:149–54.
- [17] Haukeli AD, Lie S. Controlled supply of trace amounts of oxygen in laboratory scale fermentations. *Biotechnol Bioeng* 1971; 13:619–28.
- [18] Rennie H, Wilson RJH. A method for controlled oxygenation of worts. *J I Brewing*

1975; 81:105–6.

[19] Robb WL. Thin silicone membranes: their permeation properties and some applications. *Ann NY Acad Sci* 1965; 1:119–35.

[20] Cote P. Bubble-free aeration using membranes: mass transfer analysis. *J Membr Sci* 1989; 47:91–106.

[21] Moulin P, Rouch JC, Serra C, Clifton MJ, Aptel P. Mass transfer improvement by secondary flows: Dean vortices in coiled tubular membranes. *J Membr Sci* 1996; 114:235–44.

[22] Ahmed T, Semmens MJ. Use of sealed end hollow fibers for bubbleless membrane aeration: experimental studies. *J Membr Sci* 1992; 69:1–10.

[23] Hirasa O, Ichijo H, Yamauchi A. Oxygen transfer from silicone hollow fibre membrane to water. *J Ferment Bioeng* 1991; 71:206–7.

[24] Yasuda H, Lamaze CE. Transfer of gas to dissolved oxygen in water via porous and nonporous membranes. *J Appl Polym Sci* 1972; 16:595–601.

[25] Sablayrolles JM, Barre P. Evolution of oxygen solubility during alcoholic fermentation of a grape must study with synthetical media. *Sci Alim* 1986;6:177–84.

[26] SaaP, MoenneMI, Perez-CorreaJR, AgosinE. Modeling oxygen dissolution and biological uptake during pulse oxygen additions in oenological fermentations. *Bioproc Biosyst Eng* 2012; 35:1167–78.

[27] Yang MC, Cussler EL. Designing hollow-fiber contactors. *AIChE J* 1986; 2:1910–6.

[28] Hanratty TJ. Separated flow modelling and interfacial transport phenomena. *Appl Sci Res* 1991;48:353–90.

[29] WilkeCR, ChangP. Correlation of diffusion coefficients in dilute solutions. *AIChE J* 1955;1:264–70.

[30] Hallstrom B, Gekas V, Sjolholm I, Romulus AM. Mass transfer in foods. In: Heldman DR, Lund DB, editors. *Handbook of food engineering*. 2nd edition Boca Raton, FL: CRC Press; 2007. p. 471–92.

[31] Vladislavljevic GT. Use of polysulfone hollow fibers for bubbleless membrane oxygenation/deoxygenation of water. *Sep Purif Technol* 1999; 17: 1–10.

[32] Mouret JR, Morakul S, Nicolle P, Athes V, Sablayrolles JM. Gas-liquid transfer of aroma compounds during winemaking fermentations. *LWT-Food Sci Technol* 2012; 49:238-44.

6. CONCLUSIONS

This research provided a better understanding of the oxygen dissolution patterns; the amounts of oxygen added during winemaking; the dynamics of oxygen transfer and consumption, and the characterization of a system for regulate precisely the oxygen addition. Furthermore, the experiments were carried out both at industrial and laboratory scales.

To study the oxygen incorporation and dissolution at industrial scale, different modes of adding oxygen were analysed. The results indicated that the Venturi injector incorporates approximately twice more oxygen than open pump-overs, with a clear pump contribution to dissolve the bubbles incorporated in both processes. On the other hand, as expected, closed pump-overs incorporate negligible quantities of oxygen. Hence, based on these results, the enologist can choose the better technique to its purposes, *i.e.* closed pump-over are ideal for homogenization due to the lower oxygen incorporation; open pump-overs could be used when the oxygen required are in the range of 1.4 ± 0.5 mg/L and finally Venturi injectors are ideal for high oxygen additions, ranging around 3.0 ± 1.3 mg/L according to our research. Subsequently, for improving the oxygen dissolution during pump-overs, an option could be the design of a “novel” Venturi injector capable of adding tiny bubbles rather than big bubbles, increasing the surface of exchange and therefore the OTR. In the case of open pump-overs, the oxygen dissolution is mainly carried out when the liquid splashes into the vat, so an increase of oxygen transfer at this level is more complicated.

Additionally, the oenologists need to pay attention to oxygen distribution inside large tanks. This is a very important point during oxygen addition, because the oxygen distribution is highly heterogeneous, generating gradients inside the tank with a very poor content in the lower part of the tank. Therefore, there is an urgent need to develop new techniques to improve oxygen distribution inside large tanks.

From the point of view of the kinetics of oxygen dissolution and consumption, several findings stand out. For this analysis it is necessary to divide the winemaking process in three steps: maceration, fermentation and end of fermentation. During maceration, the

native yeasts are inactive but low levels of oxygen are achieved, suggesting that the presence of high levels of free SO_2 is related to the low levels of dissolved oxygen. This agrees with the objectives of oenologists during maceration; indeed, pump-overs at this stage are carried out only with the purpose of extraction and wet the cap, not for oxygenating the must.

At the end of the fermentation, higher dissolved oxygen concentrations were observed compared with the tumultuous phase of fermentation, which agrees well with the lower yeast activity and CO_2 production rate in this stage. However, during the tumultuous phase of fermentation is when the yeast needs more oxygen to synthesize sterols and fatty acids, decreasing the risk of stuck fermentation; and not at the end of the fermentation when the sugars have already consumed and the activity of yeast decreased. Thus, we recommend to review the policies of oxygen addition to improve the oxygen dissolution during the tumultuous phase, avoiding excessive additions at the end of fermentation that could damage the final wine.

To improve the knowledge of oxygen dissolution and consumption during oenological fermentation, experiments at laboratory scale under controlled conditions were carried out. The purpose of these experiments was to achieve discrete oxygen additions in similar conditions to those encountered in oenological fermentations at industrial scale. Based on the results obtained, we confirmed the negative effect of high levels of carbon dioxide upon the mass transfer coefficient when a sparger system is employed and that the specific OUR of the *S. cerevisiae* wine strain strongly depends on the growth phase. Furthermore, the oxygen mass transfer coefficient is modified by biological uptake. It is remarkable to mention that the model developed in this part of the research can be used both under perfect mixed and non-agitated conditions, as well. Additionally, the oxygen transfer observed with biomass present is lower than without biomass and therefore the positive effect of the OUR on the OTR is not enough to compensate the increase of liquid film resistance to mass transport during fermentation. The latter could explain why during the tumultuous phase of fermentation we observed lower oxygen dissolution compared with the end phase of fermentation at industrial scale.

Our studies of the oxygen dissolution and biological uptake by direct sparging during pulse oxygen addition, showed that it is crucial to characterize a system to add precise quantities of oxygen to the liquid medium with the objective to explore the oxygen management and its effect in alcoholic fermentations. According to that, a bubble-free oxygenation system was characterized, based on the work of Blateyron et al. (Blateyron et al., 1998). This system allowed a perfect control of OTR and the model developed permitted to calculate the OTR during all the fermentation process based on the liquid flow rate, temperature of the liquid phase, the characteristics of the silicone tube and the oxygen partial pressure. Also, one of the advantages of this system was its independence of dissolved CO₂ concentration in the liquid.

One of the benefits of employing the bubble-free oxygenation system is that it can be used to study the effect of precise quantities of oxygen on the metabolism of yeast during alcoholic fermentation. In addition, the variations on aroma production under different oxygen regimes is under currently study by coupling the bubble-free oxygenation system to an online GC-MS system (article in preparation).

In summary, this research contributed to the knowledge of the fate of oxygen during winemaking. Its practical approach will contribute as a tool for oxygen management by oenologists at industrial scale as well as for precise oxygen control in experiments at laboratory scale.